Ions Released from Metal-on-Metal Hip Implants: *In Vitro* and *in Vivo* Investigations

Cathy Mélanie Tkaczyk, M.Sc.

Biomedical Engineering Department
McGill University,
Montréal, Canada

A thesis submitted to McGill University, Faculty of Graduate and Postdoctoral Studies, in partial fulfillment of the requirements of the degree of doctor of philosophy.

A mon conjoint Lilian et à ma fille Athénais Clara Constance

J'ignorais que je pouvais tant aimer

ABSTRACT

Studies have shown that Co and Cr particles and ions can enter the bloodstream and accumulate in tissues and organs of patients after metal-on-metal (MM) total hip arthroplasty (THA). These ions can generate reactive oxygen species (ROS) that can be deleterious for cells. We first assessed the biological effects of Cr(VI), Co(II), and Cr(III) by testing their effect on antioxidant enzymes (SODs, CAT, GPx, HO-1) that represent a primary defense system against ROS. We demonstrated that Cr(VI) induced the protein expression (translation) of antioxidant enzymes, whereas it had no effect on the mRNA expression (transcription). Co(II) induced the expression of both protein and mRNA of HO-1 only. Cr(III) had no effect on the activity of these enzymes. We then suggested that a difference in molecular structure may be at the origin of their differential effects and showed that Cr(III) can form precipitable complexes, whereas Co(II) and Cr(VI) cannot form complexes in the same experimental conditions. These Cr(III) complexes, formed in simulated-physiological fluids, were constituted by an organic phase (amino acids, phosphate) tangled with an inorganic phase (Cr, Ca, Na). Interestingly, these Cr(III) complexes interacted only with albumin in presence of fetal bovine serum, whereas they interacted with 8 different human serum proteins in presence of human serum. The interaction of Cr(III) complexes with serum proteins affect their internalization by macrophages, complexes formed with human serum being more easily internalized than those bound to bovine proteins. Lastly, results suggested that the

levels of Co and Cr ions in patients with MM THA are not sufficient to induce significant oxidative stress in the blood of these patients, bringing optimism over concern for the long term biological effects of Co and Cr ions released from metal-metal bearings. In conclusion, this thesis gives very valuable information on the biological effects of Cr and Co ions and gives insight into Cr metabolism.

RESUME

De nombreuses études ont montré que les particules et ions métalliques (Cr(III), Co(II) et Cr(VI)) générés par l'usure de prothèses de hanche métalliques (PHM) se retrouvent dans le flux sanguin des patients et s'accumulent également dans leurs tissus et leurs organes. Ces ions peuvent génèrer des radicaux libres qui peuvent à leur tour être nocifs pour la cellule. Nous avons déterminé les effets de ces ions sur les enzymes antioxidantes (SODs, CAT, GPx, HO-1) qui représentent la première ligne de défense cellulaire contre les radicaux libres. Nos travaux ont révélé que le Cr(VI) induit l'expression de ces protéines (traduction) mais non l'expression de leur ARNm (transcription). Le Co(II) induit l'expression de la proteine et de l'ARNm de HO-1 seulement alors que le Cr(III) n'a aucun effet sur l'expression de ces enzymes. Nous avons par la suite suggéré, que la structure moléculaire de ces ions pouvait avoir une influence sur leurs différents effets. Les résultats ont montré que le Cr(III) formait des complexes constitués d'une partie organique (acides aminés et phosphates) et d'une partie inorganique (Cr, calcium et sodium), alors que ni le Co(II), ni le Cr(VI) ne formaient de complexes dans les mêmes conditions expérimentales. En présence de sérum bovin fétal, les complexes de Cr(III) pouvent se lier seulement à l'albumine, alors qu'en présence de sérum humain, ces mêmes complexes intéragissent avec 8 protéines de nature differente. Cette intéraction avec les protéines humaines semble augmenter l'internalisation des complexes par les macrophages. Finalement, les résultats démontrent que la concentration d'ions Co et Cr présents dans le sang de patients

portant une PHM est insuffisante pour induire un stress oxydant et apportent un souffle optimiste sur les effets à long terme des ions métalliques chez les patients. Dans son ensemble ce projet apporte de nouveaux éléments de connaissances sur les effets biologiques des ions Co et Cr et sur le métabolisme du Cr.

REMERCIEMENTS

Tout d'abord, je tiens à remercier le Dr Maryam Tabrizian du Département de Génie Biomédical de l'Université McGill et le Dr Olga Huk du Département de Chirurgie Orthopédique de l'Hôpital Général Juif, de m'avoir acceptée au sein de leur laboratoire, de m'avoir fourni un excellent environnement pour ma recherche doctorale et de m'avoir permis de présenter mes travaux lors de conférences internationales.

Je suis extrêmement reconnaissante envers le Dr Maryam Tabrizian de m'avoir donné l'opportunité d'élaborer mon projet, guidée par son sens scientifique, ses conseils avertis et ses encouragements afin de travailler sur les thèmes que j'ai jugés importants. J'ai pu mettre à l'épreuve mon sens de l'initiative, perfectionner mon autonomie et acquérir un grand sens de l'adaptation inhérents à ce parcours. C'est grâce au Dr Tabrizian que j'ai pu ainsi travailler sur le projet multi-disciplinaire qui m'importait tant. Je la remercie également profondément pour sa grande gentillesse et sa compréhension. Merci pour tout Maryam, tu es mon modèle de réussite.

Je suis extrêmement reconnaissante envers Le Dr Olga Huk d'avoir été ma co-superviseur, autant disponible qu'elle le pouvait et d'avoir été un merveilleux guide pour mon projet clinique. Son analyse clinique, sa grande gentillesse et son sens de l'humanité m'ont énormement apporté. De plus, elle représente à mes yeux le médecin que tout patient devrait avoir la chance d'avoir.

Maryam et Olga, vous êtes des modèles de réussite à tous points de vue et je vous respecte et je vous admire profondément.

Je ne remercierais jamais assez le Dr Alain Petit de m'avoir supportée dans le laboratoire pendant ces années. Toujours disponible lorsque je ressentais le besoin d'avoir un conseil scientifique ou même non scientifique, il m'a apporté une aide précieuse dans ma thèse et m'a enseigné des choses fondementales. Il m'a, de ce fait, apporté ses lumières dans de nombreux domaines et ce fut ainsi très enrichissant de passer du temps avec lui. J'ose espérer qu'il lui restera encore quelques cheveux lorsque j'aurai terminé. Longue vie à toi Alain, tu es une perle.

Je remercie très chaleureusement mes superviseurs et le Dr Zukor pour leur soutien financiers sans lequel je n'aurais pu mener à bout ce travail. Je leur en suis et en serai toujours reconnaissante.

Je remercie toutes les personnes, qui de près ou de loin, ont apporté une pierre à l'édifice de ce projet: Dr Fackson Mwale pour ses discussions, les bons moments et pour m'avoir permis de travailler sur son bureau lors de ses absences, le Dr Ismail Ashraf pour m'avoir permis de venir travailler de nombreuses heures dans son laboratoire avec le spectromètre Infrarouge, Marco Di Falco de la plateforme de Protéomique de Masse de McGill pour avoir confirmer les analyses que j'avais faites sur les centaines de spectres, Suzie Poulain pour son assistance concernant les analyses en XPS, je tiens à remercier également le Dr Vali, Line Mongeon, Kelly Sears, Lucie Marcotte et tous mes collègues du Département de Génie Biomédical et de l'Institut Lady Davis que je ne nommerai pas par soucis d'espace, mais qui ont été des compagnons tres agréables et sympathiques et qui

me permettent d'associer ces années d'études à de très bons souvenirs. Je remercie Pina, Lina, Nadia et Andrew pour leur gentillesse, leur sourire et leur efficacité et diligence concernant tout le côté administratif de la thèse, Caroline Demers pour une phrase anodine qu'elle m'a dite apres une présentation et qui m'a cependant beaucoup encouragée dans mes démarches « ton projet est celui que j'aurais rêvé de faire si j'avais continué sur un PhD » et enfin je remercie toutes les personnes qui m'ont aiguillée vers des personnes ou des lieux sources.

Pour terminer, je souhaiterais exprimer ma reconnaissance à mes parents, mes frères adorés d'avoir toujours été présents pour moi, mes amis restés au pays du tournesol et des vignes, qui font partie de ma vie depuis plus de 20ans et qui sont plus que jamais présents, mes amis plus récents rencontrés au Canada, notamment au sein de l'Institut. Et enfin je remercie de tout cœur mon conjoint de m'avoir encouragée, de croire en moi et d'être constamment fier de moi. Je le remercie pour ses opinions scientifiques toujours excellentissimes ainsi que son amour et son soutien indéfectibles.

CONTRIBUTION OF AUTHORS

This thesis is presented as a collection of manuscripts which have been published or submitted. The manuscripts are based on experimental data generated from experiments designed and performed by the candidate, who was also responsible for data collection and analysis.

Dr Maryam Tabrizian (McGill University Montreal, QC) and Dr. Olga Huk (Jewish General Hospital, Montreal, QC) were involved as supervisors during the execution of the work and in the manuscript preparation. Dr Alain Petit was the collaborator the most involved at any scientific and technical standpoints. John Antoniou and Fackson Mwale had a lesser contribution in the research, but provided me with the equipment. Dr Maryam Tabrizian, Dr Olga Huk, and Dr David Zukor were involved financially in the achievement of this thesis.

TABLE OF CONTENTS

LIST OF FIGURES

LIST OF TABLES

GLOSSARY OF TERMS

•**NO**:	nitric oxide
•**O2-**:	superoxide radical
•**OH**:	hydroxyl radical
8-oxo-dG:	8-oxo-7,8-dihydro-20-deoxyguanosine
A:	Adenosine
ABTS:	2-2'-Azino-di-[3-ethylbenzthiazoline sulphonite
Arachidonic acid:	$C_{20}H_{32}O_2$
ARNm:	Acide ribonucléique messager
BHK cells:	Baby hamster kidney
C :	Carbon
C3 :	Complement C3
Ca:	Calcium
CAT:	Catalase
CHO cells:	Chinese ovarian cell
Cl:	Chlorine
Co:	Cobalt
CO:	Carbon monoxide
Cr:	Chromium
$CrPO_4$:	Chromium phosphate
Cu/Zn-SOD:	Copper-Zinc superoxide dismutase

CV: Inter-assay coefficient of variation

Cys: Cysteine

DMEM: Eagle's minimal essential medium

DNA: Deoxyribonucleic acid

EC-SOD: Extracellular superoxide dismutase

EDTA: Ethylenediaminetetraacetic acid

EDXA: Energy dispersive X-ray analysis

EPA: U.S. Environmental Protection Agency

EtOH: Ethanol

eV: Electron volt (binding energy)

FAPy-G: 2,6-diamino-5-formamido-4-hydroxypyrimidine

FBS: Fetal bovine serum

Fe(II): Ferrous ion

Fe(III): Ferric ion

Feg-SEM: Field Emission Gun Scanning Electron microscopy

FT-IR FPA: Fourier transform infra-red focal plan array

G: Guanine

GPx: Glutathione peroxidase

GSH: Glutathione

GSSR: Glutathione disulfide

H: Hydrogen

H+: Proton

H_2O: Water

H_2O_2: Hydrogen peroxide

HCl: Hydrochloric acid

HHS: Harris hip score

HNE: 4-hydrxy-2-nonenal

HO-1: Heme-oxygenase-1

HS: Human serum

IARC: International Agency for Research on Cancer

ICP-MS: Inductively coupled plasma mass spectroscopy

Ig: Immunoglobulins

LC-Q-Tof: Liquid chromatography–quadrupole–time of flight

Linoleic acid: $C_{18}H_{32}O_2$

Lipid-OOH:	Lipid peroxide
Lys:	Lysine
M:	Metallic atom
m/z:	Mass-to-charge ratio
MDA:	Malondialdehyde
Met:	Methionine
MM:	Metal-on-metal
Mn^{+}:	Ion^{+}
Mn^{2+}:	Ion^{2+}
Mn-SOD:	Manganese-superoxide dismutase
Mo:	Molybdenum
mRNA:	Messenger ribonucleic acid
MS:	Mass spectrometry
N:	Nitrogen
N_2:	Nitrogen gas (chemical formula)
Na:	Sodium
NAD(P)+:	Oxidized form of Nicotinamide adenine dinucleotide phosphate
NAD(P)H:	Reduced form of Nicotinamide adenine dinucleotide phosphate
NaOH:	Sodium hydroxide
Ni:	Nickel

O_2^-:	Superoxide anion
OH^-:	Hydroxyl anion
ONOO-:	Peroxinitrite
P:	Phosphorus
PCR:	Polymerase chain reaction
PHM:	Prothèses de hanche métalliques
PO_4:	Phosphate
Ppb:	Parts per billion
Ppm:	Parts per million
Pre-OP:	Preoperative
Pro:	Proline
R:	Gas constant (8.314)
ROS:	Reactive oxygen species
RPMI:	Roswell Park Memorial Institute medium
RSH:	Structure of thiol functional group
RT reaction:	Reverse transcriptase reaction
S:	Sulfur
SH:	Sulfudryl group
SO_2:	Sulfur dioxide
SOD:	Superoxide dismutase
T:	Temperature

TAS: Total antioxidant status

TEM: Transmission electron microscopy

THA: Total hip arthroplasty

Thr: Threonine

Ti: Titanium

Tryp: Tryptophan

Tyr: Tyrosine

UHMWPE: Ultra High molecular weight polyethylene

XPS: X-ray photoelectron spectroscopy

ΔGo: Free energy of reaction in a define standard state

ΔGred: Free energy for reduction reaction

CHAPTER 1

The Philosophy of Orthopedic Research

The fastest growing segment of the population is constituted by people over the age of 65 in Canada. Pain in older adults is often wrongly assumed to be a direct consequence of aging but in fact, it often results from specific injuries or diseases. Although the prevalence of some causes of pain, such as osteoarthritis and hip fractures increase with age, there is no reason to expect or accept pain as a consequence of aging. There is no reason as well, to accept pain in young persons who suffer from hip disorders. However, the psychological consequences of pain associated with hip troubles have not been well established but subjects with hip fracture experience confirm a significant deterioration in general health, psychological wellbeing and body image, in addition to impaired physical and social functioning. These troubles can also result in serious repercussions on their family circle.

Hip prostheses have revolutionized the treatment of osteoarthritis and are still the most effective therapy to treat the pain and disability of these patients and improve their quality-of-life. Indeed, hip implants have emerged as one of the success stories of modern orthopaedic surgery.

CHAPTER 2

Introduction

2.1. Rationale

Due to the increase of life expectancy and aging population, changes have been brought in managing degenerative conditions of the musculosketal system. Durable treatments strategies, that safety and effectively restore joint function, have thus emerged over the last 30 years. One of these treatments is the replacement of the hip joint by a biocompatible prosthesis.

In the 1960s, the concept of low-friction arthroplasty with a uniquely small ball in a cemented ultra-high molecular weight polyethylene cup appeared. Nevertheless, a high rate of osteolysis and implant loosening was observed with this metal-on-polyethylene prosthesis. Aseptic loosening was the major complication and caused a very high rate of revisions hip surgery in North America. Important efforts were made to reduce the revision rates and alternative bearings such as cobalt-chromium alloys are usually used in Total Hip Arthroplasty (THA).

Metal-on-metal (MM) prostheses, made of cobalt-chromium (Co-Cr) alloys, were first introduced in the 1960s' but have been progressively abandoned because of the high failure rate resulting from unacceptably high loosening rates. After investigations, it was determined that poor manufacturing and finishing techniques were the cause of the observed complications. Therefore, the second generation of MM bearings emerged with an improved design that gave excellent

outcome results. The implantation of MM prostheses rose an estimated of 70% from 2000 to 2002. Co-Cr-Mo alloys have the hardest, strongest and most fatigue resistant of all materials used for hip implants.

2.2. Motivation Behind the Study of Chromium and Cobalt Ions *in Vitro*

Even though Co-Cr alloys are resistant, they are subject, like all metals, to wear, corrosion, and both phenomena lead to ion release. Co and Cr ions can be generated from Co-Cr alloys by different ways; They can come directly from the corrosion of the passive layer or from the corrosion of wear particles released from the implant. Ions generated during these processes are Co^{2+} or Co(II) and hexavalent Cr^{6+}or Cr(VI), being rapidly reduced in a physiological environment to trivalent Cr^{3+} or Cr(III).

These ions are potentially toxic, since the reduction of Cr^{6+} to Cr^{3+} is accompanied by the generation of unstable and toxic intermediates such as Cr^{4+}, Cr^{5+}, and reactive oxygen species (ROS). These radicals are extremely unstable and react with molecules or other radicals to reach a stable structure. In a balanced cell state, ROS are generated as products of metabolism and are annihilated by antioxidants and the potential damages are repaired. When the level of ROS overwhelms the antioxidant level, an oxidative stress occurs, inducing deleterious effects on cells, such as lipid peroxidation, nitration and oxidation of proteins, and DNA damage.

Once Cr is ingested or released from an implant, its excretion is not fully effective and Cr ions accumulate in cells and tissues. Furthermore, Co and Cr

particles and ions released from MM hip implant can enter the bloodstream and accumulate both in surrounding tissues and organs of patients after MM total hip arthroplasty. Indeed, the main concern associated with such bearings is the presence of circulating and accumulating ions in the organism.

2.3. Hypotheses of the Thesis

This thesis was articulated in 4 parts dealing with *in vitro* and *in vivo* investigations of Co and Cr ions released from metallic hip implants.

1- Co and Cr ions are known to induce protein damage in human macrophages. Our first hypothesis was that these ions could modify the expression of antioxidant enzymes in human macrophages, which represent the first defense system against oxidative stress.

2- The second hypothesis was that a difference in molecular structure of these ions in simulated physiological fluids is the origin of their difference in toxicity.

3- Since Co and Cr are released in blood which contains numerous proteins, we hypothesized that proteins could have a predominant role in the behavior and properties *in vitro* of Cr and Co ions.

4- Lastly, we hypothesized that Co and Cr ions released from MM bearings could generate oxidative stress in patients with MM THA

2.4. Objectives of the Thesis

The overall objective of this thesis is to study the fate of Cr and Co ions released from metallic hip implants and to assess and explain their toxicity.

The detailed objectives are:

1- Compare the toxicity of Cr(VI), Cr(III), and Co(II) in human U937 cell-like macrophages

2- Determine the molecular structures of Cr(VI), Cr(III), and Co(II), that are believed to be the origin of their toxicities.

3- Attempt to understand why Cr excretion is not fully effective by determining the binding of Cr(III) complexes with serum proteins.

4- Assess the clinical relevance of increased levels of Cr and Co ions in patients with metal-on-metal implants.

CHAPTER 3

Review of Literature

3.1. Metal-on-Metal Hip Prostheses

3.1.1. Total hip arthroplasty

Millions of people in the world are affected by joint diseases, especially those of the hip articulation. One of the most predominant hip pathologies is fracture due to osteoporosis, which affects primarily elderly people. In fact, the fastest growing segment of the population is constituted by the people over age of 65 in Canada (1). Durable treatment strategies that safely and effectively restore joint function have emerged over the past 30 years. One of those is the replacement of the hip joint by a biocompatible prosthesis (2-4). Several properties are required to obtain an optimal hip implant. The material needs to be biocompatible, it must have good fatigue resistance, and its elastic modulus should be ideally the same of the bone's modulus. Total hip arthroplasty (THA) is an orthopedic procedure that involves the insertion of a prosthesis, composed of a femoral component (stem) and an acetabular component (cup), in a hip in which the head and the proximal neck of the femur have been surgically excised and the cartilage and the subchondral bone of the acetabulum removed (5). (Fig 3.1).

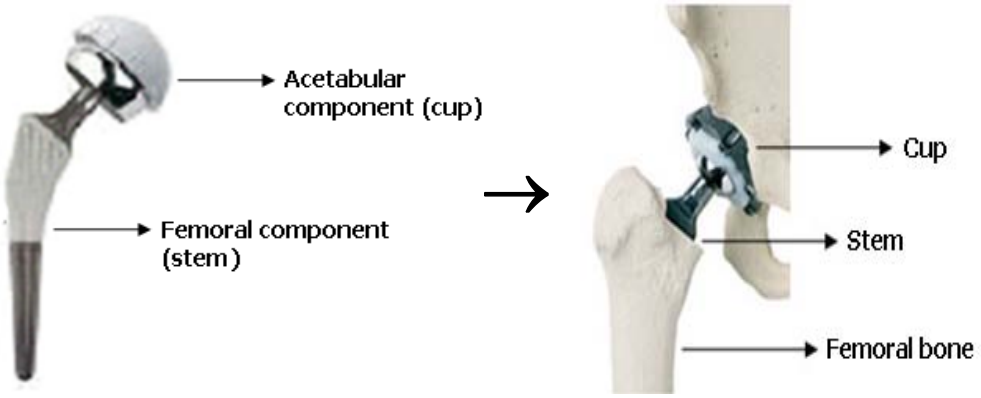

Figure 3.1. Insertion of hip prosthesis in the acetabulum (cup) and the femur (stem).

3.1.2. Metal-on-polyethylene prostheses

In the 1960s, Sir John Charnley introduced the concept of low-friction arthroplasty with a uniquely small ball (22.25 mm) in a (UHMWPE) cup (6,7). The design and bearings of this metal-on-polyethylene prosthesis led for the first time to good performance of hip arthroplasty. Nevertheless, a high rate of wear-mediated osteolysis and implant loosening was observed close to both the femoral stem and the acetabular component (8,9). Aseptic loosening, which is bone resorption around the prosthesis, was the major complication and caused a very high rate of revision hip surgery in North America. Furthermore, revision surgery is dangerous for the patient and not as effective as the primary arthroplasty (10). These problems were first thought to be generated by the use of acrylic cement in the fixation, but the most common explanation accepted was that these phenomena were generated by the presence of wear debris released from

polyethylene bearings. In fact, presence of polyethylene wear particles activate macrophages, which activate osteoclasts or become osteoclasts themselves and initiate bone resorption (11). Actually, this is the major factor limiting longevity of modern hip replacement, leading to revision surgery associated with high morbidity. Consequently, important efforts were made to reduce the revision rates and alternative bearings such as cobalt-chromium alloys are now used in THA.

3.1.3. Metal-on-metal prostheses

Metal-on-metal (MM) prostheses, made of cobalt-chromium (Co-Cr) alloys, have been first introduced in the 1960s' but have been progressively abandoned because of the high failure rate resulting from the premature design and unacceptably high loosening rates. Time has showed that despite the early failures, some excellent long-term survival could be achieved with these MM bearings. After investigation, it was demonstrated that manufacturing design limitations, were the cause of observed complications (12). Therefore, the second generation of MM bearings emerged after significant improvements in design, finishing techniques and manufacturing that gave excellent outcome results. In addition, they have shown to have less volumetric wear rate than the first generation. As a result, they were launched in the market in the late 1980's. Indeed, American Association of Orthopaedic Surgeons reported that MM hip prostheses were implanted in more than 750,000 patients in United States between 1998 and 2000 (13).

Among the available Co-Cr alloy bearings, only two of them are used as joint implants: cobalt-chromium-molybdenum (Co-Cr-Mo) and cobalt-chromium-nickel (Co-Cr-Ni). Co-Cr alloys consist of a primary Co alloy matrix phase and a secondary metal carbide phase. The metal elements are represented as followed: 62-67% Co, 27-30% Cr, 5-7% Mo, but less than 1% of nickel and manganese (14,15). In the Co phase, the presence of Cr enhances the mechanical properties of the alloy and promotes the formation of a passive oxide layer, while Mo is included to enhance corrosion resistance. Moreover, the size and distribution of the carbide phase contribute to the hardness and mechanical behavior of the alloy. Co-Cr-Mo alloys have the hardest, strongest and most fatigue resistant of all materials used for hip implants (16).

The first generation of MM prostheses was made of cast Co-Cr alloys, also designed as ASTM-F75. They were subsequently modified to make them forgeable, leading to new specifications for surgical implants: ASTM-799 for forging Co-Cr alloy and ASTM-F1537 for bar-stock (17,18). Different combinations of Co-Cr-Mo exist: cast alloys with high carbon content or those with low carbon, for instance.

3.2. Ion Properties, Characterization and Metabolism

3.2.1. Physicochemical properties

3.2.1.1. Chromium element

Chromium is the element with atomic number 24 and an atomic mass of 51.996 g/mol. Its density is 7.19 g/cm^3 at 20°C. It is unstable in oxygen and

immediately produces a thin oxide layer that is impermeable to oxygen and protects the underlying metal layers. Cr can exist under different valence states (Fig 3.2), the most common are trivalent Cr(III) (or Cr^{3+}, green in solution) and hexavalent Cr(VI) (or Cr^{6+}, orange in solution), but the most thermodynamically stable specie is Cr(III), explaining the rapid reduction of Cr(VI) to Cr(III) in solution. Cr can form different compounds such as chromium fluoride (CrF_2), Cr chloride ($CrCl_3$), Cr bromide ($CrBr_2$), Cr iodides (CrI_2), Cr oxides (CrO_2), Cr sulfides (CrS), Cr selenides (CrSe), and Cr tellurides (Cr2Te3). Cr is also known to form complexes such as hexaaquachromium nitrate ($Cr(NO_3)_3$* $9H_2O$), for instance (19,20).

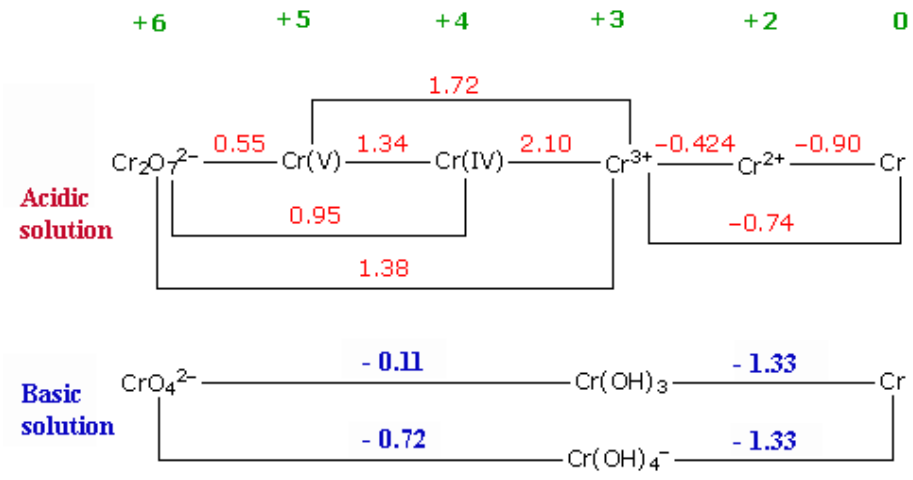

Figure 3.2: Standard reduction for chromium.

Chelation of chromium

Due to its different valences, Cr is able to bind many molecules (20). The affinity of a chelating agent for a given metal is a function of its ionic charge, hydrated ionic radius, and ligand bonding with exposed electron pairs on nitrogen and oxygen. The chelation process is also dependent on the entropy, meaning that the change of Gibbs free energy is negative. It has been demonstrated that Cr can bind to other metals, such as vanadium, iron or zinc: this binding can modify its absorption. Chelating substances such as EDTA and phytates (phytic acid or inositol hexaphosphates which are present in legumes) are known to interact with Cr (21,22). Binding to EDTA has no effect on its absorption but the interaction with phytates decreases it in the intestine of rats. Oxalates such as ethanedioate (present in spinach and rhubarb) generate an increase of the absorption (23).

Cr can also bind to some amino acids such as histidine, which chelates Cr in the small intestine (24). These amino acids prevent the precipitation of Cr at the basic pH of the intestine and thereby increase its absorption. Furthermore, Cr has been demonstrated to bind phosphate (PO_4) groups, generating CrPO4 (chromium phosphate) in phosphate buffers (25). The chelating capacity of Cr(III) is higher than that of Cr(VI).

3.2.1.2. Cobalt element

Cobalt is the element with atomic number 27 and an atomic mass of 58.933 g/mol. Its density is 8.86 g/cm^3 at 20°C. Cobalt is a silver-white, hard, lustrous, brittle element. It is a member of group VIII of the periodic table. Like

iron, it can be magnetized; it is similar to iron and nickel in its physical properties. Co is active chemically, forming many compounds. Contrary to Cr, Co is stable in air and unaffected by water, but is slowly attacked by dilute acids. Cobalt exists under 2 different valence states (Fig 3.3): Co(II) (or Co^{2+}) and Co(III) or Co^{3+} the most stable of these being Co(II). Its ionic radius is 0.078 nm for Co(II) and 0.063 nm for Co(III). Co can form different compounds such as cobalt fluoride (CoF_2), Cr chloride ($CoCl_2$), Co bromide ($CoBr_2$), Cr iodides (CoI_2), Co oxides (CoO), Co sulfides (CoS), Co selenides (CoSe), and Co tellurides (CoTe). It can also form complexes such as hexaaquocobalt dichloride ($CoCl_2.6H_2O$) (26).

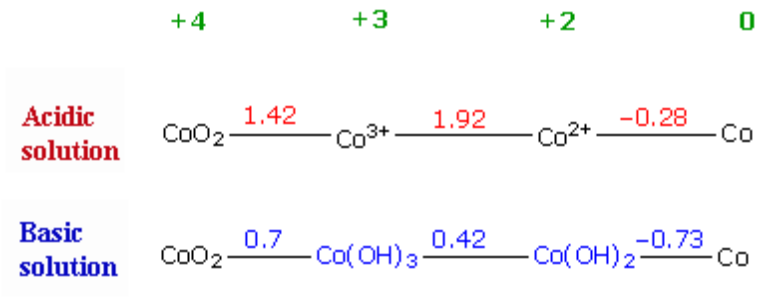

Figure 3.3. Standard reduction potentials for cobalt.

Chelation of cobalt

Co is known to have strong affinity for sulfudryl (SH) groups. It also binds EDTA, deferoxamine, a chelating agent uses to remove excess iron from the organism, and (27,28), a compound used as a precursor of pharmaceuticals or a precursor of chelating agents. However, the chelating capacity of Co is less important than that of Cr.

3.2.2. Characterization techniques for ions and ion complexes

Various techniques can be used for the characterization of ions and ions compounds. The following sections briefly describe the main techniques used in the present thesis for the characterization of Cr and Co complexes

3.2.2.1. Fourier-Transform Infra-Red Focal Plan Array (FT-IR FPA)

FT-IR is a non-destructive technique used for the characterization of chemical structures of various compounds in powder or in solution (28,29). The principal of this technique is based on the Infra-red radiation passing through a sample; some of the infra-red radiation is absorbed by the sample and some of it is transmitted. The resulting spectrum represents the molecular absorption and transmission, creating a unique molecular fingerprint of the sample. This makes infra-red spectroscopy useful for several types of analysis. For instance, it can identify unknown materials; it can determine the quality or consistency of a sample, or the amount of components in a mixture. FT-IR provides a precise measurement method which requires no external calibration.

While the two-dimensional format of an FPA provides the ability to spatially analyze a sample, a spectroscopic imaging instrument must still incorporate a method of wavelengths discrimination. FT-IR FPA functions in a similar fashion as a traditional mapping FT-IR, but in addition, it is possible to visualize the sample with a camera and to register the spectra at different specified points of the sample (29).

In the in chapter 5, FT-IR was useful to characterize complexes formed by Cr(III) ions in simulated-physiological fluids. This technique allowed us to reveal the presence of amino acids by the presence of specific bounds (such as N-H and C=O), and allowed us to determine as well the presence of phosphate groups (P=O bounds). Additionally, FT-IR FPA was useful to conclude that the chemical composition is representative of the overall Cr(III) complexes.

3.2.2.2. Carbon/ Hydrogen/Nitrogen (C/H/N) Elemental Analysis

The sample under test is weighed in using a tin capsule. The tin capsule enclosing the sample falls into the reactor chamber where excess oxygen is introduced before. At about 990°C the material is "mineralized". Formation of carbon monoxide is probable at this temperature even under these conditions of excess oxygen. The complete oxidation is reached and the resulting mixture thus consists of CO_2, H_2O und NO_x. The product gas mixture flows through a silica tube packed with copper granules. In this zone – held at about 500°C – the remaining oxygen is bound and nitric/nitrous oxides are reduced. The exiting gas stream includes the analytically important species CO_2, H_2O und N_2. Eventually, included SO_2 or hydrohalogenides are absorbed at the appropriate traps. High purity helium is used as a carrier gas. Finally the gas mixture is brought to a defined pressure/volume state and is passed to a gas chromatographic system. Separation of the species is done by so called zone chromatography. In this technique a staircase type signal is registered (30).

Complementary to FT-IR, elemental analysis confirmed the implication of amino acids in the formation of the Cr(III) complexes but allowed as well to determine the percentage of nitrogen (N), carbon (C), hydrogen (H), and sulphur (S) in this nanoscale structure. Importantly, C/N ratio made thus possible to determine only three combinations of amino acids present in Cr(III) complexes (Chapter 5).

3.2.2.3. X-ray Photoelectron Spectroscopy (XPS)

Like FT-IR, XPS provides information about the chemical binding of the chemical but only at a few nanometers of the surface. The principle of XPS is based on the photoelectric effect: photons of an adequate energy from an X-ray beam ionize atoms in a sample, resulting in the emission of core-level electrons. Photo-ionization comprises: photo absorption, photo emission, displacement of the electron within the solid and the escape of the electron from the solid into the vacuum of the spectrophotometer. According to the principle of conservation of energy, the sum of the energy of the initial state, plus the proton energy is equal to the sum of the final state plus the kinetic energy of the emitted photoelectron. As each element has characteristic core-electron binding energies, it therefore emits photoelectrons with a characteristic kinetic energy for a given photon energy. Element identification can thus be accomplished by recording the photoelectron energy distribution (spectrum), which shows intensity peaks corresponding to different element (31).

In our project, XPS analysis confirmed the presence of Cr, Ca, N, and phosphorus (P) in the Cr(III) complexes, as well as the presence of sodium (Na) and chlorine (Cl). XPS reported the presence of C-N, N-H, C-C, and P-O bond displacements, confirming once more, the presence of amino acids and phosphate groups in Cr(III) complexes (Chapter 5).

3.2.2.4. Liquid Chromatography- Quadrupole–Time of Flight Spectrometry (LC-Q-Tof)

With LC-Q-Tof, the peptides are first separated chromatographically, often by ion exchange prior to nanoscale reversed-phase HPLC. Eluting peptides are fed to a nanoflow electrospray source for ionization. During electrospray ionization the sample is dissolved in a volatile polar solvent by applying a high voltage, this creates a strong electric field that causes the solvent and sample to elute from the tip of the capillary as an aerosol of highly charged droplets. The charged droplets decrease in size as the solvent is evaporated by the flow of heated nitrogen gas that blows across the front of the ionization source. The charged ions eventually become freed from the solvent and it is then directed through a small aperture into the analyzer section where molecules are separated according to molecular mass. The basis principle of LC-Q-Tof is to generate ions from either inorganic or organic compounds to separate these ions by their mass-to-charge ratio (*m/z*) and to detect them qualitatively and quantitatively by their respective *m/z* and abundance. The Tof analyzer uses an electric field to accelerate the ions through the same potential, and then measures the time they

take to reach the detector. If the particles all have the same charge, the kinetic energies will be identical, and their velocities will depend only on their masses. Lighter ions will reach the detector first (31-33).

In chapter 6, LC-Q-Tof allowed us to confirm the presence of proteins that could bind to Cr(III) complexes and revealed their exact nature.

3.2.2.5. Inductively Coupled Plasma Mass Spectrometry (ICP-MS)

The plasma is formed in a stream of argon gas flowing through an assembly of three concentric quartz tubes known as the plasma torch. The torch is encircled at the top by an induction coil, connected to a free-running radiofrequency generator. The induction coil is cooled by the argon gas. The magnetic field generated by the generator current through the load coil induces a current in the argon gas stream. A plasma is formed almost instantaneously when the argon gas is seeded with energetic electrons. The ICP is capable of exciting/ionizing a wide range of elements, particularly metals, and it therefore allows simultaneous multi-element determination. This technique is very sensitive and allows determining ions concentration in a ppb range (31,34,35).

ICP-MS was used in chapter 7 to determine the concentration of trace metals, namely Cr and Co, in whole blood of patients wearing a metallic hip implant.

3.2.3. Metabolism of ions

3.2.3.1. Chromium metabolism

Cr is an essential nutrient for glucose metabolism and Cr is suspected to play a role in type II diabetes (36). This retention is a function of the chemical form, the age of the individual, and the presence of diabetes (37). The metabolism of Cr is dependant on its valence, its ligands, and the way in which it enters the organism. Cr is present in human diets as organic and inorganic forms (38). The hexavalent form (Cr(VI)) is present in organism diets and can also be inhaled from industrial contamination . However, Cr(VI) is unstable and is rapidly reduced via Cr(V) to Cr(III) by ascorbic acid and thiols, including reduced glutathione and cysteine (39). Not all forms of Cr(III) are biologically active. The biological active form of Cr(III) is present in the diet; it is combined to nicotinic acid or glutathione. It can also be synthesized directly by the organism (40).

Even though Cr metabolism is not fully elucidated, it is known that it is absorbed in the intestinal mucosa. In humans, the sites of absorption include the small intestine, the ileum, the duodenum, and the jejunum (41). The absorption of organic Cr salts is variable: about 0.5% for $CrCl_3$ and Cr-acetate $[(CH_3CO_2)_2Cr{\cdot}H_2O]_2$ and approximately 40% for $^{51}Cr^{3+}$ (42). The absorption of inorganic Cr (Chromium chloride ($ClCH_3$) is low, from 0.4 to 3%. but fast, (less than 15 min) and dose-dependent. Cr is preferentially excreted in the urine, hair, sweat, and bile (43). Its urinary excretion is high during the first 2 hours post-absorption. However, studies dealing with the intestinal absorption of Cr are not in total agreement.

Cr accumulates in cells and tissues but its excretion is not fully effective. Due to this partial excretion, it is believed that Cr can bind plasma proteins. Few studies have elucidated that Cr ions can bind proteins, such as transferrin or ferritin (44). Cr can be released from their carriers in the endosome or in the cytosol after binding to the DMT1 protein transporter. They can then be oxidized and generate the formation of ROS.

Some studies have shown that Cr(VI) can cross the cell membrane using anion channels while other studies suggested the use of carriers (transport proteins) (Fig 11). What is known is that Cr(VI) easily enters into the cells (45). Cr can also cross the nuclear membrane and cause damages to DNA (46). However, little is known about the internalization of Cr(III), some studies suggesting that Cr(III) could be phagocytosed, but nothing has been demonstrated yet.

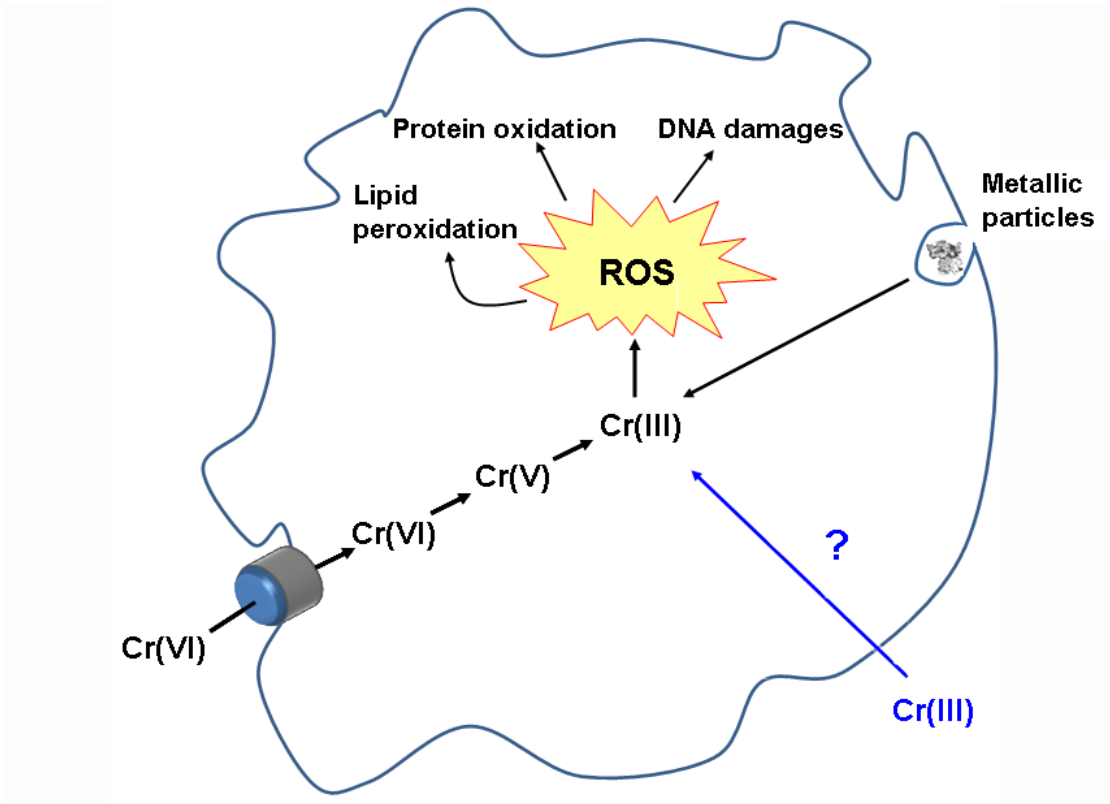

Figure 3.4: Hypothetic scheme used to illustrate the Cr ions internalization pathways.

3.2.3.2. Cobalt metabolism

Co is an essential element for the formation of vitamin B12 (hydroxocobalamin) in humans, and the main source of Co is from the diet (47). Its concentration in drinking water is about 5 mg/L, while it is present in the air at small concentrations (1–2 ng/m^3) in urban areas and somewhat less in remote areas. Once ingested, the availability of Co via the gastrointestinal tract depends on the solubility of the compound and the amount of ingested material (48). Inter-individual variations in availability also exist. Substantial uptake of Co can also occur through the lungs, while its highest concentrations are in the liver and

kidneys. The elimination of Co occurs rapidly and most of it (60-80% of the absorbed dose) appears in urine. Co usually has a biological half-life of several days, but a small amount has a half-life of several years (48).

3.3. Wear, Corrosion and Ion Release

Even though Co-Cr alloys are resistant, they are subject, like all metals, to wear and corrosion, both phenomena leading to ion release.

3.3.1. Tribocorrosion

The simultaneous mechanical (wear) and degradation (corrosion) processes is named tribocorrosion (49). Tribological design is then critical for the long term clinical performance of prostheses. When a MM hip prosthesis is implanted, its wear rate is highly dependent on the lubrication regime which is governed by tribological properties of the starting composition (low or high carbon content), the manufacturing conditions (casting, forging or powder metallurgy), and thermal treatments. More importantly, a correlation exists between the wear rate and the carbide volume fraction: the lowest wear will occur where the carbide volume fraction is largest (50).

3.3.2. Corrosion

In regard to the phenomenon of corrosion, the advantage of Co-Cr alloys resides in the fact that they form a passive oxide layer (chromium oxide), making them much more resistant to corrosion than the other metals (except titanium).

Two essential parameters determine how and why a metal corrodes. The first one concerns thermodynamic forces, which cause oxidation and reduction. During corrosion, the valence state of metal atoms increases to form ions. The thermodynamic force can be calculated using the following equation:

$$\Delta G_{red} = \Delta G^{o} + RT \ln [M]/ [M^{n+}] [e^{-}]^{n}$$

where ΔG_{red} is the free energy for the reduction reaction, ΔG^{o} is the free energy of the reaction in a define standard state, R is the gas constant, T is the temperature, and the bracketed values are the species (M = metallic atom, M^{n+} = ion, e^{-} = electron). If ΔG is greater than zero, oxidation processes will occur spontaneously.

The second parameter is determined by kinetic barriers, such as an oxidative passive layer, that limit these reactions. This is not an energetic process but a mechanical one that protects metals against oxidation and reduction processes. Passive oxide films are the best example of kinetic barriers. The passive layers of Co-Cr-Mo alloys have specific characteristics that make them really efficient. For instance, these passive layers are formed spontaneously and cover the entire surface of the material. Moreover, they are porous, allowing for better cell adhesion. Finally, they are able to remain on the surface despite stress and mechanical abrasion. However, corrosion in hip implants can occur when the passive layer is disrupted because of fretting, stress, or fatigue corrosion (51,52).

3.3.3. Generation of ions

Co and Cr ions can be generated from Co-Cr alloys in different ways. As mentioned above, they can be produced as a result of the corrosion of the passive layer or from the corrosion of wear particles. Ions generated during these processes are Co^{2+} and hexavalent Cr^{6+}, the latter being rapidly reduced in physiological environments to trivalent Cr^{3+}. This reduction is accompanied by the generation of unstable and toxic intermediates such as Cr^{4+}, Cr^{5+}, and oxygen radicals (ROS) (53,54).

3.4. Biological effects

Chromium is an element with two faces, as far as health effects are concerned. Small amounts of chromium are essential for the health of plants and animals. In humans, a chromium deficiency leads to diabetes-like symptoms, for instance. In larger amounts, chromium is harmful, particularly Cr(VI). Cr(VI) are dangerous, causing a rash or sores if spilled on the skin. They can also cause sores in the mouth and throat if inhaled. If swallowed, some chromium compounds can seriously damage the throat, stomach, intestines, kidneys, and circulatory (blood) system. Finally, they are believed to cause cancer. As a result, the U.S. Environmental Protection Agency (EPA) has established rules about the amount of chromium to which workers can be exposed (54,55).

Cobalt is widely dispersed in the environment (56). Humans may be exposed to it by breathing air, drinking water and eating food that contains cobalt. Skin contact with soil or water that contains cobalt may also enhance exposure.

Cobalt is not often freely available in the environment, but when cobalt particles are not bound to soil or sediment particles the uptake by plants and animals is higher and accumulation in plants and animals may occur.

However, high concentrations of cobalt may damage human health (55). When we breathe in very high concentrations of cobalt through air we may experience lung effects, such as asthma and pneumonia. Health effects that are a result of the uptake of high concentrations of cobalt may include: vomiting and nausea, vision problems, heart problems and thyroid damage. Cobalt dust may cause an asthma-like disease with symptoms ranging from cough, shortness of breath and dyspnea to decreased pulmonary function, nodular fibrosis, permanent disability, and death. Exposure to cobalt may also cause weight loss, dermatitis, and respiratory hypersensitivity (57). Finally, cobalt is believed to be carcinogenic. As a result, the International Agency for Research on Cancer (IARC) has listed cobalt compounds within group 2B (agents which are possibly carcinogenic to humans) (58).

3.5. Ion Toxicity

The mechanism of toxicity of these **chromium** and **cobalt** ions is not fully elucidated but there is good evidence that their cytotoxicity is a consequence of the reactive oxygen species (ROS) and/or an oxidative stress they generate (59,60). These notions are explained in the following points.

3.5.1. Oxidative stress

In a balanced cell state, ROS are generated as products of metabolism and are annihilated by antioxidants and the potential damages are then repaired. When the level of ROS overwhelms the antioxidant level, an oxidative stress occurs (61).

3.5.1.1. Reactive oxygen species

Oxygen radicals, also known as ROS, are formed by a cluster of atoms containing unpaired electron. These radicals are extremely unstable and react with molecules or other radicals to reach a stable structure. The family of ROS is composed of superoxide anion (O_2^-), superoxide radical ($\bullet O_2^-$), nitric oxide (•NO**)**, hydroxyl radical (•OH), hydroxyl anion (OH^-), and hydrogen peroxide (H_2O_2). The most reactive is •OH whereas H_2O_2 is not a radical but is a very powerful oxidizer and can be converted to •OH. H_2O_2 is stable in absence of transitional metal ions. It readily diffuses across biological membranes and forms •OH in presence of transitional metal ions, especially iron and copper by the reaction of Fenton (62):

$$Fe(III) + H_2O_2 \rightarrow Fe(II) + OH^- + \bullet OH$$

H_2O_2 is also involved in the Haber-Weiss reaction, leading to the formation of •OH as well (63):

$$\bullet O_2^- + H_2O_2 \rightarrow \bullet OH + OH^- + O_2$$

ROS can be produced from both exogenous and endogenous substances. Potential endogenous sources include mitochondria, inflammatory cell activation, and peroxisomes. Under physiological conditions, mitochondria produce a considerable quantity of H_2O_2 estimated to account for about 2% of the total oxygen uptake by an organism. Furthermore, mitochondria generate 2-3 nmol of O_2^-/min/mg of protein. In mitochondria producing a high amount of ROS, antioxidant molecules and antioxidant proteins are present in the organelle to avoid oxidative stress. O_2^- is formed on both sides of mitochondria inner and is detoxified initially to H_2O_2 and then to water by antioxidant enzymes. Macrophages and neutrophiles are additional endogenous sources of ROS. They are also present in other cells involved in cholesterol metabolism and synthesis of steroids (ovary, interstitium of the testis). As a matter of fact, activated macrophages lead to an increase in consummation of oxygen, generating a variety of ROS, including O_2^-, H_2O_2, and •NO. Additionally, peroxisomes can produce H_2O_2 under physiological conditions. Although livers are the organs where the peroxisomal contribution for H_2O_2 is the most important, other organs containing peroxisomes, are also exposed to the production of H_2O_2. ROS can also be generated by exogenous sources, such as radiations, barbiturates, and metal ions.

3.5.1.2. Reactive oxygen species generated by metal ions

In vivo, Cr^{6+} can interact with glutathione (GSH) to generate the radical GS• and Cr^{5+} (Fig 3.5, reactions 1 and 2). Once formed, Cr^{5+} can react with

hydrogen peroxide (H_2O_2) via Fenton reactions to generate Cr^{6+} and hydroxyl radical (•OH) (Fig 3.5, reaction 3) as described in the following formula:

$$M^{n+} + H_2O_2 = M^{(n+1)+} + \bullet OH + OH^-$$

where M^{n+} is a transition metal such as Co or Cr (64). This hydroxyl radical is highly reactive with a half-life in aqueous solution of less than 1 nanosecond. On the other hand, GS• radical is able to induce cellular damages and can further react with other thiol molecules (-SH) in oxygenated tissues to generate superoxide radical ($\bullet O_2^-$) (Fig 3.5, reactions 4 and 5). Superoxide radicals can also reduce Cr^{6+} in Cr^{5+} (Fig 3.5, reaction 6) that in turn can produce hydroxyl radical through a Fenton-like reaction (Fig 3.5, reaction 7) (65). Finally, cellular reductants, such as ascorbate and glutathione can also reduce Cr^{5+} to Cr^{4+} (Fig 3.5, reaction 8), which can in turn generate hydroxyl radical and Cr^{6+} through another Fenton-like reaction (Fig 3.5, reaction 9) (53).

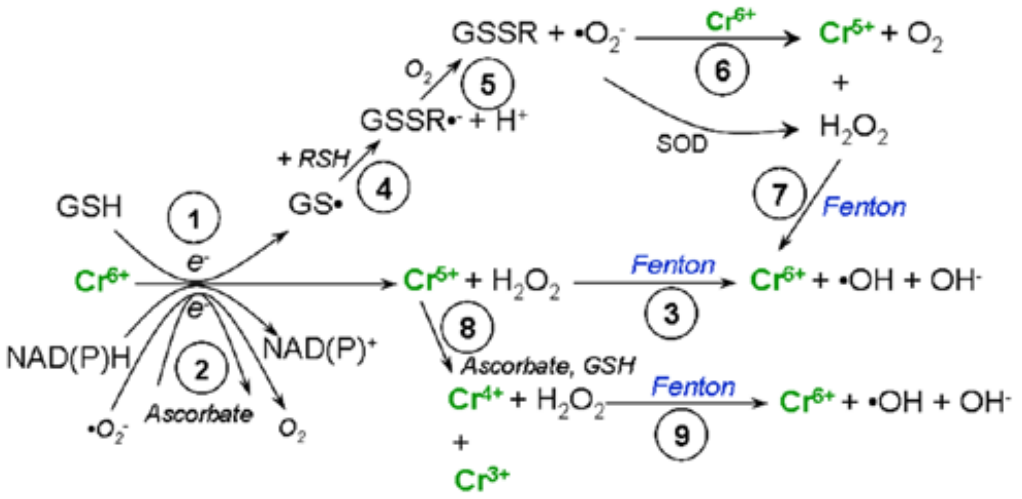

Figure 3.5: Biological reduction of Cr^{6+} and the different associated reactions producing ROS.

Co is also involved in many biological reactions and is able to generate hydroxyl radicals from hydrogen peroxide under physiological conditions. However, not all Co ions reacting with hydrogen peroxide can generate ROS. Studies have demonstrated that superoxide anions can be produced from the interaction of Co^{2+} and hydrogen peroxide. In addition, Co can be involved in a Fenton-like reaction as follows (66):

$$Co^{+} + H_2O_2 = Co^{2+} + \bullet OH + OH^{-}$$

$$2Co^{+} + H_2O_2 = Co^{3+} + \bullet OH + OH^{-}$$

3.5.2. Effect of reactive oxygen species on macromolecules

Metal ions – in this case, Co and Cr – can induce deleterious effects on cells through the formation of ROS. The effects of these ROS on macromolecules are summarized in following sections.

3.5.2.1. Lipid peroxidation

Lipids can interact with hydroxyl radical in a lipid-peroxidation process. This process occurs in three phases, the initiation, the propagation, and the termination, that can be schematized as presented in figure 3.6 (Fig3.6).

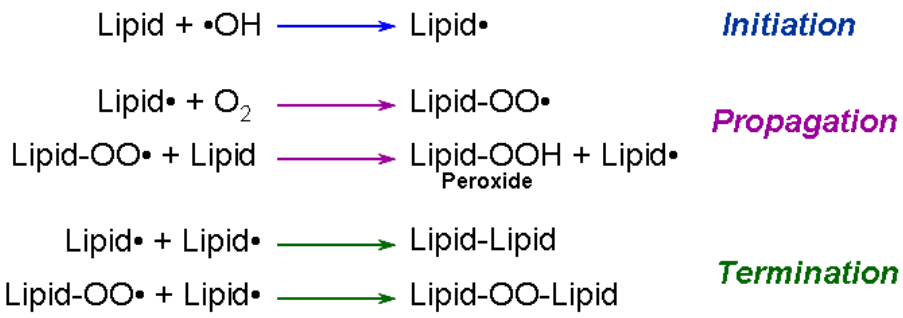

Figure 3.6: Peroxidation of lipids by ROS.

The main concern associated with the lipid oxidation is the fact they are the major constituents of cell membranes. In fact, phospholipids represent about 50% of the macromolecules of the cellular membrane (67). Because of their highly unsaturated level, they are very susceptible to oxidization. In a pure system, it has been demonstrated that 60 molecules of linoleic acids and 200 of arachidonic acids are consumed per initiation event. However, the length of lipid radicals depends on many factors in cells. Peroxidation of lipids can disturb the assembly of the membrane, causing changes in fluidity and permeability, alterations of ion transport, and inhibition of metabolic processes (68). In addition, damage generated in mitochondrial membranes can lead to additional ROS formation.

A variety of lipid byproducts can be produced as a consequence of lipid peroxidation. Malondialdehyde (MDA) and 4-hydroxy-2-nonenal (HNE) are two of the basic byproducts of lipid oxidation which have been shown to be mutagenic in bacteria and mammalian cells and frequently used as oxidative stress markers (69,70). MDA can react with DNA to form adducts to deoxyguanosine and deoxyadenosine. HNE, which can electrophilically attack many molecules such as proteins and nucleotides, causes dysfunction of these target molecules. HNE can also affect transduction signals *in vivo*, namely the extracellular signal-regulated kinase phosphorylation that is a signaling pathway associated with cellular proliferation, survival, and homeostasis.

3.5.2.2. Oxidation and nitration of proteins

Protein oxidation is defined as the covalent modification of a protein induced either directly by ROS or indirectly by reaction with secondary byproducts of oxidative stress. Depending on the ROS present, the resulting damage to the protein may take the form of oxidation or nitration of various amino acid residues. Consequently, there are numerous types of protein modifications through oxidative process.

Damages to proteins by •OH can be generated at two different sites in the polypeptide backbone: the α-carbon of amino acids and the aliphatic side chains of hydrophobic amino acids residues. These reactions lead to the formation of an alkylperoxyl radical, which generates alkylperoxide. In the presence of dioxygen radical ($•OH_2$), this alkylperoxide is converted to a radical intermediate and finally

to a hydroxyl protein derivative (Fig 3.7). It is notable that during the oxidation of proteins, the generated amino acid radicals can be propagated to secondary sites, potentially causing disproportionately modified amino acids (71). Tyr and Tryp residues are electron-rich sinks ideal for such free-radical chains. Indeed, if these residues are functionally critical, their oxidation reactions at the protein surface might disrupt or even occlude some active-site residues.

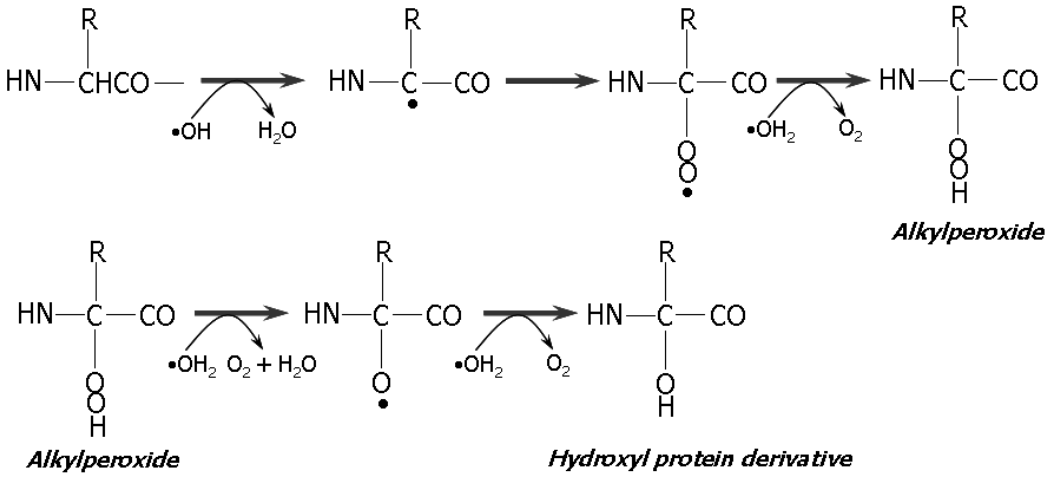

Figure 3.7: Oxidation of proteins by ROS.

The most common products of protein oxidation are the carbonyl derivatives of proline (Pro), arginine (Arg), lysine (Lys), and threonine (Thr). These protein derivatives or peptide fragments possess highly reactive carbonyl groups such as aldehydes and ketones. These derivatives may serve as markers of oxidative stress for most types of ROS.

Another byproduct of protein oxidation by ROS is nitrotyrosine (72). Nitric oxide (•NO) can rapidly react with superoxide ion ($\bullet O_2^-$) to form

peroxinitrite ($ONOO^-$). Some amino acids such as cysteine (Cys), methionine (Met), and tyrosine (Tyr) are particularly susceptible to oxidization by $ONOO^-$. When Tyr is attacked by $ONOO^-$, it is converted to a 3-nitrotyrosine (Fig 3.8). While all Tyr residues in proteins may theoretically be targets for nitration, presumably the efficiency of Tyr nitration is dependent on various biological conditions such as the local production and concentration of the reactive species, the existence and availability of antioxidants and scavengers, the accumulation of inflammatory cells and the presence of proinflammatory cytokines, as well as the proximity and compartmentation of these components (72,73).

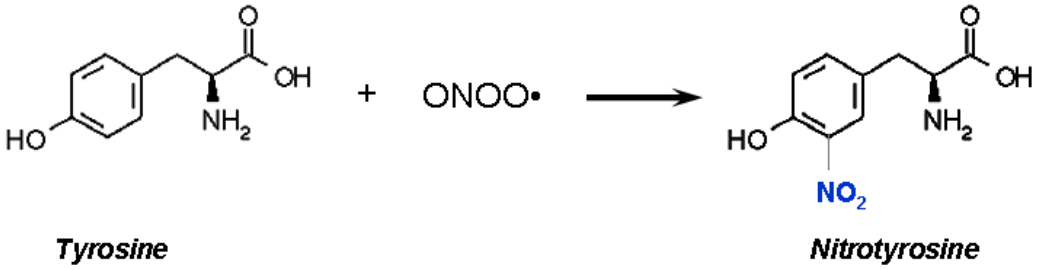

Figure 3.8: Formation of nitrotyrosine by ROS.

An accumulation of proteins damaged by oxidative modifications is associated with aging. The accumulation of oxidized proteins has also been shown in diseases such as Alzheimer's, Parkinson's, atherosclerosis, rheumatoid arthritis, respiratory distress syndrome, progeria, and muscular dystrophy (74).

3.5.2.3. DNA damage

Hydroxyl radicals can interact with DNA bases leading to a variety of oxidative products. In fact, the interaction of hydroxyl radical (•OH) with Guanine (G) generates the formation of 8-oxo-7,8-dihydro-20-deoxyguanosine (8-oxo-dG) and of 2,6-diamino-5-formamido-4-hydroxypyrimidine (FAPy-G) (Fig 3.9). 8-oxoG is a highly mutagenic miscoding lesion that can lead to G:C to T:A transversion mutations. Hydroxyl radical can also interact with Adenine (A) but these lesions are less frequent than those associated with G (75).

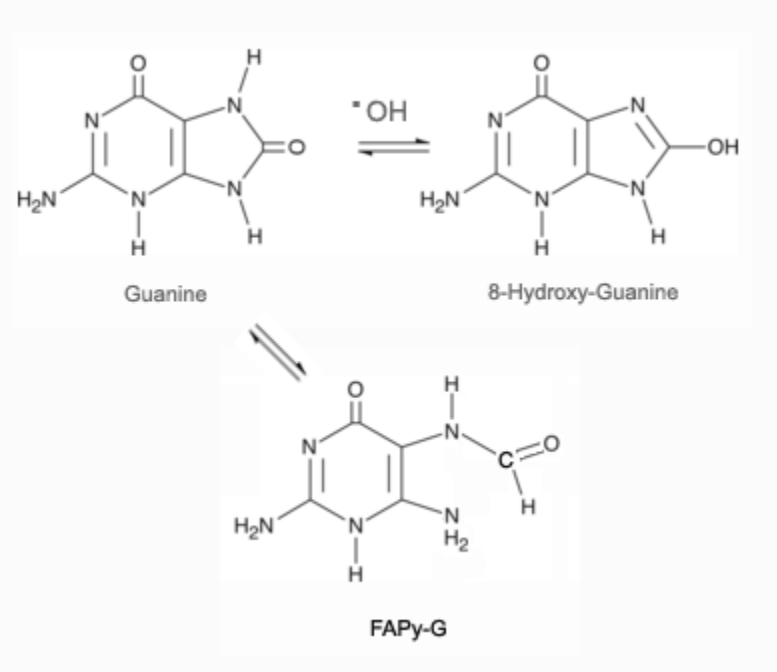

Figure 3.9: Modification of Guanine by ROS.

Oxidative lesions to DNA can lead to single-strand breaks. These lesions present mutagenic and/or cytotoxic (blocking) challenges to the cell when encountered during chromosome replication or gene transcription. Indeed, the most significant consequences in DNA lesions result in genomic instability and

various pathologies such as cancer. Oxidation of DNA is also implicated in normal aging. Due to their major physiological effects in several aspects of intracellular signaling, ROS can also indirectly interfere with the expression of several genes and signal transduction pathways (76).

3.5.3. Antioxidant systems

Biological antioxidants are natural molecules that can prevent the uncontrolled formation of free radicals and ROS or inhibit their relation with biological structures. Antioxidants can be divided in three general families. The first group is composed of small molecules such as vitamin E and C, traps radicals and prevents chain reactions. The second one made of antioxidant enzymes and metal-binding proteins, prevents the formation of new ROS. Lastly, those composed of DNA repair enzymes, repair biomolecules damaged by ROS. The focus of our research was mostly on the two first families of molecules which are further described below.

3.5.3.1. Non-enzymatic antioxidant molecules

Non-enzymatic antioxidants are scavengers that either physically quenches excited species, such as singlet oxygen, or chemically traps oxidizing free radicals and ROS. The kinetics of their scavenging reactions is very fast, making them very efficient. Importantly, free radicals reacting with scavengers decay through dismutation, recombination, or reduction by secondary scavengers. Therefore, these free radicals do not serve to initiate uncontrolled chain reactions.

Non-enzymatic antioxidant molecules exist as water soluble (free glutathione (GSH) and vitamin C (ascorbic acid), and lipid soluble (vitamins A and E) antioxidant. Bilirubin and ubiquinol, the latter being the two-electron product of ubiquinone, have the power to inhibit lipid peroxidation. Uric acid and flavonoids, which are ubiquitous in plants and contain phenolic hydroxyl groups, also have antioxidant effects (77,78).

3.5.3.2. Antioxidant enzymes

Even though non-enzymatic scavengers are essential to avoid damages induced by most ROS, their protection is not sufficient against radicals such as peroxides and hydroperoxides that are continuously produced by aerobic cells. Specific antioxidant enzymes play this essential role. The advantages of such antioxidant enzymes reside in the fact that the steady-state concentration of peroxides can be adapted to the cell requirements. Indeed, these enzymes can be induced, inhibited, or even inactivated. They also play an important role in the regulation of metabolic pathways and specific functions of aerobic cells. For this reason, their expression is modified in several diseases (Table 1) (79). The activities of the enzymes analyzed in the present research project are described below.

DISEASE	CELL TISSUS	ANTIOXIDANT
Female infertility	Luteinizing hormone (brain)	Cu/Zn-SOD
Diabetes	Beta cells (mice)	Ec-SOD
HIV	Plasma	SOD
Parkinson	Neurons	CAT, GPx, SOS
Heart diseases	Arteries	GPx, SOD
Crohn's disease	Gastro-intestinal tract	CAT, GPx, SOD
Allergy to pollen	cochlea	Cu/Zn-SOD

Table 1: Relationship between antioxidant enzymes and diseases in human. Superoxide dismutase.

Superoxide dismutase (SOD) converts superoxide radical ($\bullet O_2^-$) into hydrogen peroxide (Fig 3.10). There are three forms of human SOD: cytosolic copper/zinc-SOD (Cu/Zn-SOD), mitochondrial manganese-SOD (Mn-SOD), and extracellular-SOD (EC-SOD). Cu/Zn-SOD contains 2 subunits of 32 kDa and constitutes the first line of antioxidant defense. The Mn-SOD is a tetramer of 96 kDa that is depressed or induced by different factors such as cytokines. EC-SOD is a tetrameric enzyme of 135 kDa containing copper and zinc and is found in interstitial spaces of tissues and in extracellular fluids (synovial fluid, plasma, and

lymph). A low level of SODs is constantly generated by the cells in reaction to the formation of ROS by the respiratory chain. Interestingly, since they are induced by oxidants, they can be used as markers of oxidative stress (80).

Figure 3.10: Effect of SOD on ROS.

Catalase

Catalase (CAT) is a tetramer of 240 kDa containing one ferriprotorphyrin group per subunit. It plays a key role in the acquisition of tolerance to oxidative stress in adaptative response of cells. CAT converts hydrogen peroxide to water and oxygen (Fig 3.11) (81).

Figure 3.11: Effect of catalase on ROS.

Glutathione peroxidase

Glutathione peroxidase (GPx) is a tetramer of 80 kDa that converts hydroperoxides to water and oxygen (Fig 3.12). It is also able to catalyze the reduction of hydroperoxides into water and oxygen. Although it acts similarly as

CAT, GPx is the only enzyme that can react efficiently with other organic hydroperoxides and is crucial for cell homeostasis (82).

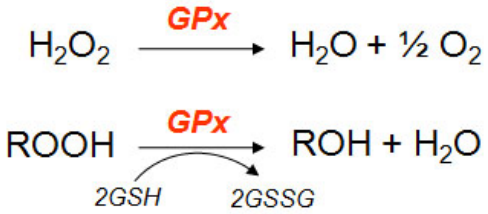

Figure 3.12: Effect of GPx on ROS.

Heme Oxygenase

Heme oxygenase (HO) is a nontraditional antioxidant enzyme exhibiting antioxidant capacities. Three isoforms (HO-1, HO-2, and HO-3) of this enzyme exist. All these isoforms are located in the membrane of the endoplasmatic reticulum and catalyze the degradation of heme into carbon monoxide, iron, and biliverdin, which is subsequently reduced to bilirubin, a potent antioxidant (Fig 3.13) (83). HO-1 is inducible by ROS and is found throughout the organs, but especially in tissues rich in reticuloendothelial cells, such as the spleen and the bone marrow. HO-1 is involved in human diseases such as Alzheimer and inflammatory diseases and its expression is down-regulated in hepatitis C.

HO-2 and HO-3 are constitutively expressed and are not inducible. HO-2 and HO-3 are widely distributed throughout the body but are especially localized in endothelial cell, adventitial nerves of blood vessels, and in neurons in autonomic ganglia (83,84).

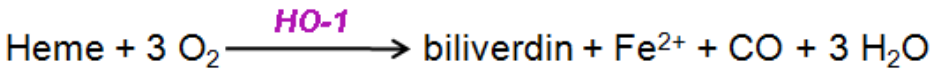

Figure 3.13: Degradation of heme by HO-1.

3.6. References.

1. Yancik R. Cancer burden in the aged: an epidemiologic and demographic overview. Cancer 1997 Oct 1;80(7):1273-1283.

2. Saikko V, Ahlroos T, Calonius O, Keranen J. Wear simulation of total hip prostheses with polyethylene against CoCr, alumina and diamond-like carbon. Biomaterials 2001 Jun;22(12):1507-1514.

3. Skinner HB. Ceramic bearing surfaces. Clin Orthop Relat Res 1999 Dec(369):83-91.

4. Tipper JL, Ingham E, Hailey JL, Besong AA, Fisher J, Wroblewski BM, et al. Quantitative analysis of polyethylene wear debris, wear rate and head damage in retrieved Charnley hip prostheses. J Mater Sci Mater Med 2000 Feb;11(2):117-124.

5. Fessy MH, Seutin B, Bejui J. Anatomical basis for the choice of the femoral implant in the total hip arthroplasty. Surg Radiol Anat 1997;19(5):283-286.

6. Donald SM. Sir John Charnley (1911-1982): inspiration to future generations of orthopaedic surgeons. Scott Med J 2007 May;52(2):43-46.

7. Wroblewski M, Siney PD, Nagai H, Fleming PA. Wear of ultra-high-molecular-weight polyethylene cup articulating with 22.225 mm zirconia

diameter head in cemented total hip arthroplasty. J Orthop Sci 2004;9(3):253-255.

8. Wroblewski BM. Osteolysis due to particle wear debris following total hip arthroplasty: the role of high-density polyethylene. Instr Course Lect 1994;43:289-294.
9. Zhu YH, Chiu KY, Tang WM. Review Article: Polyethylene wear and osteolysis in total hip arthroplasty. J Orthop Surg (Hong Kong) 2001 Jun;9(1):91-99.
10. Synder M, Kozlowski P, Marciniak M, Dorman T. Revision hip arthroplasty in aseptic loosening of total hip replacement. Ortop Traumatol Rehabil 2001;3(1):34-37.
11. Ingham E, Fisher J. The role of macrophages in osteolysis of total joint replacement. Biomaterials 2005 Apr;26(11):1271-1286.
12. Swanson SA. Engineering considerations in the design of double-cup hip replacement prostheses. Clin Orthop Relat Res 1978 Jul-Aug(134):12-18.
13. Rieker CB, Schon R, Kottig P. Development and validation of a second-generation metal-on-metal bearing: laboratory studies and analysis of retrievals. J Arthroplasty 2004 Dec;19(8 Suppl 3):5-11.
14. Higuchi F, Inoue A, Semlitsch M. Metal-on-metal CoCrMo McKee-Farrar total hip arthroplasty: characteristics from a long-term follow-up study. Arch Orthop Trauma Surg 1997;116(3):121-124.

15. Hughes AN, Lane RA. The development of high tensile properties in a wrought Co-Cr-Ni-W alloy of potential orthopaedic surgery use. Eng Med 1976 Apr;5(2):38-40.

16. Wang SC, Browne M, Ubhi HS, Starink MJ. Determination of the fatigue fracture planes of Co-Cr-Mo biomedical alloys using electron backscatter diffraction. J Microsc 2005 Feb;217(Pt 2):118-121.

17. Saldivar-Garcia AJ, Lopez HF. Microstructural effects on the wear resistance of wrought and as-cast Co-Cr-Mo-C implant alloys. J Biomed Mater Res A 2005 Aug 1;74(2):269-274.

18. Salinas-Rodriguez A, Rodriguez-Galicia JL. Deformation behavior of low-carbon Co-Cr-Mo alloys for low-friction implant applications. J Biomed Mater Res 1996 Jul;31(3):409-419.

19. Shupack SI. The chemistry of chromium and some resulting analytical problems. Environ Health Perspect 1991 May;92:7-11.

20. Kartal SN. Removal of copper, chromium, and arsenic from CCA-C treated wood by EDTA extraction. Waste Manag 2003;23(6):537-546.

21. Hazell T. Minerals in foods: dietary sources, chemical forms, interactions, bioavailability. World Rev Nutr Diet 1985;46:1-123.

22. Yu XZ, Gu JD. The role of EDTA in phytoextraction of hexavalent and trivalent chromium by two willow trees. Ecotoxicology 2008 Apr;17(3):143-152.

23. Chen NS, Tsai A, Dyer IA. Effect of chelating agents on chromium absorption in rats. J Nutr 1973 Aug;103(8):1182-1186.

24. Gammelgaard B, Jensen K, Steffansen B. In vitro metabolism and permeation studies in rat jejunum: organic chromium compared to inorganic chromium. J Trace Elem Med Biol 1999 Jul;13(1-2):82-88.

25. Zhitkovich A, Voitkun V, Costa M. Formation of the amino acid-DNA complexes by hexavalent and trivalent chromium in vitro: importance of trivalent chromium and the phosphate group. Biochemistry 1996 Jun 4;35(22):7275-7282.

26. Blackburn AC, Gallucci JC, Gerkin RE. Structure of hexaaquacobalt(II) bromate. Acta Crystallogr B 1990 Dec 1;46 (Pt 6):712-716.

27. Nagababu P, Latha JN, Pallavi P, Harish S, Satyanarayana S. Studies on antimicrobial activity of cobalt(III) ethylenediamine complexes. Can J Microbiol 2006 Dec;52(12):1247-1254.

28. Hutson TB, Mitchell ML, Keller JT, Long DJ, Chang MJ. A technique for monitoring mammalian cell growth and inhibition in situ via Fourier transform infrared spectroscopy. Anal Biochem 1988 Nov 1;174(2):415-422.

29. Stenlund H, Gorzsas A, Persson P, Sundberg B, Trygg J. Orthogonal projections to latent structures discriminant analysis modeling on in situ FT-IR spectral imaging of liver tissue for identifying sources of variability. Anal Chem 2008 Sep 15;80(18):6898-6906.

30. Keszthelyi L, Varga L, Demeter I, Hollos-Nagy K, Szokefalvi-Nagy Z. Elemental analysis of samples of biological origin relative to their protein content by means of charged particle bombardment. Anal Biochem 1984 Jun;139(2):418-426.

31. Pradier CM, Rubio C, Poleunis C, Bertrand P, Marcus P, Compere C. Surface characterization of three marine bacterial strains by Fourier transform IR, X-ray photoelectron spectroscopy, and time-of-flight secondary-ion mass spectrometry, correlation with adhesion on stainless steel surfaces. J Phys Chem B 2005 May 19;109(19):9540-9549.

32. Cordewener JH, Luykx DM, Frankhuizen R, Bremer MG, Hooijerink H, America AH. Untargeted LC-Q-TOF mass spectrometry method for the detection of adulterations in skimmed-milk powder. J Sep Sci 2009 Apr;32(8):1216-1223.

33. Chassaigne H, Norgaard JV, Hengel AJ. Proteomics-based approach to detect and identify major allergens in processed peanuts by capillary LC-Q-TOF (MS/MS). J Agric Food Chem 2007 May 30;55(11):4461-4473.

34. Deutsch AS, Cohen BI, Musikant BL. Inductively coupled plasma-emission spectroscopy and atomic absorption for the use of elemental analysis of a root canal after lasing with a holmium:YAG laser. J Endod 2003 Jun;29(6):404-406.

35. Bayon MM, Rodriguez Garcia A, Garcia Alonso JI, Sanz-Medel A. Indirect determination of trace amounts of fluoride in natural waters by ion chromatography: a comparison of on-line post-column fluorimetry and ICP-MS detectors. Analyst 1999 Jan;124(1):27-31.

36. Althuis MD, Jordan NE, Ludington EA, Wittes JT. Glucose and insulin responses to dietary chromium supplements: a meta-analysis. Am J Clin Nutr 2002 Jul;76(1):148-155.

37. Anderson RA, Kozlovsky AS. Chromium intake, absorption and excretion of subjects consuming self-selected diets. Am J Clin Nutr 1985 Jun;41(6):1177-1183.

38. Anderson RA, Bryden NA, Polansky MM, Reiser S. Urinary chromium excretion and insulinogenic properties of carbohydrates. Am J Clin Nutr 1990 May;51(5):864-868.

39. Avudainayagam S, Megharaj M, Owens G, Kookana RS, Chittleborough D, Naidu R. Chemistry of chromium in soils with emphasis on tannery waste sites. Rev Environ Contam Toxicol 2003;178:53-91.

40. McCarty MF. Chromium(III) picolinate. FASEB J 1996 Feb;10(2):365-369.

41. Dowling HJ, Offenbacher EG, Pi-Sunyer FX. Absorption of inorganic, trivalent chromium from the vascularly perfused rat small intestine. J Nutr 1989 Aug;119(8):1138-1145.

42. Borguet F, Wallaeys B, Cornelis R, Lameire N. Transperitoneal absorption and kinetics of chromium in the continuous ambulatory peritoneal dialysis patient--an experimental and mathematical analysis. Nephron 1996;72(2):163-170.

43. Donaldson DL, Smith CC, Yunice AA. Renal excretion of chromium-51 chloride in the dog. Am J Physiol 1984 Jun;246(6 Pt 2):F870-878.

44. Sun Y, Ramirez J, Woski SA, Vincent JB. The binding of trivalent chromium to low-molecular-weight chromium-binding substance (LMWCr) and the transfer of chromium from transferrin and chromium picolinate to LMWCr. J Biol Inorg Chem 2000 Feb;5(1):129-136.

45. Suwalsky M, Castro R, Villena F, Sotomayor CP. Cr(III) exerts stronger structural effects than Cr(VI) on the human erythrocyte membrane and molecular models. J Inorg Biochem 2008 Apr;102(4):842-849.

46. Quievryn G, Goulart M, Messer J, Zhitkovich A. Reduction of Cr (VI) by cysteine: significance in human lymphocytes and formation of DNA damage in reactions with variable reduction rates. Mol Cell Biochem 2001 Jun;222(1-2):107-118.

47. Tiffany ME, Spears JW, Xi L, Horton J. Influence of dietary cobalt source and concentration on performance, vitamin B12 status, and ruminal and plasma metabolites in growing and finishing steers. J Anim Sci 2003 Dec;81(12):3151-3159.

48. Barceloux DG. Cobalt. J Toxicol Clin Toxicol 1999;37(2):201-206.

49. Azzi M, Szpunar JA. Tribo-electrochemical technique for studying tribocorrosion behavior of biomaterials. Biomol Eng 2007 Nov;24(5):443-446.

50. Vandamme NS, Wayman BH, Topoleski LD. Wear behavior of carbide coated Co-Cr-Mo implant alloy. J Mater Sci Mater Med 2003 Jan;14(1):47-53.

51. Jacobs JJ, Gilbert JL, Urban RM. Corrosion of metal orthopaedic implants. J Bone Joint Surg Am 1998 Feb;80(2):268-282.

52. Cook SD, Gianoli GJ, Clemow AJ, Haddad RJ, Jr. Fretting corrosion in orthopaedic alloys. Biomater Med Devices Artif Organs 1983;11(4):281-292.

53. Tsou TC, Yang JL. Formation of reactive oxygen species and DNA strand breakage during interaction of chromium (III) and hydrogen peroxide in vitro: evidence for a chromium (III)-mediated Fenton-like reaction. Chem Biol Interact 1996 Dec 20;102(3):133-153.

54. Davidson T, Kluz T, Burns F, Rossman T, Zhang Q, Uddin A, et al. Exposure to chromium (VI) in the drinking water increases susceptibility to UV-induced skin tumors in hairless mice. Toxicol Appl Pharmacol 2004 May 1;196(3):431-437.

55. Day GA, Virji MA, Stefaniak AB. Characterization of exposures among cemented tungsten carbide workers. Part II: Assessment of surface contamination and skin exposures to cobalt, chromium and nickel. J Expo Sci Environ Epidemiol 2009 May;19(4):423-434.

56. Domingo JL. Cobalt in the environment and its toxicological implications. Rev Environ Contam Toxicol 1989;108:105-132.

57. Saglam AM, Baysal V, Ceylan AM. Nickel and cobalt hypersensitivity reaction before and after orthodontic therapy in children. J Contemp Dent Pract 2004 Nov 15;5(4):79-90.

58. Steinhoff D, Mohr U. On the question of a carcinogenic action of cobalt-containing compounds. Exp Pathol 1991;41(4):169-174.

59. Lison D, Carbonnelle P, Mollo L, Lauwerys R, Fubini B. Physicochemical mechanism of the interaction between cobalt metal and carbide particles to generate toxic activated oxygen species. Chem Res Toxicol 1995 Jun;8(4):600-606.

60. Harrop TC, Mascharak PK. Fe(III) and Co(III) centers with carboxamido nitrogen and modified sulfur coordination: lessons learned from nitrile hydratase. Acc Chem Res 2004 Apr;37(4):253-260.

61. Turi S, Nemeth I, Torkos A, Saghy L, Varga I, Matkovics B, et al. Oxidative stress and antioxidant defense mechanism in glomerular diseases. Free Radic Biol Med 1997;22(1-2):161-168.

62. Lloyd RV, Hanna PM, Mason RP. The origin of the hydroxyl radical oxygen in the Fenton reaction. Free Radic Biol Med 1997;22(5):885-888.

63. Shi XL, Dalal NS. The role of superoxide radical in chromium (VI)-generated hydroxyl radical: the Cr(VI) Haber-Weiss cycle. Arch Biochem Biophys 1992 Jan;292(1):323-327.

64. Morehouse KM, Mason RP. The transition metal-mediated formation of the hydroxyl free radical during the reduction of molecular oxygen by ferredoxin-ferredoxin:NADP+ oxidoreductase. J Biol Chem 1988 Jan 25;263(3):1204-1211.

65. Luzzatto E, Cohen H, Stockheim C, Wieghardt K, Meyerstein D. Reactions of low valent transition metal complexes with hydrogen peroxide. Are they "Fenton-like" or not? 4. The case of Fe(II)L, L = edta; hedta and tcma. Free Radic Res 1995 Nov;23(5):453-463.

66. Leonard S, Gannett PM, Rojanasakul Y, Schwegler-Berry D, Castranova V, Vallyathan V, et al. Cobalt-mediated generation of reactive oxygen species and its possible mechanism. J Inorg Biochem 1998 Jul;70(3-4):239-244.

67. Parthiban A, Vijayalingam S, Shanmugasundaram KR, Mohan R. Oxidative stress and the development of diabetic complications--antioxidants and lipid peroxidation in erythrocytes and cell membrane. Cell Biol Int 1995 Dec;19(12):987-993.

68. Arduini A, Stern A, Storto S, Belfiglio M, Mancinelli G, Scurti R, et al. Effect of oxidative stress on membrane phospholipid and protein organization in human erythrocytes. Arch Biochem Biophys 1989 Aug 15;273(1):112-120.

69. Nielsen F, Mikkelsen BB, Nielsen JB, Andersen HR, Grandjean P. Plasma malondialdehyde as biomarker for oxidative stress: reference interval and effects of life-style factors. Clin Chem 1997 Jul;43(7):1209-1214.

70. Shiraishi K, Naito K. Effects of 4-hydroxy-2-nonenal, a marker of oxidative stress, on spermatogenesis and expression of p53 protein in male infertility. J Urol 2007 Sep;178(3 Pt 1):1012-1017; discussion 1017.

71. Hawkins CL, Davies MJ. Generation and propagation of radical reactions on proteins. Biochim Biophys Acta 2001 Apr 2;1504(2-3):196-219.

72. Mattson MP, Goodman Y, Luo H, Fu W, Furukawa K. Activation of NF-kappaB protects hippocampal neurons against oxidative stress-induced apoptosis: evidence for induction of manganese superoxide dismutase and suppression of peroxynitrite production and protein tyrosine nitration. J Neurosci Res 1997 Sep 15;49(6):681-697.

73. Petit A, Mwale F, Tkaczyk C, Antoniou J, Zukor DJ, Huk OL. Cobalt and chromium ions induce nitration of proteins in human U937 macrophages in vitro. J Biomed Mater Res A 2006 Dec 1;79(3):599-605.

74. Schuessler H, Schilling K. Oxygen effect in the radiolysis of proteins. Part 2. Bovine serum albumin. Int J Radiat Biol Relat Stud Phys Chem Med 1984 Mar;45(3):267-281.

75. Ober M, Linne U, Gierlich J, Carell T. The two main DNA lesions 8-Oxo-7,8-dihydroguanine and 2,6-diamino-5-formamido-4-hydroxypyrimidine exhibit strongly different pairing properties. Angew Chem Int Ed Engl 2003 Oct 20;42(40):4947-4951.

76. Thannickal VJ, Fanburg BL. Reactive oxygen species in cell signaling. Am J Physiol Lung Cell Mol Physiol 2000 Dec;279(6):L1005-1028.

77. Franci O, Ranfi F, Scaccini C, Amici A, Merendino N, Tommasi G, et al. Differential effect of alpha-tocopherol and ascorbate on oxidative injury induced in immune cells by thermal stress. J Biol Regul Homeost Agents 1996 Apr-Sep;10(2-3):54-59.

78. Schettler V, Wieland E, Methe H, Schuff-Werner P, Muller GA. Oxidative stress during dialysis: effect on free radical scavenging enzyme (FRSE) activities and glutathione (GSH) concentration in granulocytes. Nephrol Dial Transplant 1998 Oct;13(10):2588-2593.

79. Nepomniashchikh VA, Lomivorotov VV, Deryagin MN, Lomivorotov VN, Kniazkova LG. Oxidative stress and monooxygenase liver function in patients with coronary heart disease and multiple organ dysfunction syndrome. Eur J Anaesthesiol 2009 Feb;26(2):140-146.

80. Wlaschek M, Scharffetter-Kochanek K. Oxidative stress in chronic venous leg ulcers. Wound Repair Regen 2005 Sep-Oct;13(5):452-461.

81. Cutler RG. Oxidative stress and aging: catalase is a longevity determinant enzyme. Rejuvenation Res 2005 Fall;8(3):138-140.

82. Doroshow JH. Glutathione peroxidase and oxidative stress. Toxicol Lett 1995 Dec;82-83:395-398.

83. Baranano DE, Rao M, Ferris CD, Snyder SH. Biliverdin reductase: a major physiologic cytoprotectant. Proc Natl Acad Sci U S A 2002 Dec 10;99(25):16093-16098.

84. Le WD, Xie WJ, Appel SH. Protective role of heme oxygenase-1 in oxidative stress-induced neuronal injury. J Neurosci Res 1999 Jun 15;56(6):652-658.

CHAPTER 4

Effects of Chromium and Cobalt Ions on the Expression of Antioxidant Enzymes in Human U937 Macrophage-like Cells

---

The first article presented in this chapter and accepted for publication in *Journal of Biomedical Materials Research Part A*, fulfills the first objective of this thesis which was to compare the toxicity of Cr(VI), Cr(III), and Co(II) in human U937 macrophages-like cells.

Previous studies performed in our laboratory showed that Cr(III) and Co(II) ions could induce damage to lipids and proteins in human macrophages *in vitro*. Moreover, this damage was suggested to be the result of reactive oxygen species (ROS) generated by Cr and Co ions. Consequently, one of the aims of this thesis was to understand the fate of Cr(III) and Co(II) ions in generating oxidative damage by studying *in vitro* a defense system against oxidative stress. It is known that Cr(VI) ions are the first ions generated from metallic implants and that they are rapidly reduced to Cr(III) in the body. As a result, we further investigated the effects of Cr(III), Cr(VI) and Co(II) on macrophages. Our findings showed that Cr(III) has no effect on the expression of Mn-SOD, Cu/Zn-SOD, CAT, GPx, and HO-1. Cr(VI) induced the protein expression of all the antioxidant enzymes studied but had no effect on the expression of their mRNA. Co(II) induced the expression of both proteins and mRNA of HO-1 only.

EFFECT OF CHROMIUM AND COBALT IONS ON THE EXPRESSION OF ANTIOXIDANT ENZYMES IN HUMAN U937 MACROPHAGE-LIKE CELLS

Cathy Tkaczyk[1,2,3], Olga L. Huk[2,3], Fackson Mwale[2], John Antoniou[2,3], David. J Zukor[2],

Alain Petit[2], Maryam Tabrizian[1,3,4,5]

[1]Department of Biomedical Engineering, Duff Medical Building, 3775 University Street, Montreal, QC, H3A 2B4, Canada.

[2]Division of Orthopaedic Surgery, McGill University,

Lady Davis Institute for Medical Research,

The Sir Mortimer B. Davis-Jewish General Hospital,

3755 Côte-Sainte-Catherine Road, Montreal, QC, H3T 1E2, Canada.

[3]Center of Biorecognition and Biosensors (CBB)

[4] McGill Institute for Advanced Materials, [5] Faculty of Dentistry

4.1. Abstract

The main concern associated with metal-on-metal (MM) hip prosthesis is the presence of metal ions, mainly chromium (Cr) and cobalt (Co), which are found both systemically and locally in the organism of patients. Previous studies revealed that Cr(III) and Co(II) ions could induce damages to proteins in macrophage-like cells *in vitro*, probably through the formation of reactive oxygen species (ROS). We then hypothesized that these ions can modify the expression of antioxidant enzymes in these cells. Results showed that Cr(VI) induced the protein expression of Mn-superoxide dismutase, Cu/Zn-superoxide dismutase, catalase, glutathione peroxidase, and heme oxygenase-1 (HO-1) but had no effect of the expression of their mRNA. Cr(III) have no effect on the expression of all these antioxidant enzymes. Co(II) induced the expression of both protein and mRNA of HO-1 only. In conclusion, results showed that Cr(VI), Cr(III), and Co(II) had differential effects on the expression of antioxidant enzymes in macrophage-like cells *in vitro*.

4.2. Introduction

Metal-on-metal (MM) hip prostheses, made of cobalt-chromium (Co-Cr) alloys, represent an excellent alternative to metal-polyethylene bearings in the treatment of osteoarthritis of the hip because of their substantially lower wear rates (1). However, the main concern associated with such bearings is the presence of circulating metal ions in the organism (2). These ions are potentially toxic (3,4), may cause metal hypersensitivity (5,6), chromosomal aberrations (7),

and may induce changes in the proportions of peripheral blood lymphocytes (8-10). On the other hand, epidemiological studies performed in patients with MM hip implants were unable to demonstrate any causal effect of the presence of metallic ions on the risk of cancer (11). Moreover, the mechanism of metal ion toxicity is not completely understood: it is however known that they can generate reactive oxygen species (ROS), such as superoxide ions ($O_2^{\cdot -}$), hydrogen peroxide (H_2O_2), hydroxyl radical ($OH^{\cdot}$), and nitrogen oxide ($NO^{\cdot}$) through Fenton/ Haber-Weiss chemistry (12). These ROS are involved in numerous human diseases, including degenerative lung and heart conditions, Alzheimer, rheumatoid arthritis, and aging (13). ROS are implicated in the induction of oxidative stress generating cell and tissue damage. In previous studies, we have shown that Co(II) and Cr(III) ions can induce the formation of protein carbonyls (14) and nitrotyrosines (15), two markers of ROS-induced protein damage linked to oxidative stress in human U937 macrophage-like cells and in human MG-63 osteoblast-like cells (16). However, oxidative stress may result from an increased production of oxidants (ROS) and/or a decrease in antioxidant defense. In fact, the organisms possess an efficient enzymatic defense system against these ROS, avoiding the oxidative stress status which occurs when the level of ROS overwhelms the antioxidant level.

Superoxide dismutases (SODs) are antioxidant enzymes found in three isoforms, manganese-SOD (Mn-SOD), copper/zinc-SOD (Cu/Zn-SOD), and extracellular-SOD. They catalyze the conversion of superoxide radical ($\bullet O_2^-$) into hydrogen peroxide (H_2O_2). Catalase (CAT) is another antioxidant enzyme that

assumes the next step by converting 2 molecules of hydrogen peroxide in water and oxygen. Glutathione peroxidase (GPx) supports CAT by converting one molecule of hydrogen peroxide in water and oxygen. Heme-oxygenase-1 (HO-1) is not considered as a conventional antioxidant enzyme, but it catalyses the degradation of heme in biliverdin and CO_2: these by-products have high antioxidant properties. In addition, this enzyme can be induced in an oxidative stress environment. In the present study, we aim to further understand the toxicity of Cr and Co at the cellular level by studying the effect of these ions on the expression of antioxidant enzymes in human U937 macrophage-like cells *in vitro*.

4.3. Material and Methods

4.3.1. Cell culture

Human U937 macrophage-like cells have been chosen as the cell culture model because macrophages are the main cells present in periprosthetic tissues. Moreover, macrophages are the cells that engulf foreign bodies by phagocytosis. U937 cells were cultured in RPMI 1640 medium supplemented with 5% fetal bovine serum (HyClone, Logan, UT), 100 U/mL penicillin, and 100 µg/mL streptomycin in a humidified 5% CO2 atmosphere at 37ºC. Cells were incubated for up to 72h in the absence (control) or the presence of 0-50 ppm Cr(VI) (Na_2CrO_4, Sigma-Aldrich, Oakville, ON), 0-250 ppm Cr(III) ($CrCl_3$, Sigma-Aldrich), and 0-10 ppm Co(II) ($CoCl_2$, Fisher Scientific, Montreal, QC). The choice of the ions is due to the fact that Co and Cr are the main corrosion products

of MM hip implants. Moreover, Cr(VI) are the first Cr ions released from metallic implants and are rapidly reduced to a more thermodynamically stable specie Cr(III) (17). Concentrations were chosen in function of the non-prestimulated nature of U937 cells in which higher levels of ions are necessary for stimulation. They are also based on our previous studies on the effect of Cr and Co ions on the stimulation of the oxidation of proteins in macrophages (14,15) and osteoblasts (16).

4.3.2. Protein expression

After incubation, cells were lyzed in a caspase assay lysis buffer (BioSource, Nivelles, Belgium) as previously described. Proteins were then separated on 4–20% acrylamide gels (SDS-PAGE) and transferred to nitrocellulose membranes. Anti-oxidant enzymes were detected by Western blot using anti-Mn-SOD (1:500 - Upstate, Billerica, MA), anti-Cu/Zn-SOD (1:1000 - Upstate, Billerica, MA), anti-CAT (1:1000- Abcam, Cambridge, MA), anti-GPx (1:1500 - Abcam), and anti-HO-1 (1:1000 - Abcam) antibodies. All antibodies were diluted in ChemiBlocker™:PBS-tween (0.05%) (1:1) (Chemicon International Norcross, GA). Actin (NeoMarkers, Fremont, CA) expression served as a house keeping gene for gel loading and served to normalize the results. Proteins were detected using *NEN Renaissance* chemiluminescence reagents (Perkin-Elmer, Woodbridge, ON) and analyzed using a VersaDoc image analysis system equipped with a cooled charge coupled device (CCD) 12-bit camera (Bio-Rad Laboratories, Mississauga, ON).

4.3.3. RNA Extraction

Total RNA was extracted from U937 cells by a modified method of Chomcynski and Sacchi (18) using TRIzol® reagent (Invitrogen, Burlington, ON). Purity of the RNA was measured through the A_{260}/A_{280} ratio.

4.3.4. Reverse Transcriptase (RT) Reaction

The RT reaction was performed for 50 min at 42ºC using 1.0 µg total RNA. 20 µL of reaction volume contained 50 mM Tris-HCl (pH 8.3), 75 mM KCL, 3 mM $MgCl_2$, 10 mM DTT, 50 µM dNTP mixture, and 200 units of Superscript II RNAse H reverse transcriptase (Invitrogen). The inactivation reaction was achieved at 70ºC for 15 min.

4.3.5. Polymerase Chain Reaction (PCR)

PCR was performed in a total volume of 25 µL containing 10 mM Tris-HCl (pH 8.3), 1.5 mM $MgCl_2$, 0.2 mM dNTP mixture, 0.8 µM of forward and reverse primers, 1µl of RT mixture, and 1.25 units of Taq DNA polymerase (Invitrogen). The PCR procedure was done in accordance with the standard method (19). Thirty five cycles were used for all genes. Every cycle consists of 1 min denaturation at 95°C, 1 min annealing at 51°C (GPx, HO-1) or 56°C (CAT, SODs), 1 min polymerization at 72°C, followed by a final 10 min extension at 72°C. PCR products were separated on 2% agarose gel, visualized by ethidium bromide staining, and analyzed using a Bio-Rad VersaDoc image analysis system. GAPDH was used as a house keeping gene for gel loading and served to

normalize the results. To avoid contamination with genomic DNA, DNase I treatment was performed using 1 unit of deoxyribonuclease I, (Invitrogen) at 25ºC for 1 h. DNase I was inactivated by adding 1 μL of 25 mM EDTA to the reaction mixture and by heating for 10 min at 65ºC. To confirm the lack of genomic DNA contamination of RNA samples, PCR was also performed with RNA aliquots. The primers, specific for human genes, were obtained from Invitrogen. The sequences of the primers used for PCR are described in Table 2.

Gene	Primers		Product size
HO-1	Forward	5'- ACATCTATGTGGCCCTGGAG	348
	Reverse	5'- TGTTGGGGAAGGTGAAGAAG	
CAT	Forward	5'- CTGCAGCTCCGCAATCCTAC -	229
	Reverse	5'- TCCTTCCACTGCTTCATCTGG	
GPX	Forward	5'- CCTCAAGTACGTCCGACCTG -	197
	Reverse	5'- CAATGTCGTTGCGGCACACC	
Cu-Zn-SOD	Forward	5'- AAGGCCGTGTGCGTGCTGAA-	246
	Reverse	5'- CAGGTCTCCAACATGCCTCT-	
Mn-SOD	Forward	5'- GCACATTAACGCGCAGATCA	241
	Reverse	5'- AGCCTCCAGCAACTCTCCTT -	
GAPDH	Forward	5'- CCATCACCATCTTCCAGGAG -	576
	Reverse	5'- CCTGCTTCACCACCTTCTTG -	

Table 2: Sequences of primers used for PCR.

4.4. Results

4.4.1. Effect of Cr(VI)

Figures 1 and 2 show the effect of Cr(VI) on the expression of antioxidant enzymes. Indeed, Cr(VI) induced a sustained dose-dependent expression of all studied antioxidant enzyme proteins at 24h, 48h and 72h (Fig. 4.1A and Fig. 4.2). The induction reached 2.5, 2.8, 2.9, 2.8, and 4.5 times the control with 50 ppm Cr(VI) after 72h for Mn-SOD, Cu/Zn-SOD, CAT, GPx, and HO-1 respectively. Cr(VI) had no effect on their mRNA expression in the same experimental conditions (Fig. 4.1B).

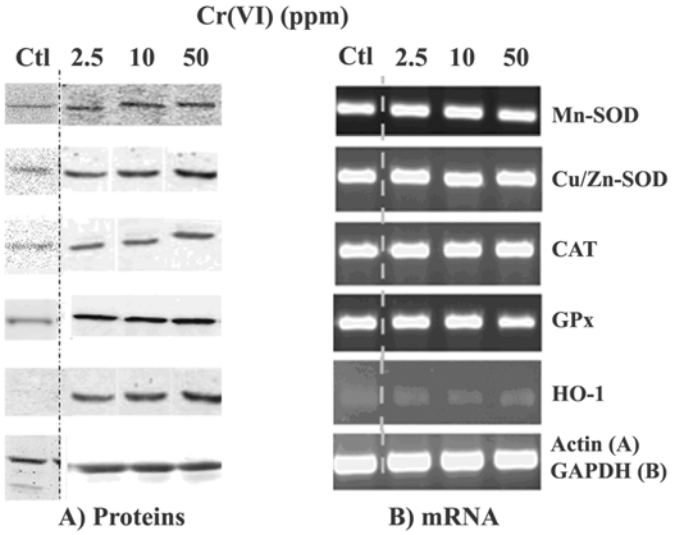

Figure 4.1: Effect of Cr(VI) on antioxidant enzyme expression. Human U937 cells were incubated for 48 h in the absence (Control) or the presence of increasing concentrations of Cr(VI). Protein expression (A) was measured by

Western blot while mRNA expression (B) was measured by PCR. Results are representative of 3-6 experiments.

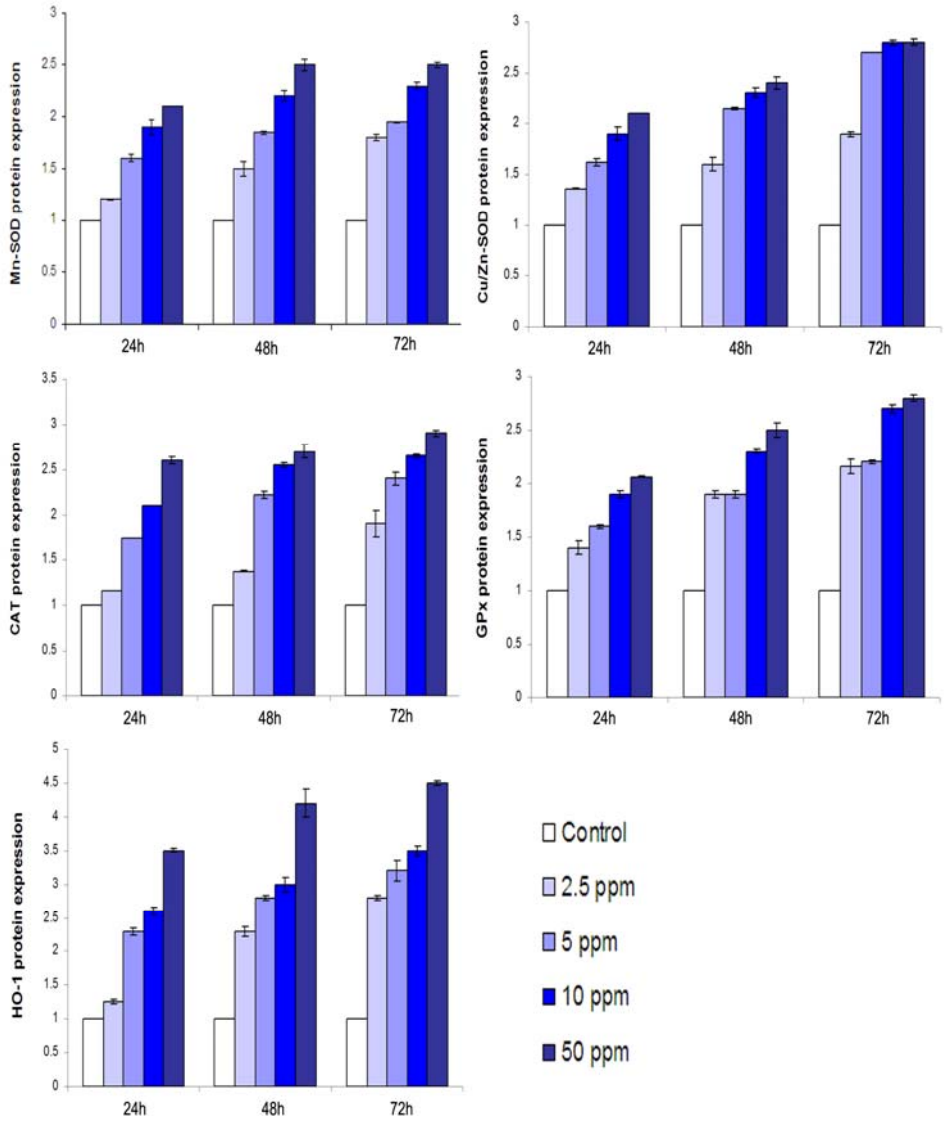

Figure 4.2: Effect of Cr(VI) on the expression of antioxidant enzyme proteins. U937 cells were incubated for up to 72h in the presence of 0-50 ppm Cr(VI). Protein expression was measured by Western blot. Results are the mean ± standard deviation of 3-4 experiments.

4.4.2. Effect of Cr(III)

Figures 4.3 and 4.4 show the effect of Cr(III) on the expression of antioxidant enzymes. After 48h, Cr(III) had no effect on the expression of antioxidant enzyme proteins (Fig. 4.3A and 4.4) and mRNA (Fig. 4.3B and 4.5) in the cell culture conditions and time of incubations used in this study. Results were similar at 24h and 72h.

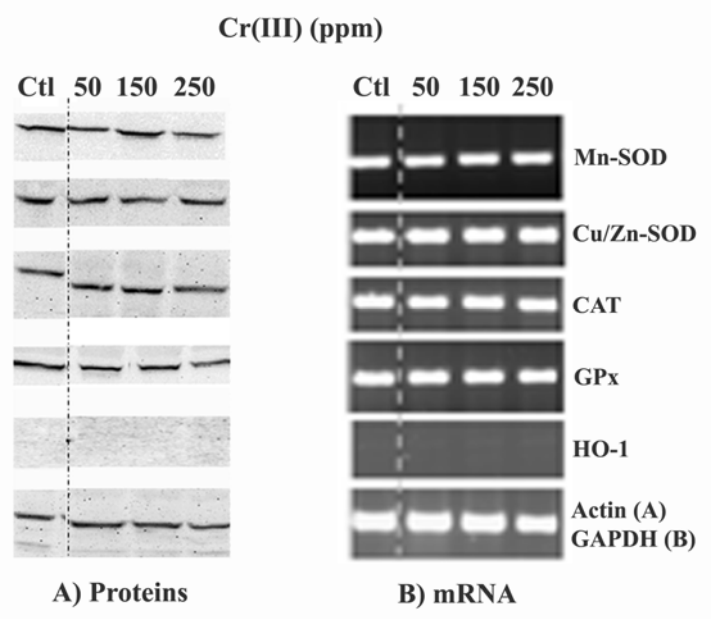

Figure 4.3: Effect of Cr(III) on the expression of antioxidant enzymes. Human U937 cells were incubated for 48 h in the absence (Control) or the presence of increasing concentrations of Cr(III). Protein expression (A) was measured by Western blot while mRNA expression (B) was measured by PCR. Results are representative of 3-6 experiments.

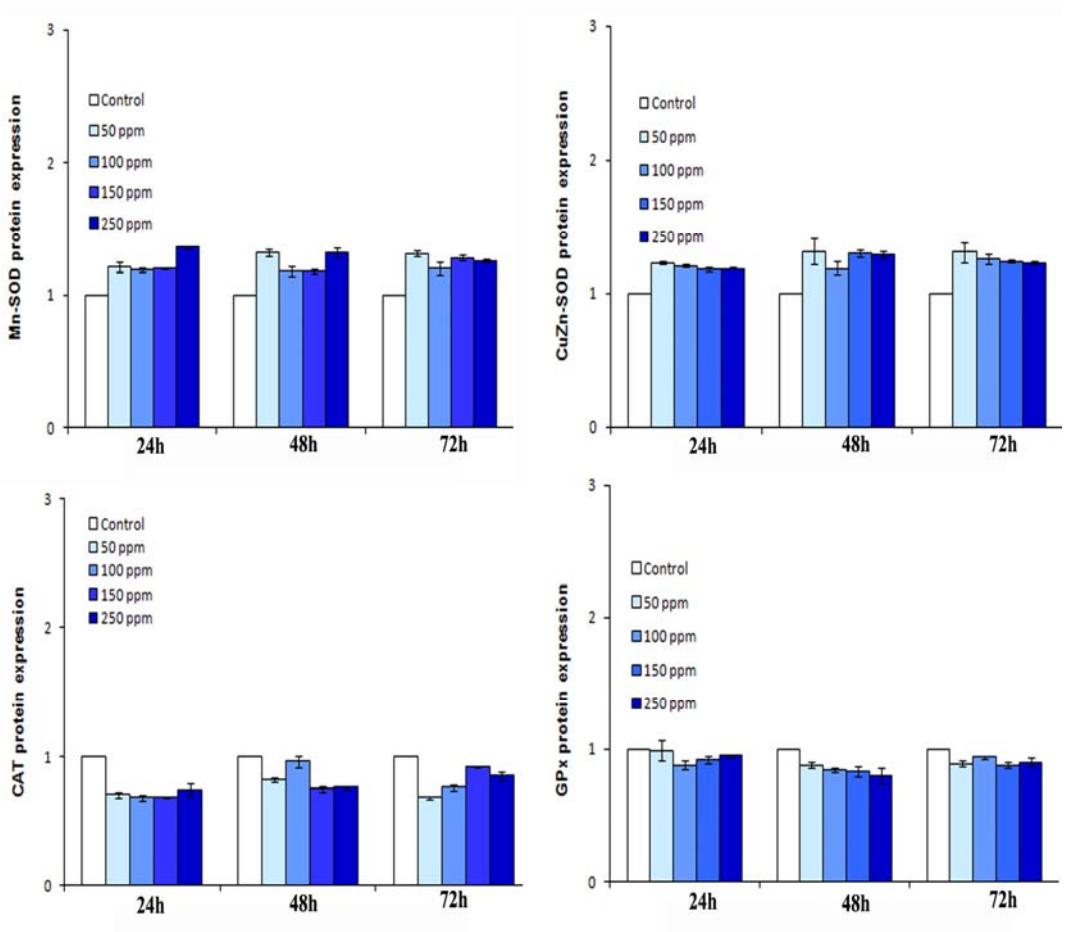

Figure 4.4: Effect of Cr(III) on the expression of antioxidant enzyme proteins. U937 cells were incubated up to 72h in the presence of 0-250 ppm Cr(III). Protein expression was measured by Western blot. Results are the mean ± standard deviation of 4-6 experiments.

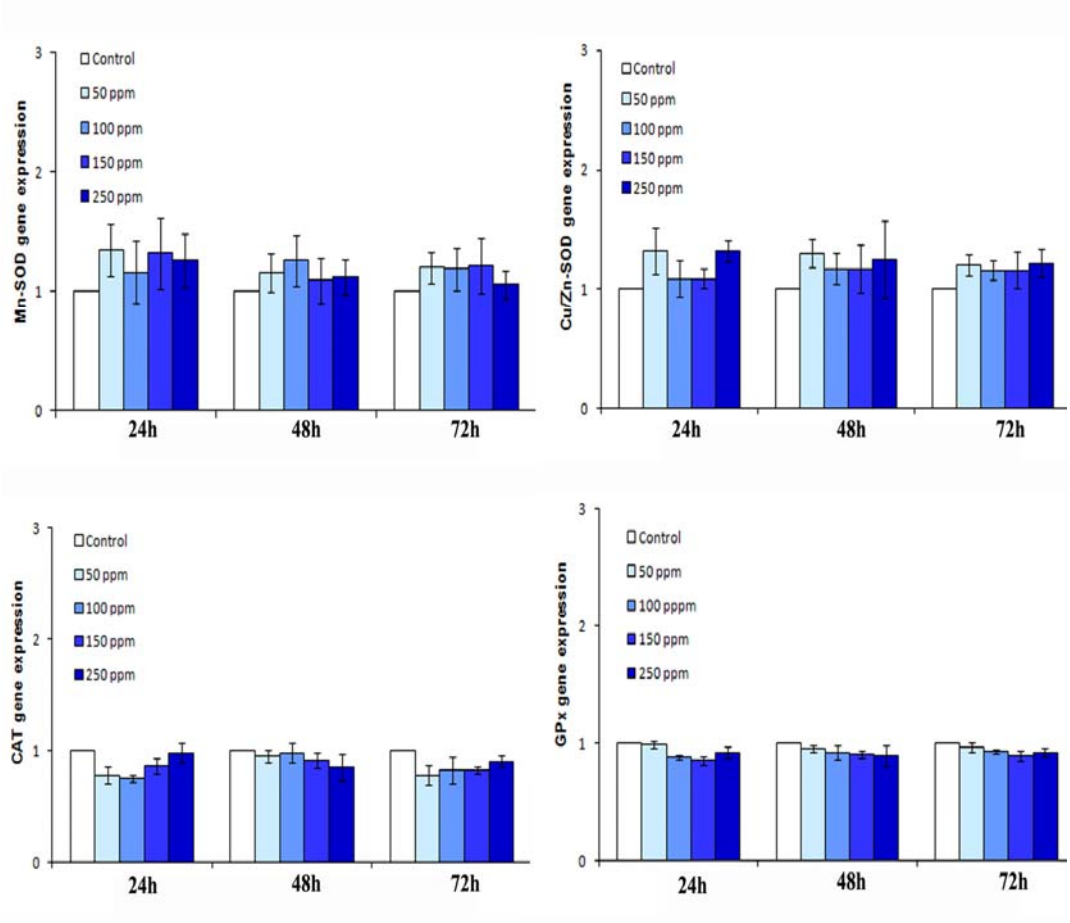

Figure 4.5: Effect of Cr(III) on the gene expression of antioxidant enzyme. U937 cells were incubated up to 72h in the presence of 0-250 ppm Cr(III). Gene expressions were measured by RT-PCR. Results are the mean ± standard deviation of 3-4 experiments.

4.4.3. Effect of Co(II)

Figures 4.6 and 4.7 show the effect of Co(II) on the expression of antioxidant enzymes. Figure 4.6A shows a representative example of the expression of proteins, while Figure 4.6B is a representative example of mRNA expression as illustrated by ethidium bromide staining of amplified sequences.

Figure 4.7 shows the semi-quantitative results of the effect of Co(II) on HO-1 expression. Results show that Co(II) had no effect on the expression of SODs, CAT, and GPx proteins (Fig. 4.6A) and mRNA (Fig. 4.6B). However, Co(II) induced a time- and dose-dependent expression of both protein and mRNA. The protein expression of HO-1 reached 0.65, 11.86, and 13.4 times the control with 10 ppm Co(II) after 24h, 48h, and 72h, respectively (Fig. 4.7A). The expression of HO-1 mRNA paralleled the protein expression with stimulation reaching 3.3, 5.9, 7.5 times the control with 10 ppm Co(II) after 72h.

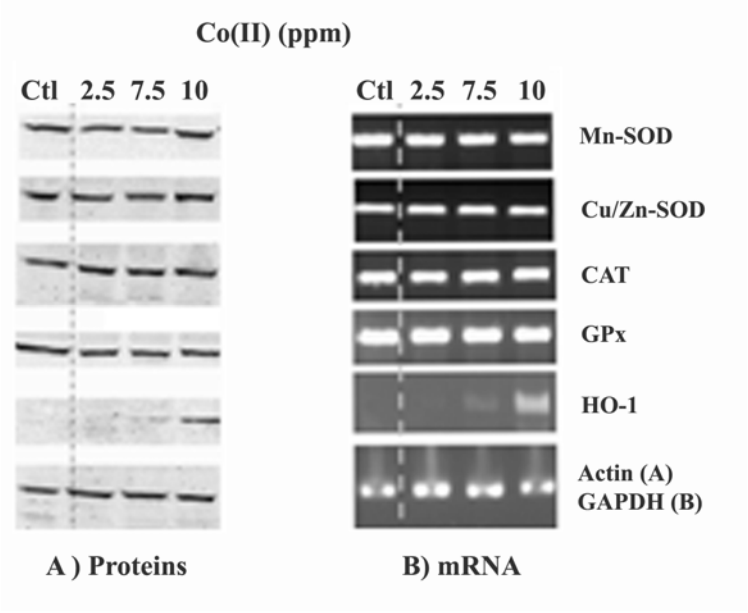

Figure 4.6: Effect of Co(II) on the expression of antioxidant enzymes. Human U937 cells were incubated for 48 h in the absence (Control) or the presence of increasing concentrations of Co(II). Protein expression (A) was measured by Western blot while mRNA expression (B) was measured by PCR. Results are representative of 3-6 experiments.

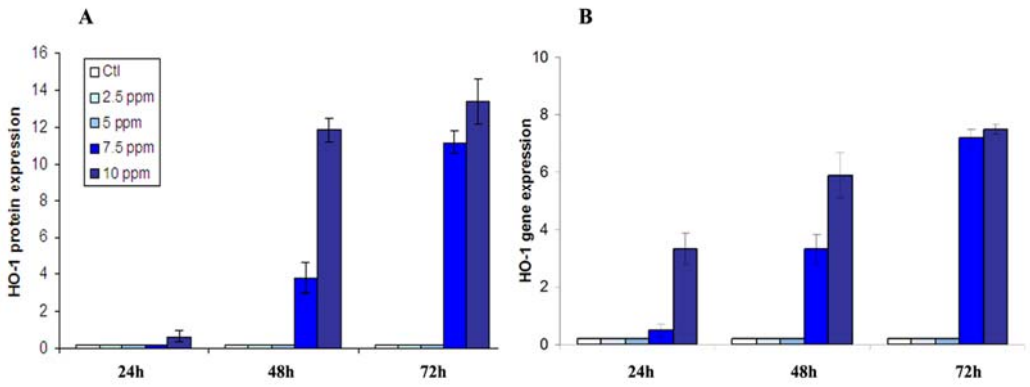

Figure 4.7: Effect of Co(II) on the expression of HO-1. U937 cells were incubated for up to 72h in the presence of 0-10 ppm Co(II). Protein expression (A) was measured by Western blot while mRNA expression (B) was measured by PCR. Results are the mean ± standard deviation of 4-6 experiments.

4.5. Discussion

Many stresses, including exposure to heavy metals, can induce damage to cells either directly or indirectly through a burst of reactive oxygen species (ROS) (20). However, mammalian cells are able to respond to elevated levels of ROS by activating their antioxidant defense systems. Results of the present study showed that Cr(VI), Cr(III), and Co(II) had differential effects on the expression of antioxidant enzymes in human U937 macrophage-like cells. More specifically, Cr(VI) induced the protein expression, but not the mRNA expression, of all the antioxidant enzymes, suggesting that several defense mechanisms are necessary to protect the U937 cells against this ion. In fact, three antioxidant groups of

molecules constitute the antioxidant defense system of the organism: the primary system prevents the formation of ROS, the secondary system eliminates radicals to prevent chain reactions, and the tertiary system works to repair damaged molecules (21). The secondary system, analyzed in the present study, is composed by Mn-SOD, Cu/Zn-SOD, and extracellular-SOD that converts superoxide radical ($\bullet O_2^-$) into hydrogen peroxide, CAT, that converts hydrogen peroxide to water and oxygen, and GPx, that converts hydroperoxide to water and oxygen (22). All these enzymes were induced by Cr(VI). Our results are in agreement with a previous study showing that long-term exposition (up to 4 weeks) to low doses of Cr(VI) induced the protein expression of SOD, CAT, and GPx in U937 cells (23). It was demonstrated that pre-stimulated macrophages, as in this study, respond to a larger extent than non-pre-stimulated cells, as in the present study (24). This implies that the concentrations necessary to induce cell response *in vitro* are more important than *in vivo* and justifies the concentrations of ions used in our study. Nevertheless, both the use of higher dose in non pre-stimulated cells or the use of repeated low doses of ions mimicking pre-stimulated cells suggests that Cr(VI) can induce the expression of antioxidant enzymes *in vitro*. Results also showed that Cr(VI) had no effect on HO-1 mRNA expression, in agreement with the lack of effect of Cr(VI) on the HO-1 mRNA expression in human airway epithelial cells *in vitro* (25).

Results also showed that Cr(III) has no effect on the expression of antioxidant enzymes (both protein and gene), suggesting that Cr(III) is less toxic than Cr(VI). In fact, most studies showed that Cr(VI) is more toxic than Cr(III)

(26). The reason for this difference of toxicity is not well known. It was however demonstrated that Cr(III) formed precipitable complexes in simulated physiological fluids, whereas Cr(VI) did not (27). Contrary to Cr(VI) which is known to enter the cells easily through anion channels (28), the Cr(III) complexes seemed to be internalized via a phagocytosis-like pathways (29) that may protect the cells from damages and may explain the difference in toxicity between the two forms of Cr.

Finally, Co(II) induced the expression of both the protein and the mRNA of HO-1, suggesting that the regulation of the expression is at the transcription level. Our results are in agreement with another study showing that $CoCl_2$ induced the expression of HO-1 mRNA in Chinese hamster ovarian cells (CHO cells) (30). Results are also in agreement with the induction of HO-1 transcription by hypochlorous acid, which is known to induce oxidative stress (31). HO-1 is a microsomal enzyme that catalyses the rate limiting step in heme degradation into carbon monoxide (CO), biliverdin, and iron with effects against apoptosis, inflammation, and oxidative stress (32). HO-1 can be induced by a variety of oxidative stress-associated agents including inflammatory cytokine, and heavy metals (33). Indeed, results suggest that the induction of HO-1 transcription may exert a cytoprotective in defense of Co(II) in human U937 macrophage-like cells. However, Co(II) had no effect on the expression of Mn-SOD, Cu/Zn-SOD, CAT, and GPx suggesting that the effects of Co(II) and Cr(VI) on ROS *in vitro* are different. The generation of these ROS by Co(II) and Cr(VI) in U937 cells remains however to be investigated. Nevertheless, our results are in agreement

with study by Kamiya *et al*, showing that Co(II) had no effect on the expression of Cu/Zn-SOD, Mn-SOD, CAT, and GPx in COS7 cells (34).

4.6. Conclusion

Using the U937 human cell lines, we have demonstrated that Cr(VI), Cr(III), and Co(II) might be involved in oxidative stress. However, their mechanism of action varies from one ion to another: Cr(VI) induced the translation of all antioxidant enzymes studied, but had no effect on their transcription. Cr(III) revealed neither effect on the transcription, nor on the translation of the same antioxidant enzymes, and finally, Co(II) had a role only on HO-1 by inducing both its transcription and translation. This might be related to a different mechanism of cellular uptake of each ion. Since Cr(III) form complexes, whereas Cr(VI) and Co(II) do not form any structure in the same experimental conditions, the mechanism would be mostly endocytosis or phagocytosis for Cr(III), as opposed to Cr(VI) and Co(II), which could mostly enter into the cell using an anion channel, generating more deleterious consequences at different cellular levels. However, because of the *in vitro* set-up (static medium without any flow) and the use of high concentrations in a ppm range, these might limit the extrapolation of *in vitro* results to *in vivo*. Ongoing research with the blood samples of patients bearing MM implants is aiming at determining the relevance of our findings in real clinical situations.

4.7. References

1. Jacobs JJ, Urban RM, Hallab NJ, Skipor AK, Fischer A, Wimmer MA. Metal-on-metal bearing surfaces. J Am Acad Orthop Surg 2009;17(2): 69-76.
2. MacDonald SJ. Can a safe level for metal ions in patients with metal-on-metal total hip arthroplasties be determined? J Arthroplasty 2004; 8:71-7.
3. Rae T. A study on the effects of particulate metals of orthopaedic interest on murine macrophages in vitro. J Bone Joint Surg [Br] 1975;57-B: 444-50.
4. Haynes DR, Rogers D, Pearcy MJ, Howie DW. The differences in toxicity and release of bone-resorbing mediators induced by titanium and cobalt-chromium-alloy wear particles. J Bone Joint Surg [Am] 1993;75-A: 825-34.
5. Hallab NJ, Merritt K, Jacobs JJ. Metal sensitivity in patients with orthopaedic implants. J Bone Joint Surg [Am] 2001;83-A: 428-36.
6. Gawkrodger DJ. Metal sensitivities and orthopaedic implants revisited: the potential for metal allergy with the new metal-on-metal joint prostheses. Br J Dermatol 2003;148: 1089-93.
7. Case CP. Chromosomal changes after surgery for joint replacement (Editorial). J Bone Joint Surg [Br] 2001;83-B: 1093-5.
8. Savarino L, Granchi D, Ciapetti, G, et al. Effects of metal ions on white blood cells of patients with failed total joint arthroplasties. J Biomed Mater Res 1999;47: 543-50.
9. Case CP, Langkamer VG, Lock RJ, Perry MJ, Palmer MR, Kamp AJ. Changes in the proportions of peripheral blood lymphocytes in patients with worn implants. J Bone Joint Sur [Br] 2000;82-B: 748-54.

10. Granchi D, Savarino L, Ciapetti G, Cenni E, Rotini R, Mieti M, Baldini N, Giunti A. Immunological changes in patients with primary osteoarthritis of the hip after total joint replacement. J Bone Joint Surg [Br] 2003;85-B: 758-64.
11. Visuri T, Pukkala E, Paavolainen P, Pulkkinen P, Riska EB. Cancer risk after metal on metal and polyethylene on metal total hip arthroplasty. Clin Orthop Relat Res 1996;329: S280-9.
12. Stohs SJ, Bagchi D. Oxidative mechanisms in the toxicity of metal ions. Free Radic Biol Med 1995;18: 321-36.
13. Spector A. Oxidative stress and disease. J Ocul Pharmacol Ther 2000;16: 193-201.
14. Petit A, Mwale F, Tkaczyk C, Antoniou J, Zukor DJ, Huk OL. Cobalt and chromium ions induce nitration of proteins in human U937 macrophages in vitro. J Biomed Mater Res A 2006;79(3): 599-605.
15. Petit A, Mwale F, Tkaczyk C, Antoniou J, Zukor DJ, Huk OL. Induction of protein oxidation by cobalt and chromium ions in human U937 macrophages. Biomaterials 2005;26(21): 4416-22.
16. Fleury C**,** Petit A**,** Mwale F**,** Antoniou J**,** Zukor DJ**,** Tabrizian M**,** Huk OL. Effect of cobalt and chromium ions on human MG-63 osteoblasts in vitro: morphology, cytotoxicity, and oxidative stress. Biomaterials 2006; 27(18): 3351-60.
17. Merritt K, Brown SA. Distribution of cobalt chromium wear and corrosion products and biologic reactions. Clin Orthop Relat Res 1996;329 (Suppl): S233-43.

18. Chomczynski P, Sacchi N. Single-step method of RNA isolation by acid guanidinium thiocyanate-phenol-chloroform extraction. Anal Biochem 1987;162: 156-9.

19. Nelea V, Luo L, Demers CN, Antoniou J, Petit A, Lerouge S, R Wertheimer M. Selective inhibition of type X collagen expression in human mesenchymal stem cell differentiation on polymer substrates surface-modified by glow discharge plasma. J Biomed Mater Res Part A. 2005;75-A(1): 216–23.

20. Stosh SJ, Bagchi D. Oxidative mechanisms in the toxicity of metal ions. Free Radical Biol Med 1995;18: 321-36.

21. Chaudière J, Ferrari-Iliou R. Intracellular antioxidants: from chemical to biochemical mechanisms. Food Chem Toxicol 1999;37(9-10): 949-62.

22. Matés JM, Sánchez-Jiménez F. Antioxidant enzymes and their implications in pathophysiologic processes. Front Biosci 1999;15(4): D339-45.

23. Raghunathan VK, Ellis EM, Grant MH. Response to chronic exposure to hexavalent chromium in human monocytes. Toxicol In Vitro 2009;23(4): 647-52.

24. S.H. Lee, F.R. Brennan, J.J. Jacobs, R.M. Urban, D.R. Ragasa and T.T. Glant, Human monocyte/macrophage response to cobalt–chromium corrosion products and titanium particles in patients with total joint replacements. J Orthop Res 1997;15: 40–9.

25. O'hara KA, Nemec AA, Alam J, Klei LR, Mossman BT, Barchowski A. Chromium (VI) inhibits heme oxygenase-1 expression in vivo and in arsenic-exposed human airway epithelial cells. J Cell Physiol 2006;209: 113-21.

26. Stasinakis AS, Thomaidis NS, Mamais D, Karivali M, Lekkas TD. Chromium species behaviour in activated sludge process. Chemosphere 2003;52: 1059–67.

27. Tkaczyk C, Huk OL, Mwale F, Antoniou J, Zukor DJ, Petit A, Tabrizian M. The molecular structure of complexes formed by chromium or cobalt ions in simulated physiological fluids. Biomaterials 2009;30: 460-7.

28. Wiegand HJ, Ottenwälder H, Bolt HM. Fast uptake kinetics in vitro of ^{51}Cr (VI) by red blood cells of man and rat. Arch. Toxicol 1985;57: 31–4.

29. Tkaczyk C, Huk OL, Mwale F, Antoniou J, Zukor DJ, Petit A, Tabrizian M. Investigation of the binding of Cr(III) complexes to bovine and human serum proteins: a proteomic approach. J Biomed Mater Res. In press, 2009.

30. Gong P, Hu B, Stewart D, Ellerbe M, Figueroa YG, Blank V, Beckman BS, Alam J. Cobalt induces heme oxygenase-1 expression by a hypoxia-inducible factor-independent mechanism in Chinese hamster ovary cells: regulation by Nrf2 and MafG transcription factors. J Biol Chem 2001;276(29): 27018-25.

31. Wei Y, Liu XM, Peyton KJ, Wang H, Johnson FK, Johnson RA, Durante W. Hypochlorous acid-induced heme oxygenase-1gene expression promotes human endothelial cell survival. Am J Physiol Cell Physiol July 22 2009, [Epub ahead of print].

32. Takahashi T, Morita K, Akagi R, Sassa S. Heme oxygenase-1: a novel therapeutic target in oxidative tissue injuries. Curr Med Chem 2004;11: 1545-61.

33. Alcaraz MJ, Fernández P, Guillén MI. Anti-inflammatory actions of the heme oxygenase-1 pathway. Curr Pharm Des 2003;9(30): 2541-51.

34. Kamiya T, Hara H, Yamada H, Imai H, Inagaki N, Adachi T . Cobalt chloride decreases EC-SOD expression through intracellular ROS generation. Free Radic Res 2008;42(11-12): 949-56.

CHAPTER 5

The Molecular Structure of Complexes Formed by Chromium or Cobalt Ions in Simulated Physiological Fluids

---

The second paper presented in this chapter, and published in *Biomaterials*, fulfills the second objective of this thesis which was to determine the molecular structures of Cr(III), Cr(VI), and Co(II) that are believed to be the origin of their toxicities.

In the first chapter, we assessed the effect of Cr(III), Cr(VI), and Co(II) on the expression of antioxidant enzymes in human U937 macrophages *in vitro*. Results suggested that Co(II) and Cr(VI) were more toxic than Cr(III). The present chapter aims at understanding this difference in toxicity. As mentioned in the Introduction (3.2.1. Metabolism of chromium), Co(II) and Cr(VI) seem to enter cells more easily than Cr(III).

We determined the molecular structure of Cr(III) nanoscale complexes. The following results present the analysis of the molecular structure of these Cr(III) complexes formed in both RPMI 1640 and DMEM high glucose media, which are commonly used in cell culture experiments and that Cr(III) can form different structures in simulated-physiological fluids.

MOLECULAR STRUCTURE OF COMPLEXES FORMED BY Cr(III) AND Co(II) IONS IN SIMULATED PHYSIOLOGICAL FLUIDS

Cathy Tkaczyk[1,3], Olga L. Huk[3,4], Fackson Mwale[3], John Antoniou[3,4], David. J Zukor[3],

Alain Petit[3], Maryam Tabrizian[1,2,4]

[1]Department of Biomedical Engineering, [2]Faculty of Dentistry,[4]Centre for Biorecognition and Bionsensors (CBB)

Duff Medical Building, 3775 University St, Montreal, QC H3A 2B4, Canada.

[3]Division of Orthopaedic Surgery, McGill University,

Lady Davis Institute for Medical Research,

The Sir Mortimer B. Davis-Jewish General Hospital,

3775 Chemin de la Côte Sainte Catherine, Montreal, QC, H3T 1E2, Canada.

5.1. Abstract

Cobalt (Co) and chromium (Cr) and their various alloys are widely used as implantable devices. Numerous studies point out elevated levels of Co and Cr ions in the serum and urine of patients with Co-Cr alloy-based articular prostheses and dental implants. It is also well recognized that workers in mines and manufacturers of hard-metals have increased risk of cancer. However, very few studies have carried out the characterization of the various chemical forms of these ions in living organisms and on their interaction with biological environments. Here, we sought to elucidate the molecular structures formed by Co and Cr ions in simulated biological fluids via transmission electron microscopy (TEM), energy dispersive X-ray analysis (EDXA), Fourier transform-infrared (FT-IR) spectroscopy, and X-ray photoelectron spectroscopy (XPS). TEM observation revealed that Cr^{3+} (or Cr(III)) formed nanoscale complexes which precipitate in both RPMI 1640 and DMEM high glucose. However, no complexes were observed with Co(II) and Cr(VI). EDXA, elementary analysis and FT-IR spectroscopy investigations showed that the Cr(III)-complexes contain phosphate ions and amino acids. In addition, FT-IR spectrum indicated that Cr(III) ions are not a form of "amino acid trap" but a real chelating entity between PO_4 groups, amino acids, and Ca. Although the exact nature of the bonds remains to be investigated, the presence of PO_4 may favour the formation of low energy hydrogen bonds. Interestingly, the nature of amino acids varied in Cr(III)-complexes formed in RPMI 1640 compared to those formed in DMEM high glucose. The absence of sulphur in the elemental analysis spectrum suggested that

amino acids containing sulphur such as methionine or cystine, are not involved in the formation of Cr(III)-complexes. Since it is known that Cr(III) is less toxic than Co(II) or Cr(VI), and that only Cr(III) ions can form complexes with media, the lower Cr(III) ion toxicity may be related to the formation of chemical complexes. These results may bring some insight in understanding the relationship between toxicity and the chelating capabilities of various metal ions *in vitro* and *in vivo*.

5.2. Introduction

Chromium and Cr alloys has been in widespread commercial use for over 100 years and several million workers worldwide are exposed to airborne fumes, mists, and dust and other components containing Cr and Co (1). Cobalt is used to make corrosion and wear-resistant alloys for aircraft engine, magnets, and in high-strength steels (2). Good mechanical and physicochemical properties, and particularly the high corrosion resistance of Co-Cr alloys, also make them very suitable for surgical devices and implants (3). Among the most popular medical applications of Co-Cr alloys is their use in total hip arthroplasty (THA) armamentarium.

Several studies have shown the presence of cobalt and chromium ions in blood, urine, and in the organs of patients after THA using Co-Cr alloy-based implants (4-8). It is also well recognized that individuals working in hard-metal production facilities have increased risk of cancer (9). This is due to the fact that ions with variable degrees of oxidation such as Cr can undergo slow oxidation, resulting in the release of higher oxidative forms, such as Cr(VI) (10, 11), which

is a human carcinogen, primarily affecting the respiratory tract (12). A generally accepted mechanism of Cr(VI)-induced genotoxicity includes the active transport of Cr(VI) into cells through ion channels for water soluble chromates or by phagocytosis of insoluble chromates (13). Inside cells, Cr(VI) undergoes reduction via a process associated with the production of unstable Cr(V), Cr(IV),Cr (III) ions, and organic radicals (14-16). Cr(V) and Cr(VI) are able to link to amino acids during their reduction step by the thiol group of glutathione (17). However, phosphate groups are necessary for the interaction of Cr(III) with DNA (18). Nevertheless, the biological significance of these complexes is difficult to assess because of their unknown composition.

Literature has also reported on the cytotoxic effects of Co ions on/in macrophages (19,20) and osteoblasts (21). In fact, the toxicity of Co(II) is much higher than the toxicity of Cr(III), 25 times less Co(II) being necessary to generate the same level of toxicity within cells. Moreover, Co(II) induces the oxidation (22) and the nitration (23) of proteins, which both contribute to cell damage (24,25), with a higher potency than Cr(III).

Although many reports are available on the biological and toxic effects of Co and Cr *in vitro,* there has been little or no attempt to determine the chemical form of implant-derived metal ions in adjacent tissues or in biofluids. We hypothesized that Cr(III) interacts in a different way with cells as a consequence of its interaction with cell membranes compared to Co(II) and Cr(VI), and thereby affects the cell viability in a different manner. We used two different types of cell culture media namely RPMI 1640 and DMEM high glucose media, to determine

the nature of the media interaction with Co and Cr ions as a mean to simulate biological fluids. Transmission electron microscopy (TEM) was used to visualize any Co or Cr complexes formed with the cell culture media Fourier transform-infrared (FT-IR) spectroscopy and high resolution X-ray photoelectron spectroscopy (XPS) were employed to identify the chemical structure of the complexes.

5.3. Materials and Methods

5.3.1. Materials.

Cr (III) and Cr (VI) ($CrCl_3$ and Na_2CrO_4 respectively) were purchased form Sigma-Aldrich (Oakville, ON, Canada) and Co(II) ($CoCl_2$), $CrPO_4 \bullet xH_2O$ and amino acids were supplied by Fisher Scientific (Ville St-Laurent, QC, Canada). RPMI 1640 and DMEM high glucose media were obtained from Hyclone (Logan, UT). The media composition and content are reported in Table 3. Both media were chosen in function of their composition similarity with physiological fluids. They are commonly used to harvest prostheses surrounding cells and to assess the different metallic ions toxicity.

	DESCRIPTION	RPMI (mg/L)	DMEM (mg/L)
INORGANIC SALTS	$Ca(NO_3)_2 \cdot 4H_2O$ $CaCl_2$ (anhydrous) $Fe(NO_3) \cdot 9H_2O$ KCl $MgSO_4$ NaCl NaH_2PO_4 (anhydrous) $NaH_2PO_4 \cdot H_2O$	100.00 **0** **0** 400.00 48.84 6000.00 800.00 **0**	**0** 200.00 0.10 400.00 97.67 6400.00 **0** 125.00
AMINO ACIDS	L-Arginine L-Asparagine L-Aspartic Acid L-Cystine 2HCl L-Glutamic Acid L-Glutamine Glycine L-Histidine FB L-Hydroxyproline L-Isoleucine L-Leucine L-Lysine HCl L-Methionine L-Phenylalanine L-Proline L-Serine L-Threonine L-Tryptophan L-Tryosine $2Na \cdot 2H_2O$ L-Valine	200.00 50.00 20.00 65.15 20.00 300.00 10.00 15.00 20.00 50.00 50.00 40.00 15.00 15.00 20.00 30.00 20.00 5.00 28.83 20.00	84.00 **0** **0** 62.57 **0** 584.00 30.00 42.00 **0** 104.80 104.80 146.20 30.00 66.00 **0** 42.00 95.20 16.00 103.79 93.60
VITAMINS	d-Biotin D-Ca Pantothenate Choline Chloride Folic Acid Myo-Inositol Niacinamide Pyridoxine HCl Riboflavin Thiamine HCl Vitamin B-12	0.20 0.25 3.00 1.00 35.00 1.00 1.00 0.20 1.00 0.0050	**0** 4.00 4.00 4.00 7.00 4.00 4.00 0.40 4.00 **0**
OTHER	D-Glucose Para-Aminobenzoic Acid Glutathione(Reduced) Phenol Red (Sodium) $NaHCO_3$	2000.00 1.00 1.00 5.30 **0**	4500.00 **0** **0** 15.90 3700.00

Table 3: Formulations of RPMI 1640 and high glucose DMEM media.

5.3.2. Isolation of Co(II), Cr(III), and Cr(VI) complexes

Fifty (50) ppm of Cr (III), Cr (VI) and Co(II) ($CoCl_2$) were incubated separately for 1h at 37°C in 1 mL of RPMI 1640 or DMEM high glucose. After incubation, structures were isolated by centrifugation at 5000 x *g* for 20 min, washed 3 times with water and once with ethanol (EtOH). Pellets were dried for 4h at 18°C and resuspended in different volumes of EtOH (10 to 100 µl).

5.3.3. Electron Microscopy Analyses

One drop of isolated precipitates was deposited on a copper grid, dried, and then analyzed by transmission electron microscopy (TEM) using a JEOL 2000FX TEM (Akishima, Tokyo, Japan) at an accelerating voltage of 80 kV. Isolated precipitates were processed for field-emission-gun scanning electron microscopy (Feg-SEM, S-3000N Variable Pressure, Hitachi, Japan) at an accelerating voltage of 20 kV. Samples were critical-point dried, mounted on aluminum pin stubs, and coated with a 5-nm layer of platinum-palladium. Platinum-palladium coating was assessed using an Agar Scientific high-resolution sputter fitted with an Agar Scientific thickness monitor.

5.3.4. Energy Dispersive X-Ray Analysis (EDXA)

Qualitative analysis of the elemental composition of isolated precipitates was performed using an energy-dispersive spectrometer (Princeton Gamma Tech, Princeton, NJ, USA) equipped with an ultrathin window for the detection of low

atomic number elements. Data acquisition time was set at 100 sec and 20 spectra were collected with a take-off angle of 70°.

5.3.5. Fourier Transform-Infra-red Spectroscopy

Fourier transform-infrared (FT-IR) spectroscopy, in both transmittance and reflectance (ATR) modes, was performed to obtain the IR spectra of isolated precipitates along with the spectrum of each amino acid present in the cell culture media used as a control (Table 3). One drop of the precipitate in ethanol was deposited on a zinc-selenium (ZnSe) slide (75mm×25mm×1mm) and examined with a UMA-600 infrared microscope (Digilab, Randolph, MA, USA) coupled to a charge-coupled device CDD camera. FT-IR analyses was performed using a Digilab Excalibur imaging spectrometer equipped with a Digilab UMA-600 infrared microscope with a 32×32 mercury-cadmium-telluride (MCT) focal plane array detector with a cut-off at 950 cm^{-1} and operating under Win-IR Pro 3.3 software. All spectra were collected by co-adding 256 scans at a resolution of 8 cm^{-1} from 4000 to 950 cm^{-1} and were normalized against a background spectrum recorded from a bare section of the microscope slide. A constant flow of dry air was used to purge the spectrometer and the microscope in order to limit spectral contributions from carbon dioxide and atmospheric water vapor. A focal plan area (FPA)-FT-IR spectrometer equipped with an n×n array detector (n^2 pixels) collects data simultaneously from n^2 spatially adjacent points within the microscope's field of view. A total of 1024 spectra were recorded simultaneously

from an area of 180 μm×180 μm, corresponding to a spatial resolution of about 5.6 μm, in a total acquisition time of about 2 min.

5.3.6. Elemental Analysis

Elemental analysis was performed by carbon, hydrogen, nitrogen, sulphur (CHNS) dynamic flash combustion on a Fison EA 1108 (Fison Instruments, Rodano, Italy).

5.3.7. X-ray Photoelectron Spectroscopy (XPS)

The X-ray photoelectron spectroscopy (XPS) experiments were performed using a VG Scientific ESCA LAB MK-II spectrometer equipped with a magnesium-aluminium (Mg–Al) X-ray spectroscope (Thermo Electron Corporation, Waltham, MA, USA). Only an Al excitation source was used, selected for its ultrahigh-energy resolution (300W, 15 kV, 1486,6 eV).

The basal pressure in the sample chamber was controlled in the range of 10^8 to 10^9 Torr. Emitted photoelectrons were collected from an approximately 3 mm diameter circle of the sample. High-resolution spectra were recorded at a take-off angle of 0° by a concentric hemispherical analyzer operating in the constant-pass-energy mode.

5.4. Results

Figure 5.1 shows TEM micrographs of ion complexes formed in cell culture media. The presence of vesicle-like complexes in the nanoscale range

were observed with Cr(III) in both RPMI 1640 and DMEM high glucose (Fig. 5.1A and B, respectively), whereas no such structures were identified with Cr (VI) and Co(II).

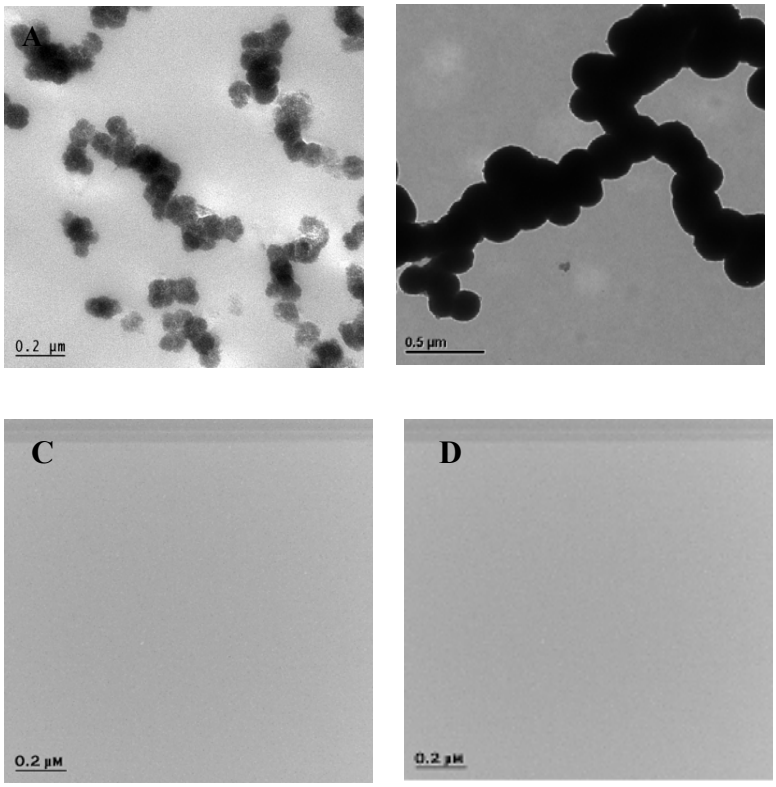

Figure 5.1: Formation of ion complexes in cell culture media. Complexes obtained with Cr(III) in RPMI 1640 (A) or in DMEM high glucose (B) and with Cr(VI) (C) and Co (D) in RPMI 1640 were analyzed by TEM. Magnification: x 85000.

We cannot however exclude the formation of Co(II) and Cr(VI) complexes smaller than 0.4 nm, which is the sensitivity limit of TEM. The Cr (III) complexes in RPMI 1640 were smaller (Fig. 1A) than those in DMEM high

glucose (Fig. 5.1 B) (~60 nm vs. 100 nm). FEG-SEM studies confirmed the formation of the Cr(III) complexes in RPMI 1640 (Fig. 5.2A) and in DMEM high glucose (Fig. 5.2B) with similar aspects.

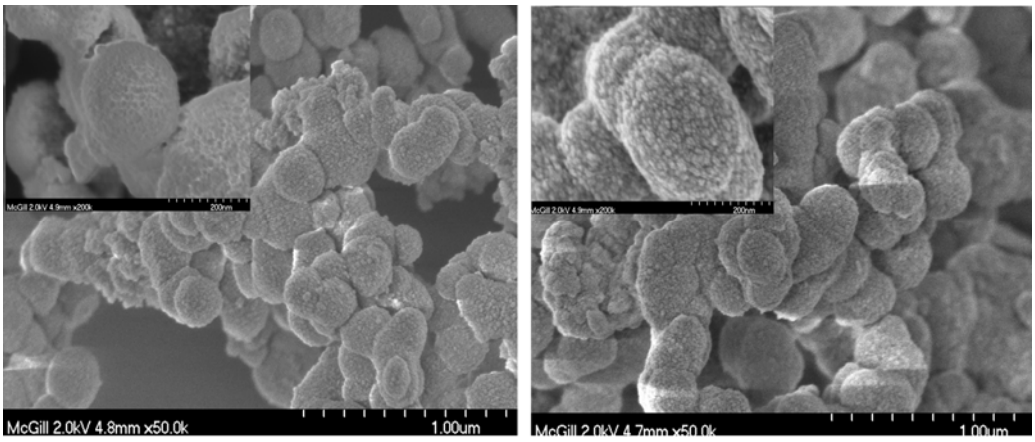

Figure 5.2: FEG-SEM pictures of Cr(III) complexes. Nanoscale complexes were formed in both RPMI 1640 (left) and DMEM high glucose (right). Pictures show agglomeration of complexes at 10k magnification. Inlet shows a higher magnification (200k) of complexes. However, closer examination of complex morphology revealed a slight variation between the two types of complex. Cr (III) complexes formed in DMEM show increased surface roughness.

EDXA spectra of Cr(III)-complexes isolated from RPMI 1640 (Fig. 5.3) and from DMEM high glucose (Fig. 5.3B) media showed similar structural composition. The major peaks in these spectra corresponded to Cr, phosphate (PO_4), and calcium (Ca), indicating an interaction between Cr(III), Ca, and PO_4 present in the media allowing complex formation. In addition, the EDXA spectra

taken from numerous points on the complexes showed identical patterns, suggesting that the complex composition is homogenous.

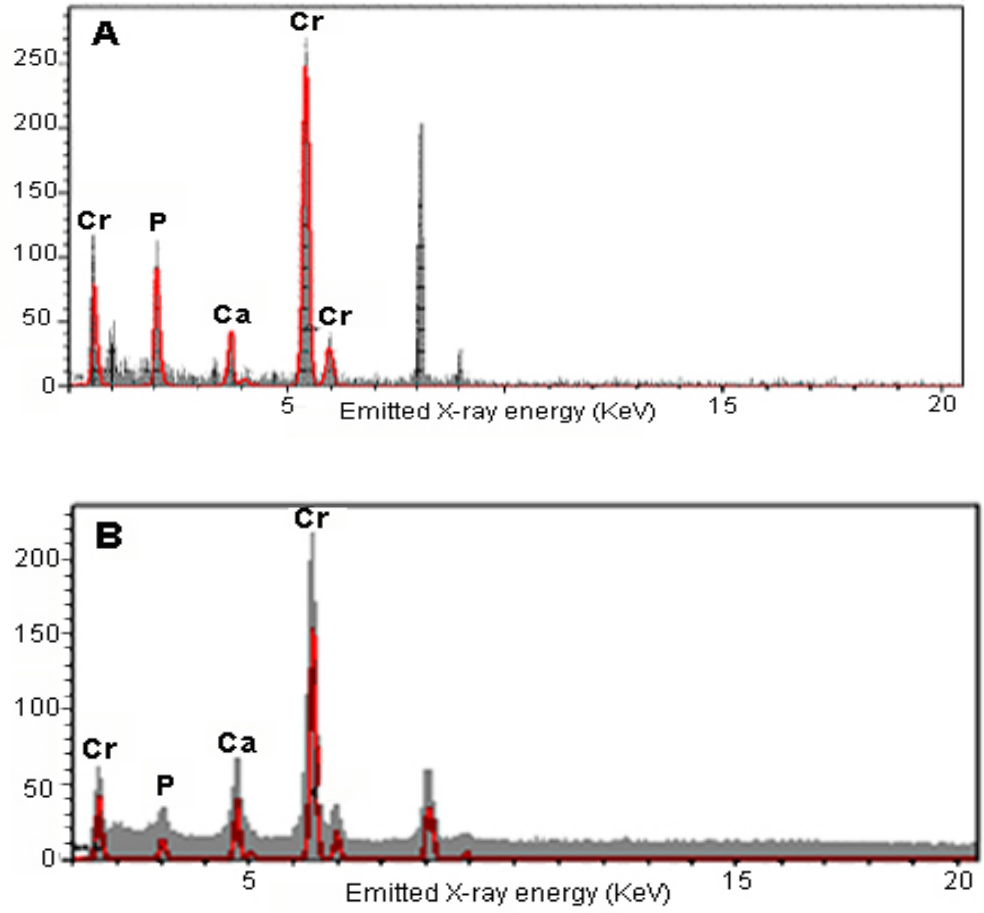

Figure 5.3: Heavy atoms present in Cr(III) complexes. Cr(III) complexes prepared in RPMI 1640 (A) and in DMEM high glucose (B) were analyzed by EDXA. Copper peaks visible on the right of the spectra (8-9 keV) are generated by the grids

Transmittance FT-IR spectroscopy was then used to further characterize the composition and compare the Cr(III) complexes formed in RPMI 1640 and DMEM high glucose (Fig. 5.4).

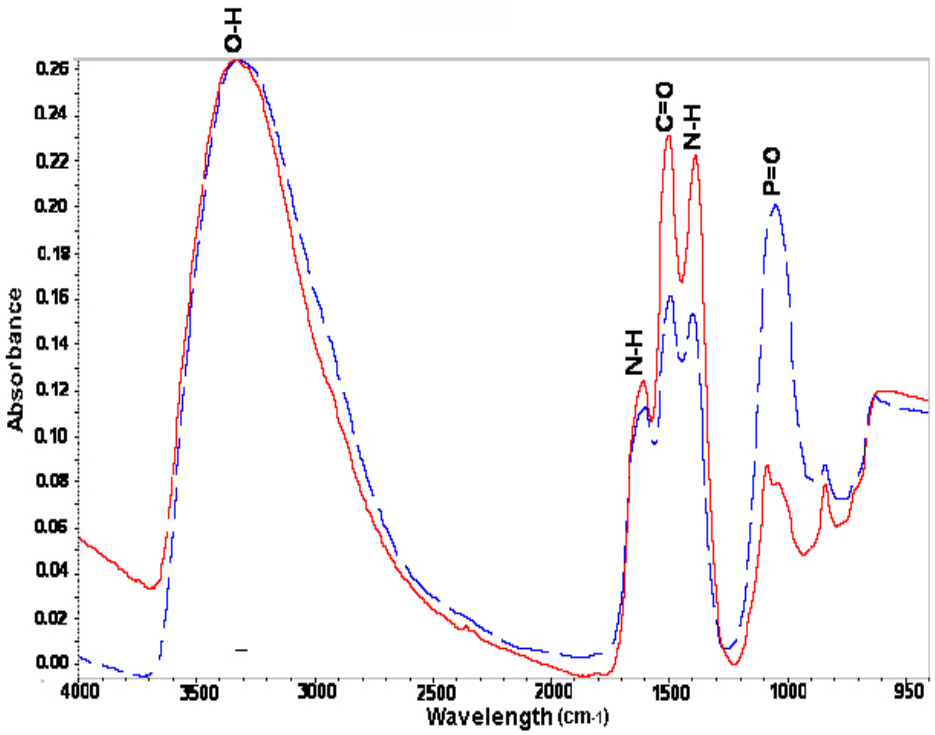

Figure 5.4: Analysis of Cr(III)-complexes by transmittance FT-IR. Spectra were obtained for structures prepared in RPMI 1640 (dashed line) and in DMEM high glucose (full line).

Spectra showed the presence of P=O groups at 1040 cm^{-1} and the presence of three peaks characteristic of amino acids at 1395 cm^{-1}, 1500 cm^{-1}, and 1602 cm^{-1}, corresponding respectively to N-H, C=O, and N-H bonds. The presence of the O-H stretch (2770 cm^{-1} to 3650 cm^{-1}) corresponded to moisture from the air. The results indicated the presence of both amino acids (organic phase) and PO_4 groups

(inorganic phase) in the Cr(III)-complexes formed within the two media. The spectra also showed that the intensity ratio of P=O/amino acids was different for complexes obtained in RPMI 1640 and in DMEM high glucose. This may be related to the higher concentration of PO_4 found in RMPI 1640 (800 mg/L) compared to DMEM high glucose (125 mg/L). Finally, the smoothness of the curves suggested that amino acids were chemically bound to Cr(III), but not free in the complexes. The polynomial baseline correction of the FT-IR results confirmed the presence of amino acids in Cr(III)-complexes with characteristic peaks of C-H bonds at 1640 cm^{-1}, 2840 cm^{-1}, 2940 $cm^{-1}$and 2900 cm^{-1} in RPMI, and at 2935 cm^{-1}, 2920 cm^{-1} and 2860 cm^{-1} in DMEM high glucose (results not shown).

In order to further determine the contribution of PO_4 in forming Cr(III)-complexes, FT-IR was used to compare Cr(III)-complexes and commercial chromium phosphate. Results showed that the peak corresponding to P=O in Cr(III)-complexes (Fig. 5A and 5B) had the same aspect and wavelength than the peak of P=O in $CrPO_4$ (Fig. 5C), suggesting that Cr(III) is covalently bound to PO_4.

Complementary to FT-IR, elemental analysis not only confirmed the implication of amino acids in the formation of the Cr(III)-complexes but also allowed determination of the percentage of nitrogen (N), carbon (C), hydrogen (H), and sulphur (S) in this nanoscale structure (Table 4).

50 ppm Cr(III) in RPMI 1640		50 ppm Cr(III) in DMEM high glucose	
Nitrogen (%)	1.34 ± 0.4	Nitrogen (%)	1.71 ± 0.4
Carbon (%)	7.85 ± 0.4	Carbon (%)	6.21 ± 0.4
Hydrogen (%)	3.60 ± 0.4	Hydrogen (%)	3.74 ± 0.4
Sulphur (%)	0	Sulphur (%)	0
C/N	5.85 ± 0.2	C/N	3.63 ± 0.2

Table 4: Elemental analysis of nitrogen, carbon, hydrogen, and sulphur in Cr(III) complexes. Results are presented as the % of atoms present in the structures

Results showed similar chemical compositions, but not identical concentrations of N, C, and H in the two media. The C/N ratio was higher in the complexes formed in RPMI 1640 (C/N = 5.85) than in that formed in DMEM high glucose (C/N = 3.63). Since the percentage of H present is difficult to evaluate by this technique due to the presence of moisture, the C/H ratio was not taken into account in the calculation. Interestingly, the absence of sulphur suggests that amino acids containing sulphur, such as methionine or cystine, are not involved in the formation of Cr(III) complexes.

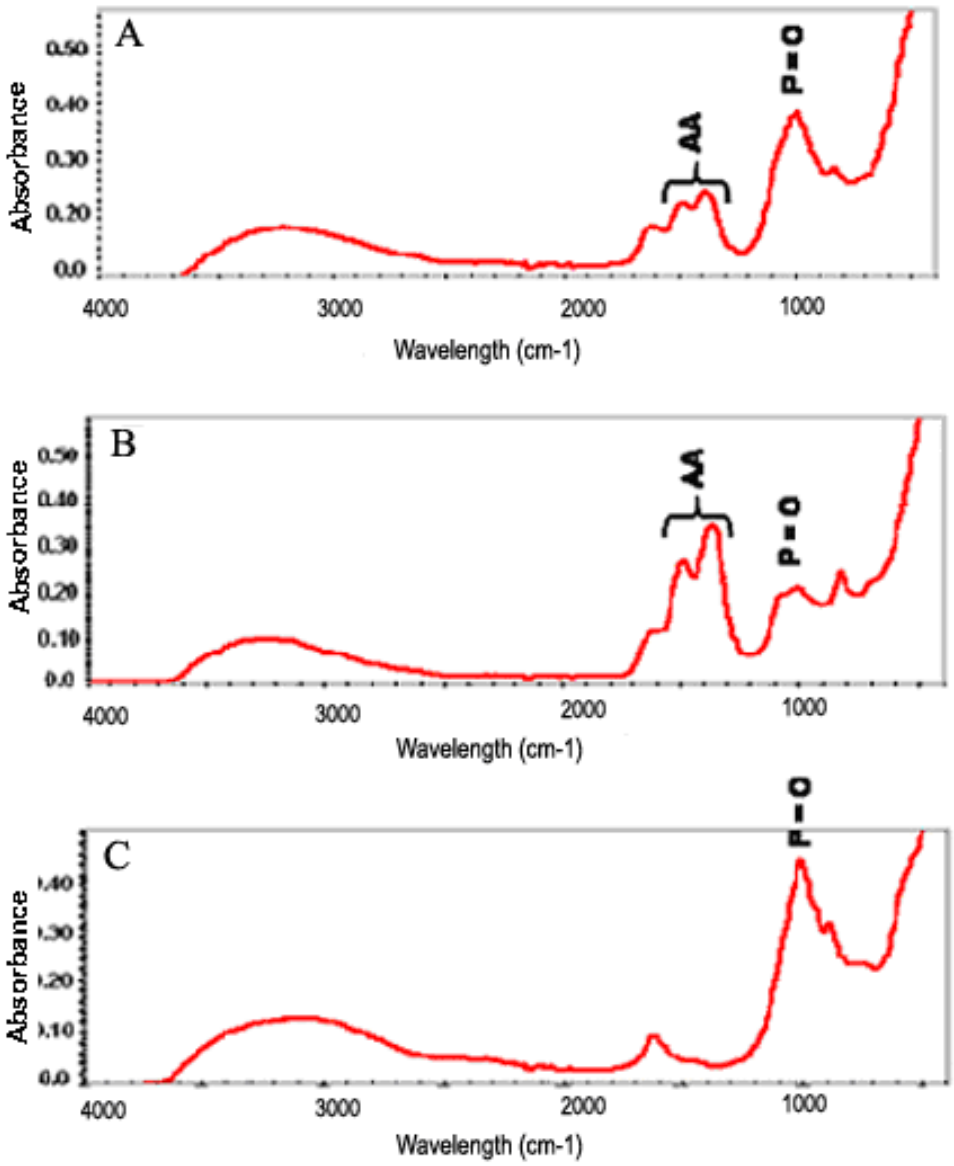

Figure 5.5: Analysis of Cr(III)-complexes by ATR FT-IR. Cr(III) complexes obtained in RPMI 1640 (A) and DMEM high glucose (B) were compared to $CrPO_4$ (C). AA: amino acid characteristic pics.

To show the chelating role of Cr(III) governing the formation of complexes in cell culture media, nanoscale structures containing various

concentrations of Cr(III) have been isolated from media and then weighted. The linearity of the results showed that the amino acids and PO_4 were in sufficient concentrations to interact with Cr(III) up to 500 ppm in both RPMI 1640 and DMEM high glucose (Fig. 5.6). This also suggests that the formation of the complexes was only limited by the concentration of Cr(III) and not by the availability of various components of the media.

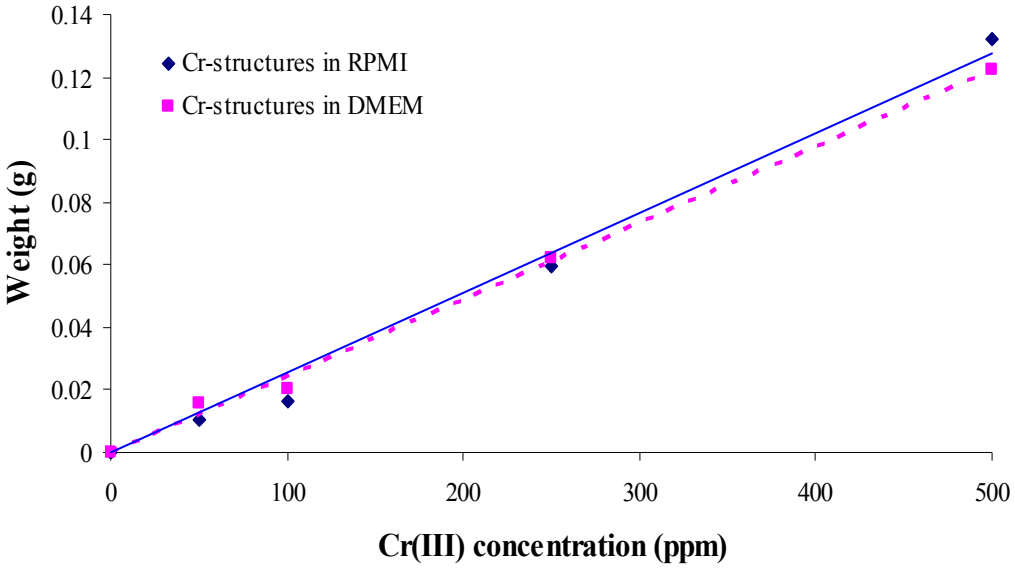

Figure 5.6: Effect of the concentration of Cr(III) on the weight of Cr(III) complexes. RPMI 1640 (R^2=0.989) and DMEM high glucose (R^2=0.997) media were incubated with Cr(III) from 0 to 500 ppm. Pellets obtained after centrifugation were air dried and weighted.

X-ray photoelectron spectroscopy (XPS) analysis confirmed the presence of Cr, Ca, N, and phosphorus (P) in the Cr(III)-complexes, as well as the presence

of sodium (Na) and chlorine (Cl), but in different ratios (Fig. 5.7, Table 5). The presence of oxygen in the survey spectrum was attributed to the presence of moisture and therefore has not been taken into account in the calculation. Cr and Cl were predominant, followed by N and P. Table IV reports on the presence of C-N, N-H, C-C, and P-O bond displacements and their relative ratios as identified by high resolution XPS (spectra not shown) confirming once more the role of Cr(III) in chelating amino acids and PO_4 and to form nanoscale structures.

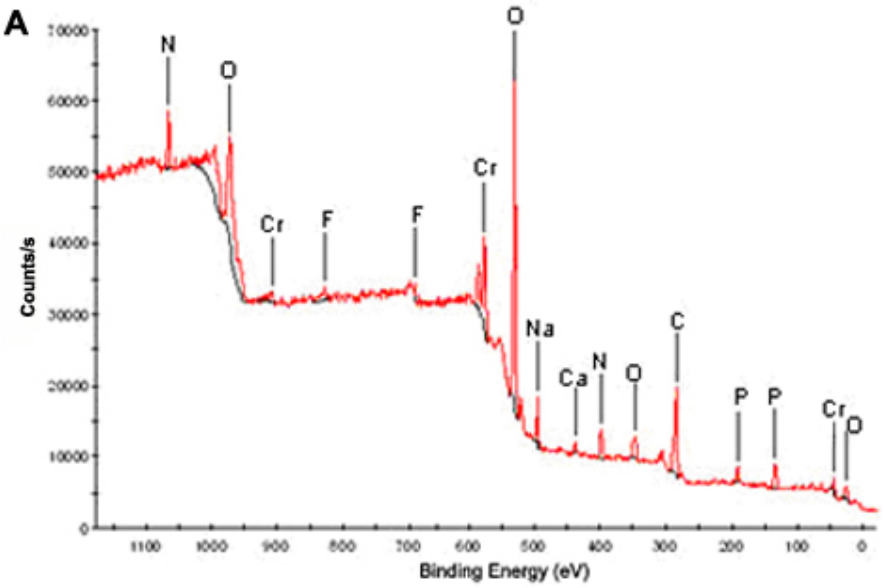

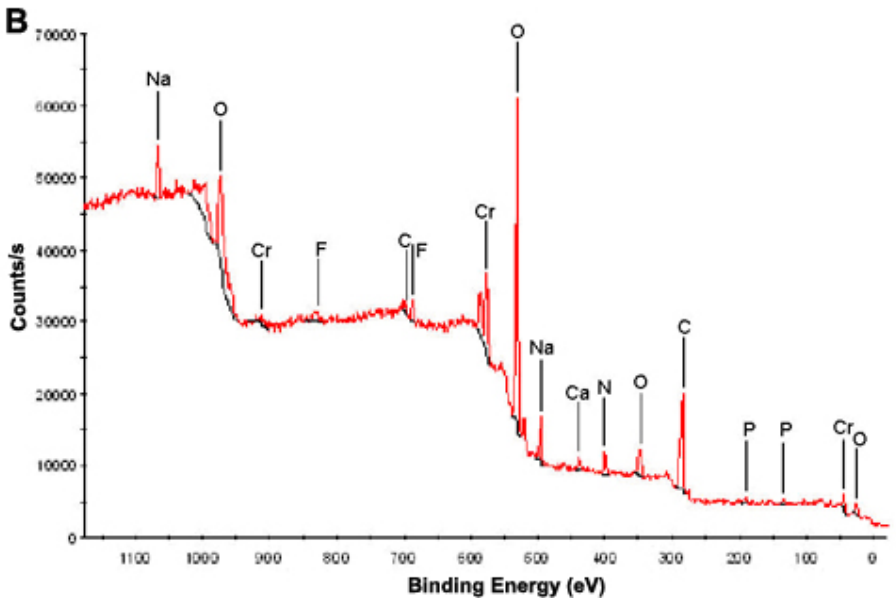

Figure 5.7: X-ray photoelectron spectroscopy analysis of Cr(III) complexes. Spectra were obtained from complexes formed in both RPMI 1640 (A) and DMEM high glucose (B). Spectra show the presence of Cr, Na, P, C and O.

Element	Binding Energy	Relative %atom		Sensitivity Factor
	(eV)	**DMEM**-Cr(III) complexes	**RPMI**-Cr(III) complexes	
Na	1067	3.0	3.1	2.30
Cl	285	39.19	34.56	1.00
Cr	576	6.0	5.5	2.30
O	531	42.6	44.7	0.66
N	400	4.4	5.5	0.42
Ca	347	1.9	1.3	1.58
C	285.0	39.2	34.6	0.25
P	134	1.0	4.1	0.39

Table 5: Atoms present in Cr(III) complexes. Table summarizes the results obtained by XPS (Figure 5.7) and shows the different elements present in the DMEM and RPMI nanostructures (noticed DMEM Cr(III) complexes and RPMI-Cr(III) complexes in the table 5 and their relative amount. Sensitivity factor are

dependent various factors, the well-known parameters include the intrinsic properties of the elements (cross section of different orbits of different elements), illumination condition and analyzer transmission (instrument geometry and analyzer setting), and the sample (surface) itself. Each element has its atomic sensitivity factor (indicated in the table).

Name of peak	Binding Energy	Identification	Relative % atomic	
	(eV)		Cr(III) complexes formed in DMEM	Cr(III)-complexes formed in RPMI
C1	285.0	C-C	14.2	17.0
C2	285.9	C-O; C-H ; C-N	17.1	18.0
C3	287.0	C=O ; C_6H_5NH	6.0	4.1
C4	288.8	C=O	2.8	2.8
O1	531.8	P-Ox ; Cr-O	12.1	17.1
O2	532.8	PO_4 ; C=O	21.4	15.4
O3	533.9	C-O	4.7	3.3
Ca	348.5	Ca CO_3	2.5	2.3
N1	399.8	Cr-N ; C-N	0.7	0.3
N2	400.9	C-NH	1.7	1.4
N3	401.7	NH_4^+	1.3	-
N4	402.3	NH_4^+ ; N_2	-	0.6
N5	406.4	R-NO_3	-	0.2
Cr	578.4	Cr-O_x	8.1	6.8
P1	135.9	P-O	-	3.9
P2	137.3	?	-	0.6

Table 6: Nature of the atomic bounds in the Cr(III) complexes. Results were obtained by high resolution XPS of Cr(III)-nanostructures formed in both RPMI 1640 and DMEM high glucose and show the signification of the most important peaks (results not shown) and their relative concentration.

5.5. Discussion

Few publications to date have focused on the characterization of the chemical nature of implant-derived metal ions in biofluids, relating the chemical structure to their relative toxicity. The present work is an attempt to characterize the molecular structure of Co(II), Cr(III) and Cr(VI) in simulated biological fluids.

It is known that cobalt-chromium metallic implants release cobalt and chromium ions in organism, by the natural corrosion process. However, a complexation phenomenon is instantaneous, making impossible to extract implant-derived metal ions *in vivo*, before their involvement in any chemical process. Although commercial ions are used in this study, they are similar to those generated from metallic surfaces.

We showed that of the group only Cr(III) could form insoluble nanoscale complexes by interacting with the media components after centrifugation (5000 x g, 20 min). The absence of precipitate with Co(II) and Cr(VI) was persistent even though harsher experimental conditions were used (i.e. 16000 x *g* for 40 min centrifugation). The Cr(III) complexes could not be dissolved in either acidic or basic solutions. Solution pH has been modified in order to obtain a large range of pH from basic to acidic by adding respectively NaOH or HCl. For further investigations, isolated complexes were immerged in pure NaOH or HCl. No solubilisation was observed. Polar and non-polar organic solvents also failed to dissolve the precipitates. 27 solvents with different polarities have been used from 0.043 solvent polarity parameter (triethylamine) to 1.00 (water), including

common solvents such as toluene (0.099), chloroform (0.259), acetone (0.355), methanol (0.762) and more specifically solvents such as dioxane (0.164) hexamethylphosphoramide (0.315) or methoxyether (0.667). The low solubility of the complexes caused some limitations when using liquid phase analytical methods for characterization of the complex (NMR for example).

Our results, which are mostly based on solid phase characterization of the complexes, indicated that Cr(III) binds PO_4, Ca, and amino acids in cell culture media . Complexes with a size ranging from 70 nm to 100 nm are formed in RPMI 1640 and DMEM high glucose, respectively. This finding is in agreement with the work of Zhikovitch *et al* who showed the formation of chemically inactive $CrPO_4$ in phosphate buffer containing Cr(III) (26).

Some studies showed that $CrPO_4$ compounds have been found in tissues surrounding orthopaedic implants (27). Other studies have demonstrated that Cr(III) interacts with DNA and that the PO_4 groups were necessary for that interaction (28). Cr-DNA could be formed as a ternary complex involving amino acids or glutathione bridges (29). These findings support our hypothesis concerning the interaction of Cr, PO_4, and amino acids for the formation of Cr(III)-complexes in both RPMI 1640 and DMEM high glucose. Since the concentration of amino acids was 100 times higher than the concentration of vitamins in the media, it is highly unlikely the vitamins are significantly involved in the formation of these complexes, if at all.

In order to define the exact molecular structure of the Cr(III)-complexes, crystallization assays with various solvents were performed. X-ray diffraction

analysis showed that at the most only 33% crystallization of the complexes can be achieved in cell culture media. Our attempt to match the crystal structure with one of those available in the latest X-ray database failed. Elemental analysis however clearly indicated that the amino acids composition of the Cr(III)-complexes formed in RPMI 1640 is significantly different than the one formed in DMEM high glucose. Ratio of 5.81 for C/N is obtained in RPMI 1640 media, while a ratio of 3.63 was observed in DMEM high glucose (Table 4).

Considering the types of amino acids and their respective concentrations, only three combinations of amino acids could correspond to the C/N ratio in the RPMI 1640 Cr(III)-complexes:, 1) phenylalanine, proline, serine, and tryptophane for a C/N=5.85; 2) tyrosine, proline, serine, or tryptophane for a C/N=5.85; and 3) phenylalanine, tyrosine, serine, and tryptophane for a C/N=5.88. Furthermore, the C/N ratio in DMEM high glucose could be represented by the following two combinations of amino acids: 1) aspartic acid, threonine, valine, serine, and isoleucine/leucine for a C/N=3.75; 2) aspartic acid, threonine, valine, serine, and glutamic acid for a C/N=3.60. The presence of C_6H_5 groups in high resolution XPS spectrum (Table 5) suggests that the likely involvement of phenylalanine or tyrosine in the formation of complexes.

Since the 256 scans of FPA-FT-IR at a single point, on 30 different spots of the samples having a diameter of 1 cm (vs. ~70 nm for the Cr(III)-complexes) had the same profile, we can conclude that the chemical composition as defined by the C/N ratios are representative of the overall Cr(III)-structures. In addition, the aspect of the FT-IR spectrum indicated that Cr(III) ions are not a type of

"amino acids trap" but a chelating entity between PO_4 groups, amino acids, and Ca. Although the exact nature of the bonds remains to be investigated, the presence of PO_4 may favour the formation of low energy hydrogen bounds. The efficacy of a given metal as a chelating agent in a biological system depends on the binding constants of the chelator, the concentration of the metals, and the presence and concentrations of other ligands competing for binding with the chelating metal. In our case, it seems that Cr(III) ions are better chelating agents than Co(II) or Cr(VI) ions in biological media under our experimental conditions. Our results are in agreement with some studies reporting on the higher chelating ability of Cr(III) compared to that of Co(II) and Cr(VI) (30,31). This is extremely interesting because chelation is a very important process in biology. Chelating therapy, for example, could be used as a medical treatment of thalassaemia, which is a genetic disease that interferes with a person's ability to make hemoglobin (32).

The presence of Ca, coming from inorganic salts available in high concentration in RPMI 1640 (100 mg/L of $Ca(NO_3)_2$) and in DMEM high glucose (200 mg/L of $CaCl_2$), is another interesting finding. Indeed, this is in agreement with the study of Harris *et al* (33) that showed a strong co-localization of Cr with Ca in small areas of cytoplasm in A549 human lung adenocarcinoma epithelial cells.

pH also seems to play a role in the formation of Cr-complexes. The pH of the two chosen media is slightly basic, which precipitates both Cr(III) complexes and commercial $CrPO_4$. In fact, amino acids are zwitterions (PKa of COOH is

between 1.8 and 2.2 and PKa of NH_2 is between 8.8 and 10.6) resulting in a major concentration of COO^-. Since Cr(III) has a strong affinity towards O^-, it interacts either with PO_4 groups or with the carboxylic groups of amino acids. Also, both glutamic acid and aspartic acid have their side chain negatively charged (PKa of COOH side chain = 4.7) at the pH of the media. This would allow a strong interaction between the Cr ions and these amino acids via the COO^- group in DMEM high glucose media. This may also explain the difference in the morphology of complexes formed in the two different media, as observed by TEM (Fig. 5.1).

These findings strongly suggest that there is a relationship between the formation of Cr(III) nanoscale complexes and the lower toxicity of Cr(III) compared to Cr(VI) (34-39). We believe that due to the size and nature of the Cr(III) nanoscale-complexes, their cellular internalization follow different mechanisms which in turn might lead to their lower toxicity. As demonstrated by some *in vivo* studies, Cr(III) ions are primarily taken up by cells and internalized via the cell membrane (40,41) while Cr(VI) ions have the ability to enter cells through ion channels and accumulate inside cells at concentrations of up to a hundred-fold greater than the extracellular concentration (42,43). Since we found that neither Co(II) or Cr(VI) form complexes in the tested media, it should affect their overall toxicity.

5.6. Conclusion

Our results show that among three ions, namely Co (II), Cr (III) and Cr (VI), only Cr(III) formed nanoscale complexes in simulated physiological fluids, namely in RPMI 1640 and DMEM high glucose. Although the use of many analytical techniques allowed us to identify the involvement of phosphate, calcium and amino acids in the chemical composition of the Cr(III)-complexes formed in RPMI 1640 and in DMEM high glucose, they could not be matched to any organic or inorganic crystal structure available to date in X-ray diffraction databases. Formation of metal ion complexes in biological fluids is of great importance for the understanding of ion cytotoxicity *in vivo* and our findings could explain the difference between chromium and cobalt ions toxicity.

5.7. References

1. Brockett C, Williams S, Jin Z, Isaac G, Fisher J. Friction of total hip replacements with different bearings and loading conditions. J Biomed Mater Res B Appl Biomater 2007; 81 :508-15.
2- Sargeant A, Goswami T. Pathophysiological aspects of hip implants. J Surg Orthop Adv 2006; 15:111-2.
3- Ren WP, Markel DC, Zhang R, Peng X,Wu B, Monica H, Wooley PH. Association between UHMWPE particle-induced inflammatory osteoclastogenesis and expression of RANKL, VEGF, and Flt-1 in vivo. Biomaterials 2006; 30:5161-9.

4- Geller JA, Malchau H, Bragdon C, Greene M, Harris WH, Freiberg AA. Large diameter femoral heads on highly cross-linked polyethylene: minimum 3-year results. Clin Orthop Rel Res 2006; 447:53-9.

5- Sharkey PF, Hozack WJ, Dorr LD, Maloney WJ, Berry D. The bearing surface in total hip arthroplasty: evolution or revolution. Instr Course Lect 2000; 49:41-56.

6- Williams S, Tipper JL, Ingham E, Stone MH, Fisher J. In vitro analysis of the wear, wear debris and biological activity of surface-engineered coatings for use in metal-on-metal total hip replacements. Proc Inst Mech Eng [H] 2003; 217:155-63.

7- Jacobs JJ, Skipor AK, Patterson LM, Hallab NJ, Paprosky WG, Black J, Galante JO. Metal release in patients who have had a primary total hip arthroplasty. A prospective, controlled, longitudinal study. J Bone Joint Surg [Am] 1998; 80:1447-58.

8- Jacobs JJ, Skipor AK, Doorn PF, Campbell P, Schmalzried TP, Black J, Amstutz HC. Cobalt and chromium concentrations in patients with metal on metal total hip replacements. Clin Orthop Ret Res 1996; (329 Suppl):S256-63.

9- Langkamer VG, Case CP, Heap P, Taylor A, Collins C, Pearse M, Solomon L. Systemic distribution of wear debris after hip replacement. A cause for concern? J Bone Joint Surg [Br] 1992; 74:831-9.

10- Merritt K, Brown SA. Distribution of cobalt chromium wear and corrosion products and biologic reactions. Clin Orthop Rel Res 1996; (329 Suppl):S233-43.

11- Zhitkovich A, Peterson-Roth E, Reynolds M. Killing of chromium-damaged cells by mismatch repair and its relevance to carcinogenesis. Cell Cycle 2005; 8:1050-2.

12- Levina A, Harris HH, Lay PA. Binding of chromium(VI) to histones: implications for chromium(VI)-induced genotoxicity. J Biol Inorg Chem 2006; 11:225-34.

13- Moghaddas S, Gelerinter E, Bose RN. Mechanisms of formation and decomposition of hypervalent chromium metabolites in the glutathione-chromium (VI) reaction. J Inorg Biochem 1995; 57:135-46.

14- Stearns DM, Kennedy LJ, Courtney KD, Giangrande PH, Phieffer LS, Wetterhahn KE. Reduction of chromium(VI) by ascorbate leads to chromium-DNA binding and DNA strand breaks in vitro. Biochemistry 1995; 34:910-9.

15- Gez S, Luxenhofer R, Levina A, Codd R, Lay PA**.** Chromium(V) complexes of hydroxamic acids: formation, structures, and reactivities. Inorg Chem 2005; 44:2934-43.

16- Moghaddas S, Gelerinter E, Bose RN. Mechanisms of formation and decomposition of hypervalent chromium metabolites in the glutathione-chromium (VI) reaction. J Inorg Biochem 1995; 57:135-46.

17- Voitkun V, Zhitkovich A, Costa M. Cr(III)-mediated crosslinks of glutathione or amino acids to the DNA phosphate backbone are mutagenic in human cells. Nucleic Acids Res 1998; 6:2024-30.

18- Cobb AG, Schmalzreid TP. The clinical significance of metal ion release from cobalt-chromium metal-on-metal hip joint arthroplasty. Proc Inst Mech Eng [H] 2006; 220:385-98.

19- Catelas I, Petit A, Vali H, Fragiskatos C, Meilleur R, Zukor DJ, Antoniou J, Huk OL. Quantitative analysis of macrophage apoptosis vs. necrosis induced by cobalt and chromium ions in vitro. Biomaterials 2005; 26:2441-53.

20- Fleury C, Petit A, Mwale F, Antoniou J, Zukor DJ, Tabrizian M, Huk OL. Effect of cobalt and chromium ions on human MG-63 osteoblasts in vitro: morphology, cytotoxicity, and oxidative stress. Biomaterials 2006; 27:3351-60.

21- Petit A, Mwale F, Tkaczyk C, Antoniou J, Zukor DJ, Huk OL. Induction of protein oxidation by cobalt and chromium ions in human U937 macrophages. Biomaterials 2005; 26:4416-22.

22- Petit A, Mwale F, Tkaczyk C, Antoniou J, Zukor DJ, Huk OL. Cobalt and chromium ions induce nitration of proteins in human U937 macrophages in vitro. J Biomed Mater Res A 2006; 79A:599-605.

23- Salnikow K, Su W, Blagosklonny MV, Costa M. Carcinogenic metals induce hypoxia-inducible factor-stimulated transcription by reactive oxygen species-independent mechanism. Cancer Res 2000; 60:3375-8.

24- Kitahara J, Yamanaka K, Kato K, Lee YW, Klein CB, Costa M. Mutagenicity of cobalt and reactive oxygen producers. Mutat Res 1996; 370:133-40.

25- Zhitkovich A, Voitkun V, Costa M. Formation of the amino acid-DNA complexes by hexavalent and trivalent chromium in vitro: importance of

trivalent chromium and the phosphate group. Biochemistry 1996; 35:7275-82.

26- Case CP, Langkamer VG, James C, Palmer MR, Kemp AJ, Heap PF, Solomon L. Widespread dissemination of metal debris from implants. J Bone Joint Surg [Br] 1994; 76:701-12.

27- Chaudhary S, Pinkston J, Rabile MM, Van Horn JD. Unusual reactivity in a commercial chromium supplement compared to baseline DNA cleavage with synthetic chromium complexes. J Inorg Biochem 2005; 99:787-94.

28- Messer J, Reynolds M, Stoddard L, Zhitkovich A. Causes of DNA single-strand breaks during reduction of chromate by glutathione in vitro and in cells. Free Radic Biol Med 2006; 40:1981-92.

29- Harris HH, Levina A, Dillon CT, Mulyani I, Lai B, Cai Z, Lay PA. Time-dependent uptake, distribution and biotransformation of chromium(VI) in individual and bulk human lung cells: application of synchrotron radiation techniques. J Biol Inorg Chem 2005; 10:105-18.

30- Walter PB, Macklin EA, Porter J, Evans P, Kwiatkowski JL, Neufeld EJ, Coates T, Giardina PJ, Vichinsky E, Olivieri N, Alberti D, Holland J, Harmatz P. Inflammation and oxidant-stress in beta-thalassemia patients treated with iron chelators deferasirox (ICL670) or deferoxamine: an ancillary study of the Novartis CICL670A0107 trial. Haematologica 2008; 93:817-23.

31- Cai L, Li XK, Song Y, Cherian MG. Essentiality, toxicology and chelation therapy of zinc and copper. Curr Med Chem 2005; 12:2753-63.

32- Abdel-Latif S, El-Roudi O, Mohamed M. Chelation behaviour of nitroso-pyrazolones with Mn(II), Co(II), Ni(II), Cu(II) AND Zn(II). Journal of Thermal Analysis and Calorimetry 2003; 73: 939-50.

33- Bagchi D, Stohs SJ, Downs BW, Bagchi M, Preuss HG. Cytotoxicity and oxidative mechanisms of different forms of chromium. Toxicology 2002; 180:5-22.

34- Bagchi D, Bagchi M, Stohs SJ. Chromium (VI)-induced oxidative stress, apoptotic cell death and modulation of p53 tumor suppressor gene. Mol Cell Biochem 2001; 222:149-58.

35- Blasiak J, Kowalik J. A comparison of the in vitro genotoxicity of tri- and hexavalent chromium. Mutat Res 2000; 469:135-45.

36- Shelnutt SR, Goad P, Belsito DV. Dermatological toxicity of hexavalent chromium. Crit Rev Toxicol 2007; 37:375-87.

37- Nethercott J, Paustenbach D, Adams R, Fowler J, Marks J, Morton C, Taylor J, Horowitz S, Finley B. A study of chromium induced allergic contact dermatitis with 54 volunteers: implications for environmental risk assessment. Occup Environ Med 1994; 51:371-80.

38- Goulart M, Batoréu MC, Rodrigues AS, Laires A, Rueff J. Lipoperoxidation products and thiol antioxidants in chromium exposed workers. Mutagenesis 2005; 20:311-5.

39- Sipowicz MA, Anderson LM, Utermahlen WE Jr, Issaq HJ, Kasprzak KS. Uptake and tissue distribution of chromium(III) in mice after a single intraperitoneal or subcutaneous administration. Toxicol Lett 1997; 93:9-14.

40- Suzuki T, Miyata N, Horitsu H, Kawai K, Takamizawa K, Tai Y, Okazaki M. NAD(P)H-dependent chromium (VI) reductase of Pseudomonas ambigua G-1: a Cr(V) intermediate is formed during the reduction of Cr(VI) to Cr(III). J Bacteriol 1992; 174:5340-5.

41- Buttner B, Beyersmann D**.** Modification of the erythrocyte anion carrier by chromate. Xenobiotica 1985; 15:735-41.

42- Biedermann KA, Landolph JR. Role of valence state and solubility of chromium compounds on induction of cytotoxicity, mutagenesis, and anchorage independence in diploid human fibroblasts. Cancer Res 1990; 50:7835-42.

43- Sathwara NG, Patel KG, Vyas JB, Patel S, Trivedi MR, Dave LM, Madia MM, Kulkarni PK, Parikh DJ, Saiyed HN. Chromium exposure study in chemical based industry 2007; 28:405-8.

CHAPTER 6

Interactions of Cr(III) Complexes with Serum Proteins

The 3rd paper presented here, and accepted for publication in *Journal of Biomedical Materials Research Part* (Ref.: JBMR-A-09-0371.R2), fulfills the objective of this thesis which aimed at understanding why Cr excretion is not fully effective by determining the binding of Cr(III) complexes with serum proteins.

Our previous *in vitro* studies suggested that Cr(III) are less toxic than Cr(VI) and Co(II) and that this difference in toxicity may be explained by the formation of Cr(III) complexes in physiological fluids. It is known that the retention of organic Cr in the organism is much higher than the retention of inorganic Cr compounds. This suggests that Cr ions circulating in blood can interact with serum proteins, generating complexes with a high organic density.

In the present chapter, we determined through a proteomic approach the nature of proteins bound to Cr(III) complexes in both bovine and human serum and investigated their effect on the internalization of these complexes by macrophages. Our main finding showed that Cr(III) complexes could bind only to bovine albumin in bovine serum but to 8 proteins in human serum. We also demonstrated that Cr(III) complexes formed in both RPMI 1640 and DMEM high glucose and in the presence of human serum were more easily internalized by macrophages than the complexes formed in bovine serum, suggesting that human proteins playing a role of opsonins.

INVESTIGATION OF THE BINDING OF Cr(III) COMPLEXES TO HUMAN AND BOVINE SERUM PROTEINS: A PROTEOMIC APPROACH

Cathy Tkaczyk[1,2,3], ✉ Olga L. Huk[1,3], Fackson Mwale[1], John Antoniou[1,3], David. J Zukor[1],

Alain Petit[1], ✉ Maryam Tabrizian[2,3,4,5]

[1]Division of Orthopaedic Surgery, McGill University,

Lady Davis Institute for Medical Research,

The Sir Mortimer B. Davis-Jewish General Hospital,

3755 Côte-Sainte-Catherine Road, Montreal, QC, H3T 1E2, Canada.

✉ ohuk@jgh.mcgill.ca

Fax: (514) 340-7502

[2]Department of Biomedical Engineering, [3]Center of Biorecognition and Biosensors (CBB),

[4] McGill Institute for Advanced Materials, [5] Faculty of Dentistry,

Duff Medical Building, 3775 University Street, Montreal, QC, H3A 2B4, Canada.

✉ : maryam.tabrizian@mail.mcgill.ca

Fax: (514) 398-7461

6.1. Abstract

One of the main concerns in the use of cobalt-chromium (Co-Cr) alloys-based implants is the long-term fate of Co and Cr ions present in the blood, organs, and urine of patients. Our previous studies have shown that Cr(III) can form complexes in different cell culture media alone, whereas Co(II) and Cr(VI) do not form any detectable structure under the same conditions. Since Cr(VI) and Co(II) are known to be more toxic than Cr(III), we hypothesized that the difference in their molecular structure could be the origin of the difference in their toxicity. Herein, we investigated the interaction of the Cr(III) complexes formed in RPMI 1640 and DMEM high glucose media with serum proteins and their internalization by macrophages. Electrophoresis gels stained by Coomassie Blue showed the presence of proteins for complexes formed in both media. Using a liquid chromatography–quadrupole–time of flight (LC-Q-Tof) mass spectrometer, we showed that in the presence of fetal bovine serum, Cr(III) complexes interacted only with albumin, while they interact mainly with albumin, transferrin and immunoglobulins (Ig) in the presence of human serum. Other proteins, such as complement C3, alpha-2-macroglobulin, ceruloplasmin, plasminogen, and apolipoprotein B may also interact with Cr(III) complexes but with lower probability. The cellular uptake of Cr(III) complexes, visualized by transmission electron microscopy, was also higher in RPMI 1640. Furthermore, Cr(III) complexes were more easily engulfed by macrophages when they were formed with human serum. To the best of our knowledge, this is the first report on Cr ions

and their interaction with macrophages in the presence of bovine and human serum proteins.

6.2. Introduction

Numerous studies reported on the chromium (Cr) compounds toxicity to organisms (1). Workers exposed to Cr often suffer from allergies, dermatitis, asthma, and cancer. While Cr(VI) has been considered the main culprit for "heavy" responses, Cr(III) has been shown to react more as an irritant (2). As far as the orthopedic community is concerned, several studies have shown the presence of Cr ions in the blood, urine, and organs of patients after metal-on-metal (MM) total hip arthroplasty (THA) (3). The most significant concern on the use of these implants, made of cobalt-chromium alloys, is the production of metal ions, which could lead to cellular toxicity (4,5), metal hypersensitivity (6,7), and chromosomal changes (8,9). In addition, these ions have the potential to generate an oxidative stress that can impair cells via DNA damage, lipid peroxidation or protein oxidation (10). Some investigations have also shown that Cr ions may be responsible for protein nitration in human macrophages (11) and morphological changes in human osteoblasts (12). Cr(VI) is known to be more toxic than Cr(III), both *in vitro* and *in vivo* (13). So far, one study has been directed towards understanding the molecular forms of these ions in biological fluids after their release from metallic implants. Cr-phosphate corrosion products have been found around retrieved hip implants and surrounding tissues (14). However, no further

investigation was performed to determine either their composition or to relate this chemical composition to their level of toxicity.

Some studies attempted to elucidate the kinetic and the mechanism of urinary exchange of Cr (15), and found that the urinary excretion of Cr is not fully effective and Cr ions tend to accumulate in tissues and red blood cells (16,17). As an explanation for such behavior, the literature points out possible interactions of Cr with proteins (18). Organic Cr complexes have then been described to have a higher retention coefficient in organs than inorganic Cr complexes or other forms of Cr (19). However, the exact nature and mechanism of Cr interactions with proteins and Cr complex retention still need to be understood.

Conversely, some investigations relate the lower toxicity of Cr (III) in comparison to Cr(VI) to its mechanism of uptake through a phagocytosis-like process (20). In a previous *in vitro* study, we have shown that Cr(III) formed complexes in RPMI 1640 and DMEM high glucose cell culture media, whereas Cr(VI) did not produce any detectable complexes under the same conditions (21). Furthermore, the Cr(III) complexes were composed of organic and inorganic components, tangled with Cr(III) ions. The organic compounds included amino acids and phosphates, while calcium, sodium, and chromium were the main compounds present in the inorganic phase. This study enabled us to relate, to some extent, the chemical form of Cr to their mechanism of uptake and therefore to their potential toxicity.

In light of these findings, the aim of this work was to provide new insight on the predominant role of organic compounds, particularly of proteins, in the

formation of Cr(III) complex and their behavior and properties *in vitro*. To elucidate the cellular uptake of Cr(III) ions, $CrCl_3$ salt generating Cr(III) ions was used. It was demonstrated that only Cr(III) is present in the crystal salt of $CrCl_3$ (22) and is first released in the solution. However, Cr(II) and Cr(VI) may theoretically also be formed from Cr(III). However, Cr(III) is the most thermodynamically stable species and does not tend to reduce to Cr(II) or oxidize to Cr(VI) that are more unstable. The valence of the ion is then similar to what is observed in metal implants in which Cr(III) is released by the natural corrosion process (23). Since the main cells present around orthopedic implants are macrophages (24), the U937 cells, a monoblastoid cell line of human histiocytic lymphoma (macrophage-like cells) (25) was used as cell culture model. They are well known to engulf foreign bodies via different mechanisms. The "standard" one is phagocytosis and involves immunoglobulins (Ig) and/or complement C3 playing the role of opsonins (26). In fact, opsonins are serum components acting as attachment sites on the foreign bodies, which aid the internalization process. Most of *in vitro* studies are performed with media supplemented with fetal bovine serum (FBS). Therefore, the RPMI 1640 and DMEM high glucose media were supplemented with FBS to determine biological differences with human serum (HS) and point out the limitation of the use of FBS for *in vitro* studies.

This will help to improve our understanding of the fate and transit of metal ions as well as the possible biological consequences of their interactions with proteins both *in vitro* and *in vivo*. More than 600 proteins are present in sera, albumin, transferrin, and fibrinogen being amongst the most abundant. There are

however, important differences in terms of protein composition and concentration between FBS and HS as outlined in Table 7.

HUMAN SERUM (HS)	FETAL BOVINE SERUM (FBS)
Albumin	Albumin
Transferrin	Alpha-1-Antiproteinase
Fibrinogen	Plasminogen
IgA total	Lactoperoxidase
Alpha-2-macroglobulin	Kininogen
IgM total	NADH-Ubiquinine-oxidoreductase
Alpha-1-Antitrypsin	IgA total
C3 complement	Alpha-2-Glycoprotein
Haptoglobin	Hemiferrin

Table 7: Comparison of the most abundant proteins present in human and fetal bovine serum**.**

6.3. Materials and Methods

6.3.1. Isolation of Cr(III) Complexes

The concentration of Cr(III) used in the present study is based on a previous *in vitro* work showing that Cr(III) concentrations in the ppm range are necessary to elicit a U937 cell response (11,27,28) and on our previous work on

the formation of Cr(III) complexes in cell culture media. (21). Fifty (50) ppm of Cr ions ($CrCl_3$, Sigma-Aldrich, Oakville, ON) were added to RPMI 1640 and DMEM high glucose (HyClone, Logan, UT) supplemented with 5% FBS (Hyclone) and 5% HS Sigma-Aldrich, Oakville, ON) as described below:

1) 50 ppm Cr(III) + RPMI 1640 + 5% FBS

2) 50 ppm Cr(III) + RPMI 1640 + 5% HSS

3) 50 ppm Cr(III) + DMEM high glucose + 5% FBS

4) 50 ppm Cr(III) + DMEM high glucose + 5% HS

After incubation for 1 h at 37°C, precipitates were isolated by centrifugation at 5000 x g for 20 min, washed 3 times with water as previously described (21) and loaded on 4-20% acrylamide gel. Proteins were then separated by SDS-PAGE and gels stained with Coomassie Blue.

6.3.2. Detection of Proteins by Mass Spectrometry

Bands of proteins visible on acrylamide gels stained with Coomassie Blue were cut out of the gels and taken for in-gel digestion on a robotic MassPrep Workstation (Micromass; Waters Corp., Milford, MA). The gel pieces were destained, reduced with 10 mM dithiothreitol, alkylated with 55 mM iodoacetamide, and incubated with 6 ng/µl trypsin for 5 h at 37°C. Peptides were then extracted with 1% formic acid/2% acetonitrile. Identification of the digested proteins was completed using a Liquid Chromatography–Quadrupole–Time of Flight (LC-Q-Tof) Mass Spectrometer (Micro Mass, Milford, MA). The digests were loaded into a 10 cm capillary PicoFrit column filled with C18 stationary

phase and eluted by linear gradient of 5–70% acetonitrile in 0.1% formic acid at the flow rate 200 µl/min. The eluted peptides were electrosprayed into Q-Tof and the precursor ions were subjected to fragmentation by collision with argon (MS/MS). The MS/MS data were submitted to Mascot (Matrix Science, London, UK) for a search against the NCBI nonredundant database.

6.3.3. TEM Microscopy

U937 human macrophages (ATCC, Rockville, MD) were cultured in RPMI 1640 and DMEM high glucose (Hyclone, Logan, UT) supplemented with 5% FBS or 5% HS, 100 U/ml penicillin, and 100 µg/ml streptomycin at 37°C under 5% CO_2 humidified atmosphere at a density of 5×10^5 cells/ml. Cells were incubated with 50 ppm of Cr(III) for 30 min at 37°C. After incubation, cells were centrifuged at $500 \times g$ for 6 min, supernatants were removed, and pellets were fixed overnight in 0.5 ml of 2.5% glutaraldehyde. After centrifugation at $16{,}000 \times g$ *for* 20 min, supernatants were removed and 0.5 ml of 1% osmium tetroxide was added for 2 h. Cells were then dehydrated by increasing concentrations of acetone (from 30% to 100%) to wash the pellets. After centrifugation at $16{,}000 \times g$ for 20 min, supernatants were removed and epon:acetone with a ratio of 1:1 was added for 1 h, followed by epon:acetone with a ratio of 2:1 for 1 h, and epon:acetone with a ratio of 3:1 overnight. At least 0.3 ml of pure epon resin was added and samples were incubated for 3 h under vacuum to avoid any air bubble. After polymerization at 60°C for 48 h, the plastic tubes were removed to obtain solid pieces of resin with cells pellets at the bottom.

These pellets were then sectioned in thin diamond knife cuts (about 90 nm). Cells were observed using a JEOL 2000FX transmission electronic microscope (TEM) (Akishima, Tokyo, Japan) at an accelerating voltage of 80 kV. To determine the percentage of internalization, 500 cells from randomly selected fields were counted and analyzed for the presence of nano-sized complexes (dark spots on the TEM microphotographs). Finally, energy dispersive X-ray analysis (EDXA) was used to confirm the nature of the internalized structures.

6.4 Results

Figure 6.1 shows that Cr(III) complexes obtained in different media interacted with serum proteins. No proteins were found when Cr(III) was incubated with media without serum, which was used as negative control. No pelleted proteins could either be obtained after centrifugation of media and serum without Cr(III) (results not shown), or after centrifugation of Cr(III) and serum without medium dilution (21). The patterns of electrophoresis were similar for complexes formed in the presence of FBS in RPMI 1640 (Fig. 6.1a) to those formed in DMEM high glucose (Fig. 6.1b) with bands visible at 69 and 200 kDa. In HS (Fig. 6.1c), major protein bands were detected at 10, 66, 68, 77, and 90 kDa with similar electrophoresis patterns in both media.

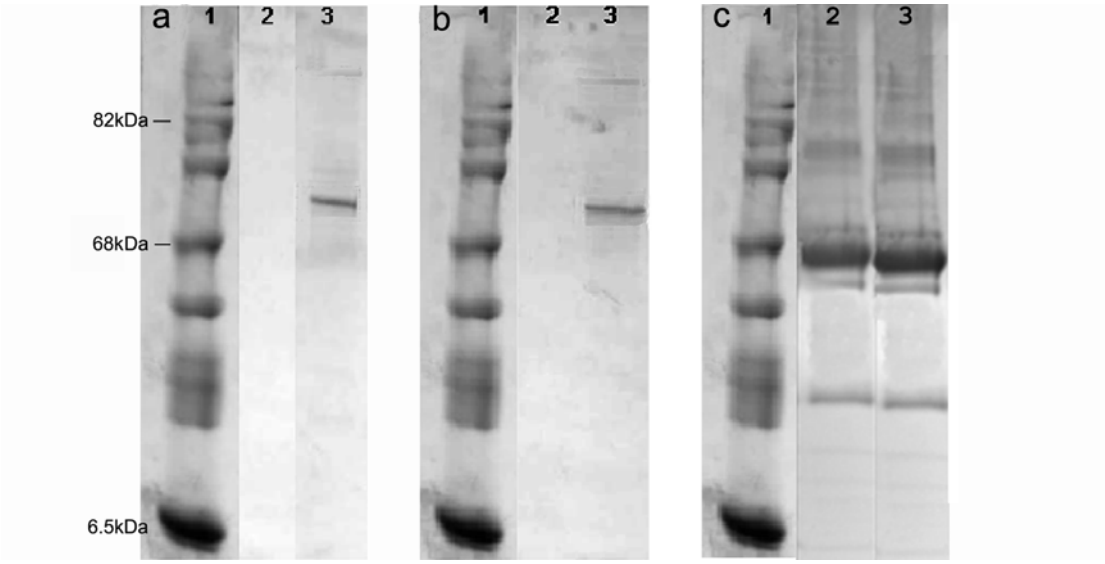

Figure 6.1: Electrophoresis gels of Cr(III) complexes formed in the presence of serum. Fifty (50) ppm of $CrCl_3$ was incubated with the different media as indicated in Materials and Methods. Proteins were separated on 4-20% acrylamide gels and stained with Coomassie Blue.

a) Lane 1: molecular weight marker; Lane 2: RPMI + 50 ppm Cr^{3+}; Lane 3: RPMI + 5% FBS + 50 ppm Cr^{3+}.

b) Lane 1: molecular weight marker; Lane 2: DMEM + 50 ppm Cr^{3+}; Lane 3: DMEM + 5% FBS + 50 ppm Cr^{3+}.

c) Lane 1: molecular weight marker; Lane 2: RPMI + 5% HS + 50 ppm Cr^{3+}; Lane 3: DMEM + 5% HS + 50 ppm Cr^{3+}.

Figure 6.2 shows an illustration of MS/MS spectrum corresponding to the fragmentation of the peptide CCTESLVNR by the MS. The generated data was submitted to Mascot, a mass spectrometry search engine, in order to retrieve

proteins from primary sequence databases. The experimental mass value was compared with calculated peptide mass or fragment ion mass values, obtained by applying cleavage rules to the entries in a comprehensive primary sequence database.

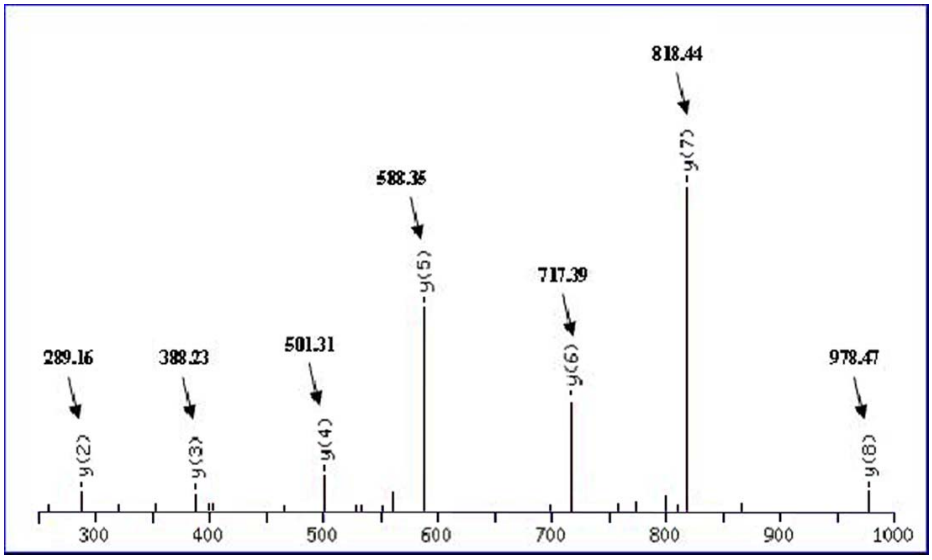

Figure 6.2: MS/MS spectrum of the peptide CCTESLVNR (serum albumin, Homo sapiens) showing different ion fragments and their relative mass (mass/charge (M/Z)). Electrophoresis gel bands of Cr(III) complexes in the presence of FBS or HS were cut and digested with trypsin. The resulting peptide mixture was analyzed by mass spectrometry and MS/MS.

By using an appropriate scoring algorithm, the closest match or matches were identified. Results for the RNVLSETCC peptide are presented in Table 8. In this example, 8 ion fragments on 70 matched with albumin for a peptide score of 60.1, demonstrating the presence of a human albumin. Ions score is 10*Log (P),

where P is the probability that the observed match is a random event. Individual ions scores > 45 indicate identity or extensive homology ($p<0.05$).

#	b	b^{++}	b*	b^{*++}	b^{0}	b^{0++}	Seq.	y	y^{++}	y*	y^{*++}	y^{0}	y^{0++}	#
1	161.04	81.02					**C**							**9**
2	321.07	161.04					**C**	**978.47**	489.74	961.44	481.22	960.46	480.73	**8**
3	422.12	211.56			404.11	202.56	**T**	**818.44**	409.72	801.41	401.21	800.43	400.72	**7**
4	551.16	276.08			533.15	267.08	**E**	**717.39**	359.20	700.36	350.68	699.38	350.19	**6**
5	638.19	319.60			620.18	310.59	**S**	**588.35**	294.68	571.32	286.16	570.34	285.67	**5**
6	751.27	376.14			733.26	367.14	**L**	**501.31**	251.16	484.29	242.65			**4**
7	850.34	425.68			832.33	416.67	**V**	**388.23**	194.62	371.20	186.11			**3**
8	964.39	482.70	947.36	474.18	946.38	473.69	**N**	**289.16**	145.08	272.14	136.57			**2**
9							**R**	**175.12**	88.06	158.09	79.55			**1**

Table 8: Mascot analysis of the fragmentation of the RNVLSETCC peptide.

Spectrum is shown in Figure 2. The table shows the different peptides (protein fragments or ion fragments) possible for the sequence (Seq.), which is read from the bottom to the top of the table. The ions "y" (or charged peptides) represent the results from the analyzed samples while the other columns represent the Mascot database for comparison. For instance, the peptide RNVLSETC generated from the fragmented samples has a mass/charge (M/Z) of 978.47. The ions "b" indicate a $C^{-}\rightarrow$ N sequence, while the ions "y" represent an $N^{-}\rightarrow$ C sequence. The ions "y++" with an M/Z of 489.74 is a corresponding peptide in the database with 2 positive charges with the sequence RNVLSETC. The symbols "*"and "^{0}" mean that the peptide lost a NH^{3+} molecule (978 – 17 = 961) or a H_2O molecule (978 – 18 = 960) respectively.

All bands from Figure 6.1 were analyzed in the same way. It is important to note that our choice was limited to proteins having at least 8 corresponding peptides with ion scores over 45 in order to ascertain their presence in the Cr(III) complexes. Results showed that with FBS, only albumin (123 peptides with scores from 45 to 90) interacts with the Cr(III) complexes. With HS, albumin (132 peptides with scores from 45 to 102), transferrin (98 peptides with scores from 45 to 89), immunoglobulins (99 peptides with scores from 45 to 98), apolipoprotein B (12 peptides with scores from 45 to 97), complement C3 (11 peptides with scores from 45 to 87), ceruloplasmin (11 peptides with scores from 45 to 79), alpha-2-macroglobulin (9 peptides with scores from 45 to 81), and plasminogen (8 peptides with scores from 45 to 69) are all possibly interacting with the Cr(III) complexes. The results obtained for albumin and transferrin are summarized in Table 9.

	Protein Name	Gel position	Accession no.	MW
BOVINE	Albumin	1 & 2	gi| 162648	71244
	Albumin	1 & 2	gi| 229552	68083
HUMAN	Albumin	1, 2, 4, 5 & 6	gi| 23307793	71344
	Albumin	1, 2, 4, 5 & 6	gi| 28592	71316
	Transferrin	3 & 4	gi| 553788	55207
	Transferrin	3 & 4	gi| 31415705	79280
	Transferrin	3 & 4	gi| 37747855	79329

Table 9: Most probable protein candidates in bovine and human sera interacting with Cr(III) complexes. All bands from electrophoresis gels were analyzed by MS/MS. The generated data was submitted to Mascot and the best matches were identified as shown in Table 8.

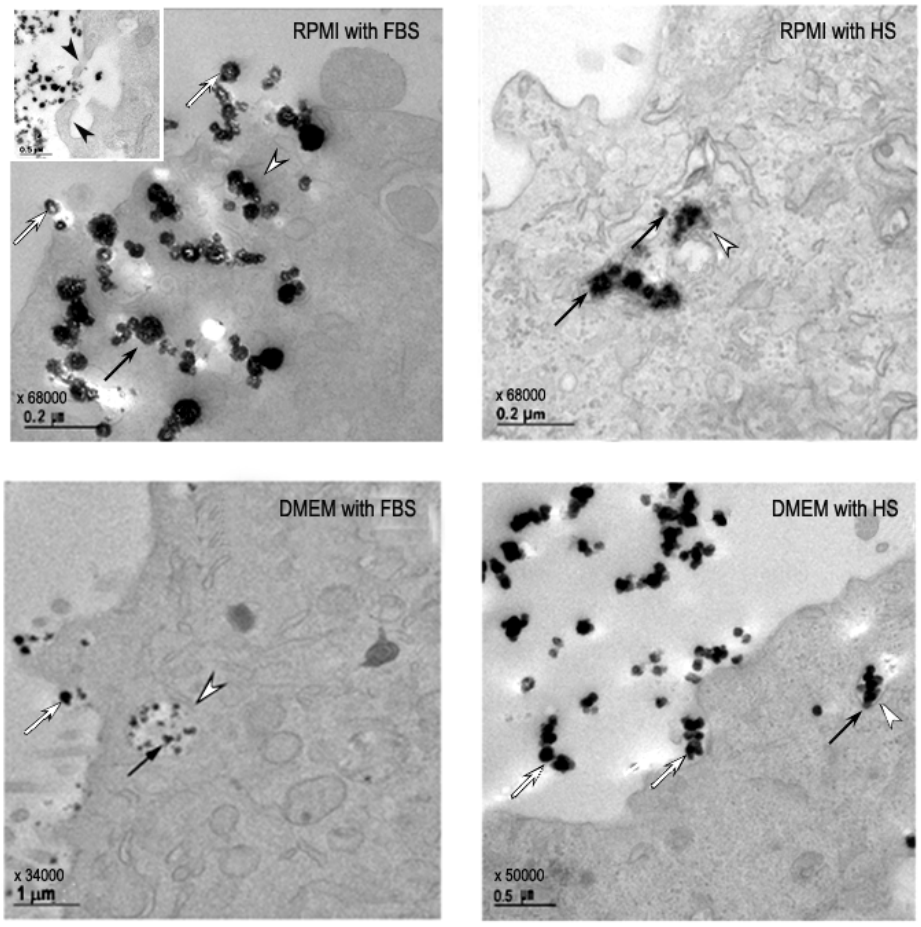

Figure 6.3: TEM pictures of Cr(III) complexes with U937 macrophage-like cells in serum supplemented media. Black arrows show Cr(III) complexes inside the cells while white arrowheads show Cr(III) complexes outside the cells. Note the presence of internalized vesicles (black arrow head). The black arrowhead in the insert (RPMI with FBS) shows the formation of pseudopodia.

TEM images (Figure 6.3) along with EDXA analysis (Figure 6.4) clearly indicated the presence of Cr(III) complexes in U937 macrophage-like cells or interacting with them. The size of these complexes varied from 60 nm when

formed in RPMI 1640 (in both FBS and HS) to 100 nm when formed in DMEM high glucose (in both FBS and HS).

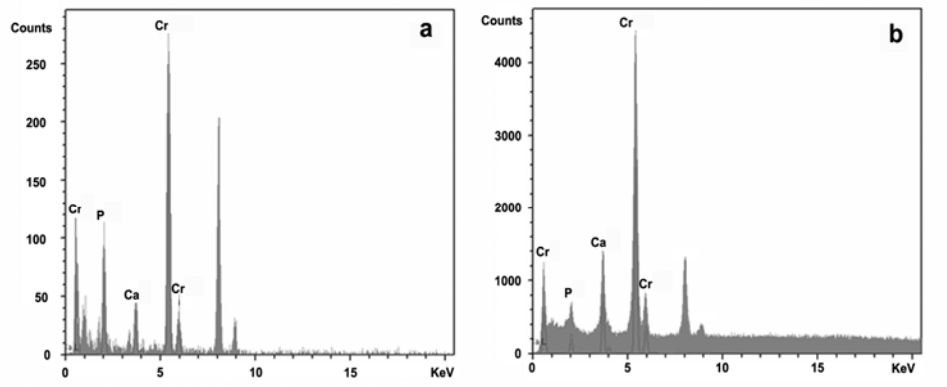

Figure 6.4: EDXA spectra of Cr(III) complexes internalized by U937 macrophage-like cells in RPMI 1640 with FBS (a) and in DMEM high glucose supplemented with FBS (b). EDXA spectra obtained in HS are the same (data not shown). Copper peaks visible on the right of the spectra (8-9 keV) are generated by the grids. Note the presence of chromium (Cr), phosphate (P) and calcium (Ca) in both Cr(III) complexes.

Figure 6.5 shows the percentage of U937 cells that internalized Cr(III) complexes (integrated into the cytoplasm, black arrow), as obtained by evaluating 500 cells under TEM for each medium/serum condition. A more important cellular uptake of Cr(III) complexes was observed in RPMI 1640 than in DMEM high glucose. The internalization of the Cr(III) complexes was also facilitated by HS compared to FBS. Notably, 21% and 48% of U937 cells contained Cr(III) complexes or interacting with Cr(III) complexes in RPMI 1640 in presence of

FBS and HS, respectively. Conversely, only 6% and 21% of U937 cells contained Cr(III) complexes in DMEM high glucose in the presence of FBS and HS, respectively.

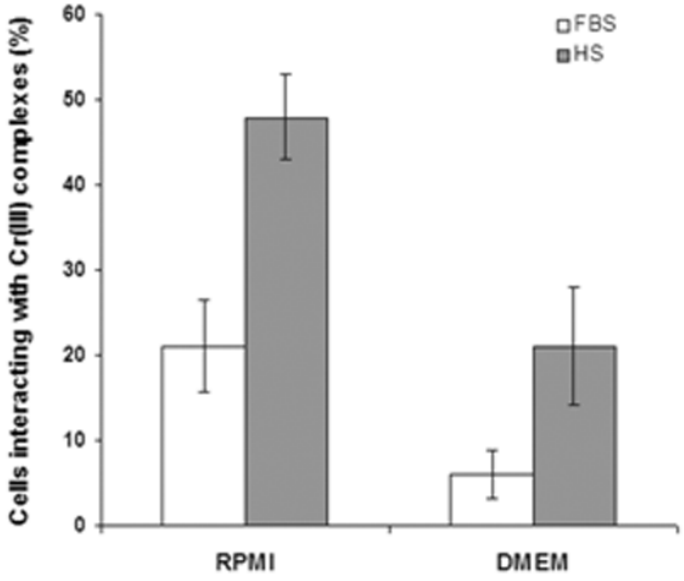

Figure 6.5: Internalization of Cr(III) complexes by U937 macrophage-like cells. Results are presented as the percentage (± standard deviation) of cells that internalized the Cr(III) complexes over the total number of cells.

6.5. Discussion

Proteomic approach was used to study the interaction of Cr(III) complexes formed in cell culture media (21) with serum proteins. Although proteomic is an established technology for protein detection and discovery, it is not a widely used methodology for determining the interactions between metal and proteins. We found that Cr(III) complexes interacted only with albumin in the presence of FBS,

while they interacted with albumin, transferrin, and immunoglobulins in the presence of HS. Alpha-2-macroglobulin, ceruloplasmin, plasminogen, immunoglobulin, complement C3, and apolipoprotein B also seem to interact with the Cr(III) complexes in HS. It is also interesting to point out the fact that although albumin, transferrin, complement C3, alpha-2-macroglobulin, ceruloplasmin, plasminogen, and apolipoprotein B are parts of the "standard proteins" of plasma, they are not necessarily the most abundant ones (29), suggesting that the concentration of proteins is not the prime factor to promote their interaction with Cr(III) complexes and their internalization by U937 macrophage-like cells.

Our findings support a previous study demonstrating that ^{51}Cr can bind to transferrin and albumin in patients on continuous ambulatory peritoneal dialysis [30] and also enforce other studies showing the transfer of Cr(III) ions from blood to urine in the presence of insulin (31-32). In fact, human albumin is known to bind and transport a multitude of ligands such as bilirubin, fatty acids, retinoids, steroids, heavy metals, and various drugs (33-35). The primary, secondary, and tertiary structure of albumin provides the unique capability to bind, covalently or reversibly, a great number of various endogenous and exogenous compounds (36-39) with hydrophobic properties. However, heavy metals are also known to bind to this protein (40-43) as it is the major transport protein in blood for Zn^{2+}, which is necessary for various physiological processes such as protein and DNA synthesis, cell growth and division (44). It can also interact with Cd^{2+} and Cl^- ions (45-49). The presence of Cl^- ions in Cr(III) complexes, as shown in our previous

study (21), suggests that Cl^- might promote the interaction of Cr(III) complexes with albumin.

Bovine and human albumin presents a 76% identical sequence (50). The main difference between the two proteins is the presence of two tryptophan residues (W^{131} and W^{214}) in bovine albumin, whereas human albumin has only one (W^{214}) (51). This difference can play a role in their interactions with other components. For instance, in a study on the interactions of both human and bovine albumin with different detergents, spectroscopic results suggested distinct interactions of detergent molecules with W^{131} and W^{214} (52). Moreover, it seems that the binding of surfactants to HS is more complex than for FBS (53). This complexity of binding of albumin is in agreement with the fact that more different human proteins interact with Cr(III) complexes in human serum than in bovine serum. This might also be the reason behind having a greater internalization by U937 macrophage-like cells. Since it was demonstrated that cell lines of the monocytic lineage had lower uptake of titanium oxide (TiO_2) particles than macrophages (54), it is possible that our results underestimated the capacity of macrophages to internalize Cr(III) particles.

Like albumin, transferrin is involved in ion transport and is known as an iron transporter protein. Ti(IV) can bind to transferrin, be recognized by the transferrin receptor, and be up taken by the cells (55). Transferrin belongs to the family of monomeric glycoproteins of~80 kDa which comprises two lobes (N and C) (56), with each lobe containing a single metal-binding center. However, despite substantial structural similarity between the two lobes, the existence of

significant differences in the lobes' metal-binding properties has been demonstrated (57). Indeed, TEM study showed that the Cr(III) complexes formed with human serum are more easily internalized than those formed with bovine serum. This difference can be explained by the absence of transferrin as a mediator of cellular uptake of Cr(III) complexes when the medium is supplemented with FBS (58).

Interestingly, no immunoglobin was involved in the formation of Cr(III) complexes in the presence of FBS while they were involved in the formation of Cr(III) complexes in HS, even though both human and bovine sera are composed of 8-26% (5-18 mg/ml) of immunoglobins (59). While the reason for this difference still needs to be investigated, we found that Cr(III) complexes formed in HS interacted with immunoglobins and complement C3 and that these complexes were more easily engulfed by human U937 cells than Cr(III) complexes formed in FBS. Macrophages and monocytes can internalize molecules and complexes mainly through 3 different pathways. When the material is small (i.e. nutriments), it can be internalized by pinocytosis or endocytosis. Larger substances are internalized by phagocytosis, in which opsonins are involved. Indeed, our results suggest that the internalization of Cr(III) complexes formed in HS occurs through the classical phagocytosis pathway where immunoglobins and complement C3 are the opsonins that are facilitating the recognition of foreign bodies by macrophages (26). However, the absence of opsonin in the Cr(III) complexes formed in FBS suggests that pinocytosis and/or endocytosis pathways may also be involved. This remains to

be investigated. Most importantly, it seems that Cr(III) ions enter cells by different way than Cr(VI) that enter via anions channels (20). Those differences might explain the difference of toxicity of these ions. Thus, the formation of Cr(III) complexes along with the presence of proteins may be the origin in the difference of toxicity between Cr(VI) and Cr(III). Moreover, our previous study demonstrated that Cr(III) complexes cannot be dissolved at low pH (21), suggesting that the Cr(III) complexes are not destroyed in the intracellular endosomes following endocytosis/pinocytosis or in the phagosomes following phagocytosis. This may also explain the high cellular and tissue retention of Cr comparatively to Co that is easily eliminated in urine (16).

Results also suggest the presence of alpha-2-macroglobulin, known to be involved in controlling inflammatory responses to different pathogens, in the Cr(III) complexes formed in HS. Some studies have demonstrated that alpha-2-macroglobulin has a very similar histidine and cysteine-rich region as albumin (60). Additionally, alpha-2-macroglobulin is able to bind zinc (Zn^{2+}) and manganese (Mn^{2+}) ions (61). Therefore, the ability of alpha-2-macroglobulin and its similarity with albumin may explain the capacity of this protein to bind Cr(III) complexes. In addition, alpha-2-macroglobulin shares the copper pool of plasma with albumin and ceruloplasmin, an α2-glycoprotein that binds 90–95% of blood plasma copper (62).

6.6. Conclusion

This work is the very first that uses a proteomic approach to study the interaction of Cr(III) ions with bovine and human proteins present in sera. Our results showed that Cr(III) complexes were able to bind albumin, transferrin, and immunoglobulins in HS but only to albumin in FBS even though the other protein were present in FBS. They also suggest a mechanism, the formation of organic Cr complexes, for their retention in organ and cells. This study provides valuable information on the specificity of interactions between Cr(III) complexes and proteins in simulated physiological fluids.

6.7. References

1. Langard S. One hundred years of chromium and cancer: a review of epidemiological evidence and selected case reports. Am J Ind Med 1990;17:189-215.
2. Iyer VJ, Banerjee G, Govindram CB, Kamath V, Shinde S, Gaikwad A, Jerajani HR, Raman G, Cherian KM. Role of different valence states of chromium in the elicitation of allergic contact dermatitis. Contact Dermatitis 2002;47:357-360.
3. MacDonald SJ, Brodner W, Jacobs JJ. A consensus paper on metal ions in metal-on-metal hip arthroplasties. J Arthroplasty 2004;19(Suppl 3):12-16.
4. Haynes DR, Rogers SD, Hay S, Pearcy MJ, Howie DW. The differences in toxicity and release of bone-resorbing mediators induced by titanium and

cobalt-chromium-alloy wear particles. J Bone Joint Surg [Am] 1993;75-A:825-834.

5. Rae T. A study on the effects of particulate metals of orthopaedic interest on murine macrophages in vitro. J Bone Joint Surg [Br] 1975;57:444-450.
6. Gawkrodger DJ. Metal sensitivities and orthopaedic implants revisited: the potential for metal allergy with the new metal-on-metal joint prostheses. Br J Dermatol 2003;148:1089-1093.
7. Hallab NJ, Mikecz K, Jacobs JJ. A triple assay technique for the evaluation of metal-induced, delayed-type hypersensitivity responses in patients with or receiving total joint arthroplasty. J Biomed Mater Res 2000;53:480-489.
8. Case CP. Chromosomal changes after surgery for joint replacement. J Bone Joint Surg [Br] 2001;83:1093-1095.
9. Moriwaki H, Osborne MR, Phillips DH. Effects of mixing metal ions on oxidative DNA damage mediated by a Fenton-type reduction. Toxicol In Vitro 2008;22:36-44.
10. Stohs SJ, Bagchi D, Hassoun E, Bagchi M. Oxidative mechanisms in the toxicity of chromium and cadmium ions. J Environ Pathol Toxicol Oncol 2001;20:77-88.
11. Petit A, Mwale F, Tkaczyk C, Antoniou J, Zukor DJ, Huk OL. Cobalt and chromium ions induce nitration of proteins in human U937 macrophages in vitro. J Biomed Mater Res Part A 2006;79:599-605.
12. Fleury C, Petit A, Mwale F, Antoniou J, Zukor DJ, Tabrizian M, Huk OL. Effect of cobalt and chromium ions on human MG-63 osteoblasts in vitro:

morphology, cytotoxicity, and oxidative stress. Biomaterials 2006;27:3351-3360.

13. McGregor DB, Baan RA, Partensky C, Rice JM, Wilbourn JD. Evaluation of the carcinogenic risks to humans associated with surgical implants and other foreign bodies - a report of an IARC Monographs Programme Meeting. Eur J Cancer 2000;36:307-13.
14. Jacobs JJ, Urban RM, Gilbert JL, Skipor AK, Black J, Jasty M, Galante JO. Local and distant products from modularity. Clin Orthop Relat Res 1995;319:94-105.
15. O'Flaherty EJ, Kerger BD, Hays SM, Paustenbach DJ. A physiologically based model for the ingestion of chromium(III) and chromium(VI) by humans. Toxicol Sci 2001;60:196-213.
16. Bitsch RG, Zamorano M, Loidolt T, Heisel C, Jacobs JJ, Schmalzried TP. Ion production and excretion in a patient with a metal-on-metal bearing hip prosthesis. A case report. J Bone Joint Surg [Am] 2007;89-A:2758-2763.
17. Granadillo VA, Parra de Machado L, Romero RA. Determination of total chromium in whole blood, blood components, bone, and urine by fast furnace program electrothermal atomization AAS and using neither analyte isoformation nor background correction. Anal Chem 1994;66:3624-3631.
18. Kottwitz K, Laschinsky N, Fischer R, Nielsen P. Absorption, excretion and retention of 51Cr from labelled Cr-(III)-picolinate in rats. Biometals 2009;22:289-295.

19. Kerger BD, Paustenbach DJ, Corbett GE, Finley BL. Absorption and elimination of trivalent and hexavalent chromium in humans following ingestion of a bolus dose in drinking water. Toxicol Appl Pharmacol 1996;141:145-158.
20. Wiegand HJ, Ottenwalder H, Bolt HM. Recent advances in biological monitoring of hexavalent chromium compounds. Sci Total Environ 1988;71:309-315.
21. Tkaczyk C, Huk OL, Mwale F, Antoniou J, Zukor DJ, Petit A, Tabrizian M. The molecular structure of complexes formed by chromium or cobalt ions in simulated physiological fluids. Biomaterials 2009;30:460-467.
22. Kuhlov B. Magnetic ordering in $CrCl_3$ at the phase transition. Phys. Stat.sol(a) 1982; 72:161-168.
23. Merritt K, Brown SA. Distribution of cobalt chromium wear and corrosion products and biologic reactions. Clin Orthop Relat Res 1996;329 (Suppl):S233-S243.
24. Ingham E, Fisher J. The role of macrophages in osteolysis of total joint replacement. Biomaterials 2005;26:1271-1286.
25. Baek YS, Haas S, Hackstein H, Bein G, Hernandez-Santana M, Lehrach H, Sauer S, Seitz H. Identification of novel transcriptional regulators involved in macrophage differentiation and activation in U937 cells. BMC Immunol 2009;10:18 (15 pages).
26. Stuart LM, Ezekowitz RA. Phagocytosis: elegant complexity. Immunity 2005;22:539-550.

27. Catelas I, Petit A**,** Zukor DJ, Antoniou J, Huk OL. TNF-α secretion and macrophage mortality induced by cobalt and chromium ions in vitro - Quantitative analysis of apoptosis. Biomaterials 2003;24:383-391.

28. Petit A, Mwale F, Tkaczyk C, Antoniou J, Zukor DJ, Huk OL. Induction of protein oxidation by cobalt and chromium ions in human U937 macrophages. Biomaterials. 26: 4416-4422, 2005.

29. Issaq HJ, Xiao Z, Veenstra TD. Serum and plasma proteomics. Chem Rev 2007;107:3601-3620.

30. Borguet F, Cornelis R, Delanghe J, Lambert MC, Lameire N. Study of the chromium binding in plasma of patients on continuous ambulatory peritoneal dialysis. Clin Chim Acta 1995;238:71-84.

31. Clodfelder BJ, Emamaullee J, Hepburn DD, Chakov NE, Nettles HS, Vincent JB. The trail of chromium(III) in vivo from the blood to the urine: the roles of transferrin and chromodulin. J Biol Inorg Chem 2001;6:608-617.

32. Clodfelder BJ, Vincent JB. The time-dependent transport of chromium in adult rats from the bloodstream to the urine. J Biol Inorg Chem 2005;10:383-393.

33. Chen J, Fitos I, Hage DS. Chromatographic analysis of allosteric effects between ibuprofen and benzodiazepines on human serum albumin. Chirality 2006;18:24-36.

34. Fasano M, Curry S, Terreno E, Galliano M, Fanali G, Narciso P, Notari S, Ascenzi P. The extraordinary ligand binding properties of human serum albumin. IUBMB Life 2005;57:787-796.

35. Kandagal PB, Ashoka S, Seetharamappa J, Shaikh SM, Jadegoud Y, Ijare OB. Study of the interaction of an anticancer drug with human and bovine serum albumin: spectroscopic approach. J Pharm Biomed Anal 2006;41:393-399.

36. Colmenarejo G. In silico prediction of drug-binding strengths to human serum albumin. Med Res Rev 2003;23:275-301.

37. Curry S, Mandelkow H, Brick P, Franks N. Crystal structure of human serum albumin complexed with fatty acid reveals an asymmetric distribution of binding sites. Nat Struct Biol 1998;5:827-835.

38. Sudlow G, Birkett DJ, Wade DN. The characterization of two specific drug binding sites on human serum albumin. Mol Pharmacol 1975;11:824-832.

39. Sugio S, Kashima A, Mochizuki S, Noda M, Kobayashi K. Crystal structure of human serum albumin at 2.5 A resolution. Protein Eng 1999;12:439-446.

40. Filipe P, Morliere P, Patterson LK, Hug GL, Maziere JC, Freitas JP, Fernandes A, Santus R. Oxygen-copper (II) interplay in the repair of semi-oxidized urate by quercetin bound to human serum albumin. Free Radic Res 2004;38:295-301.

41. Liang H, Huang J, Tu CQ, Zhang M, Zhou YQ, Shen PW. The subsequent effect of interaction between Co(2+) and human serum albumin or bovine serum albumin. J Inorg Biochem 2001;85:167-171.

42. Stewart AJ, Blindauer CA, Berezenko S, Sleep D, Sadler PJ. Interdomain zinc site on human albumin. Proc Natl Acad Sci (USA) 2003;100:3701-3706.

43. Wang J, Zhang H, Yang K, Niu C, Ni J. Computer simulation of Zn(II) speciation and effect of Gd(III) on Zn(II) speciation in human blood plasma. Biol Trace Elem Res 2003;96:125-131.

44. Ahel I, Ahel D, Matsusaka T, Clark AJ, Pines J, Boulton SJ, West SC. Poly(ADP-ribose)-binding zinc finger motifs in DNA repair/checkpoint proteins. Nature 2008;451:81-85.

45. Bal W, Christodoulou J, Sadler PJ, Tucker A. Multi-metal binding site of serum albumin. J Inorg Biochem 1998;70:33-39.

46. Goumakos W, Laussac JP, Sarkar B. Binding of cadmium(II) and zinc(II) to human and dog serum albumins. An equilibrium dialysis and 113Cd-NMR study. Biochem Cell Biol 1991;69:809-820.

47. Sadler PJ, Tucker A, Viles JH. Involvement of a lysine residue in the N-terminal Ni2+ and Cu2+ binding site of serum albumins. Comparison with Co2+, Cd2+ and Al3+. Eur J Biochem 1994;220:193-200.

48. Tinoco AD, Valentine AM. Ti(IV) binds to human serum transferrin more tightly than does Fe(III). J Am Chem Soc 2005;127:11218-11219.

49. Zhou Y, Hu X, Dou C, Liu H, Wang S, Shen P. Structural studies on metal-serum albumin. IV. The interaction of Zn(II), Cd(II) and Hg(II) with HSA and BSA. Biophys Chem 1992;42:201-211.

50. Sen P, Fatima S, Khan JM, Khan RH. How methyl cyanide induces aggregation in all-alpha proteins: a case study in four albumins. Int J Biol Macromol 2009;44:163-169.

51. Peters T, Jr. 1985 Serum albumin. Adv Protein Chem 37:161-245.

52. Gelamo EL, Tabak M. Spectroscopic studies on the interaction of bovine (BSA) and human (HSA) serum albumins with ionic surfactants. Spectrochim Acta A Mol Biomol Spectrosc 2000;56-A:2255-2271.

53. Gelamo EL, Silva CH, Imasato H, Tabak M. Interaction of bovine (BSA) and human (HSA) serum albumins with ionic surfactants: spectroscopy and modelling. Biochim Biophys Acta 2002;1594:84-99.

54. Stringer B, Imrich A, Kobzik L. Flow cytometric assay of lung macrophage uptake of environmental particulates. Cytometry 1995;20:23–32.

55. Tinoco AD, Eames EV, Valentine AM. Reconsideration of serum Ti(IV) transport: albumin and transferrin trafficking of Ti(IV) and its complexes. J Am Chem Soc 2008;130:2262-2270.

56. Sun H, Li H, Mason AB, Woodworth RC, Sadler PJ. N-lobe versus C-lobe complexation of bismuth by human transferrin. Biochem J 1999;337 (Pt 1):105-111.

57. Guo M, Sun H, McArdle HJ, Gambling L, Sadler PJ. Ti(IV) uptake and release by human serum transferrin and recognition of Ti(IV)-transferrin by cancer cells: understanding the mechanism of action of the anticancer drug titanocene dichloride. Biochemistry 2000;39:10023-10033.

58. Aisen P. Transferrin, the transferrin receptor, and the uptake of iron by cells. Met Ions Biol Syst 1998;35:585-631.

59. Stoica GH, Samborschi C, Michiu V. Influence of sex and age on serum immunoglobulin concentrations in healthy subjects. Med Interne 1978;16:23-31.

60. Moriya M, Ho YH, Grana A, Nguyen L, Alvarez A, Jamil R, Ackland ML, Michalczyk A, Hamer P, Ramos D, Kim S, Mercer JF, Linder MC. Copper is taken up efficiently from albumin and alpha2-macroglobulin by cultured human cells by more than one mechanism. Am J Physiol Cell Physiol 2008;295:C708-C721.

61. Gettins P, Cunningham LW. A unique pair of zinc binding sites in the human alpha 2-macroglobulin tetramer. A 35Cl and 37Cl NMR study. Biochemistry 1986;25:5004-5010.

62. Fehily D, Kiswani AS, Jenkins DM, Cremin FM. Redistribution of plasma zinc between albumin and alpha 2-macroglobulin in pregnancy. J Trace Elem Electrolytes Health Dis 1987;1:63-68.

CHAPTER 7

EVALUATION OF OXIDATIVE STRESS *IN VIVO*

The 4th and last paper presented in this chapter, submitted to *Journal of Arthroplasty* (Ref 09-0432U), fulfills the last objective of the present thesis, which was to assess the clinical relevance of increased levels of Co and Cr ions in patients with MM implants.

The previous chapters suggested that the formation of Cr(III) complexes in physiological fluids may explain the lowest toxicity of Cr(III) *in vitro* in comparison to Cr(VI) and Co(II). The last aim of the present project was to assess the relationship between the *in vitro* findings and the *in vivo* clinical situations.

In this chapter, we determined the concentrations of Cr and Co ions in five groups of patients having a 28 mm-head metal-on-metal (MM) primary total hip replacement for up to 10 years. We also measured the level of oxidative stress markers (total antioxidants, peroxides, and nitrotyrosines) and the expression of antioxidant enzymes (SODs, CAT, GPx, and HO-1). Results showed an increase of both Cr and Co ion levels in the blood of these patients. However, these increases had no effect on oxidative stress markers and very slight effect on the expression of SOD and HO-1 expression, suggesting that the increased levels of Co and Cr ions are not associated with significant oxidative stress damage *in vivo*.

SIGNIFICANCE OF ELEVATED BLOOD METAL ION LEVELS IN PATIENTS WITH METAL-ON-METAL PROSTHESES: AN EVALUATION OF OXIDATIVE STRESS MARKERS

Cathy Tkaczyk[1,3,4], Olga L. Huk[3,4], Fackson Mwale[3], John Antoniou[3,4], David. J Zukor[3],

Alain Petit[3], Maryam Tabrizian[1,2,4]

[1]Department of Biomedical Engineering, [2]Faculty of Dentistry,[4]Centre for Biorecognition and Biosensors (CBB)

Duff Medical Building, 3775 University St, Montreal, QC H3A 2B4, Canada.

[3]Division of Orthopaedic Surgery, McGill University,

Lady Davis Institute for Medical Research,

The Sir Mortimer B. Davis-Jewish General Hospital,

3755 Chemin de la Côte Sainte Catherine, Montréal, QC, H3T 1E2, Canada.

7.1. Abstract

The main concern associated with Metal-on-Metal hip prostheses made of chromium (Cr)-cobalt (Co) alloys, is the release of chromium and cobalt ions in the blood and their accumulation in organs of patients. Moreover, it is widely known that Cr and Co ions can enhance the production of reactive oxygen species (ROS), known to be damageable for cells. In a matter of fact, these ROS have the capacity to disturb the redox status of cells, leading to the oxidative stress which generates damage at different levels in cells, from the extracellular environment to the nucleus.

Different antioxidants are present in cells in order to prevent cell damage, to stop the chain reactions generated by ROS and finally to repair the damage caused by the oxidative stress. Antioxidant enzymes, such as superoxide dismutases (SOD), catalase (CAT) and glutathione peroxidase (GPx) and a non-classical one, heme-oxygenase-1 (HO-1) represent the major antioxidant defense system in organism and have been widely studied recently because of their involvement in many human diseases.

The aim of this work was to establish a relation between Cr and Co ions released in serum of patients with a metal-metal hip implant and their capacity to generate an oxidative stress. To answer this question, we assessed the antioxidant enzymes, namely SOD, CAT, GPx and HO-1 at different time points. In addition, we studied the presence of lipid and protein oxidation, which is a sign of oxidative stress. Our findings suggested that SOD activity is related to ions concentrations, suggesting that it could be used as oxidative stress biomarker *in*

vivo. Taken together, results showed that Cr and Co ions did no generate any oxidative stress in patients, suggesting the efficacy of the complex antioxidant system present in serum. This work is the very first to study the effects of metallic ions released from metallic prostheses in the serum of patients, in term of oxidative stress and to propose a biomarker to study oxidative stress *in vivo*.

7.2. Introduction

Metal-on-metal (MM) hip prostheses, made of cobalt-chromium (Co-Cr) alloys, represent an excellent alternative to metal-polyethylene bearings in the treatment of osteoarthritis of the hip because of their substantially lower wear rates (1). However, the main concern associated with such bearings is the presence of circulating ions in the organism (2). These metal alloys undergo corrosion, either electrochemically or mechanically, and release metallic particles and ions that disperse systemically (3). Indeed, several studies have shown that Co and Cr particles and ions can enter the bloodstream and accumulate both in surrounding tissues and organs of patients after MM total hip arthroplasty (THA) (4-6). These ions are potentially toxic (7,8), may cause metal hypersensitivity (9,10), and chromosomal aberrations (11), and may induce changes in the proportions of peripheral blood lymphocytes (12-14).

The mechanism of metal ion toxicity is not completely understood but it is known that they can generate reactive oxygen species (ROS), such as superoxide ions ($O_2^{\cdot -}$), hydrogen peroxide (H_2O_2), hydroxyl radical ($OH^{\cdot}$), and nitrogen oxide ($NO^{\cdot}$) through Fenton/ Haber-Weiss chemistry (15). These ROS are known to be

involved in numerous human diseases, including degenerative lung and heart conditions, Alzheimer disease, rheumatoid arthritis, and aging (16). ROS are implicated in the induction of oxidative stress generating cell and tissue damage. Oxidative stress may result from an increased production of oxidants and/or a decrease in antioxidant defense. Since the damage that a ROS produces depends on its origin and type, the most accurate and clinically relevant measurement of oxidative damage is to measure multiple products of this damage (17).

In the present study, we hypothesized that metal ions released from MM bearings, namely Co and Cr, could generate oxidative stress in patients with MM THA. We first measured the concentration of both Co and Cr ions in blood of patients with MM 28 mm-head prostheses. We then evaluated the concentrations of total antioxidants (TAS), peroxides, and nitrated protein as markers of oxidative stress in the plasma of these patients. TAS measures the overall antioxidant capacity of serum samples while peroxides were used as a marker of lipid peroxidation and nitrated proteins (nitrotyrosines) as a marker of damage to proteins. Since the induction of oxidative stress is also related to the activity of specific antioxidant enzymes, in a second step we measured the activity of some of these enzymes in the plasma of these patients. We specifically looked at classical antioxidant enzymes (18) such as catalase (CAT), glutathione peroxidase (GPx), and superoxide dismutase (SOD), as well as the non-classical antioxidant enzyme heme oxygenase-1 (HO-1) (19). These enzymes were chosen because their expression (CAT, GPX, and SOD) is modulated by Co and Cr ions in human MG-63 pre-osteoblasts *in vitro* (20), and are implicated in multiple human disease

processes (18) and because the induction of HO-1 is a general response to oxidative stress in mammalian cells (21).

In a recent study (22), it has been showed that the levels of oxidative stress markers are not elevated in the plasma of patients 1 year after the implantation of MM bearings. To the best of our knowledge, this is the very first study of its kind attempting to further understand the clinical significance of elevated metal ion levels by evaluating their long-term effect at the cellular oxidant/antioxidant level.

7.3. Materials and Methods

7.3.1. Study groups

A total of 127 patients having a 28 mm-head MM articulating interface (Metasul, Zimmer, Warsaw, IN) and who gave a total of 156 blood samples were included in the study. The serum of 46 patients scheduled for THA served as control. The patients were separated into 5 groups: 1) the control group includes 46 patients; 2) 40 patients were included in the “less than 6 months” group; 3) 23 patients were included in the “1-2 years” group; 4) 28 patients were included in the “3-4 years” group; 5) 19 patients were included in the “more than 4 years” group. The age of patients at the time of blood sampling was similar for the 5 groups with a percentage of smokers varying from 14% of the patients (less than 6 months group) to 7% in the control group (Table 10). The UCLA activity and the Harris Hip scores were also similar, except for the control and the less than 6

months groups that had lower results. Prior ethics committee approval and informed written consent were obtained.

	Age (range)	UCLA	HHS	Smoker
Pre-OP	55 ± 9 (39-76 y)	4.8 ± 2.3	47 ± 14	7%
≤ 6 months	60 ± 10 (42-71 y)	4.7 ± 1.9	75 ± 16	14%
1-2 years	56 ± 11 (31-72 y)	6.0 ± 1.3	85 ± 14	11%
3-4 years	51 ± 8 (32-64 y)	6.6 ± 1.6	87 ± 13	8%
>4 years	52 ± 8 (33-65 y)	7.1 ± 1.6	90 ± 11	8%

Table 10: Demographic and outcome measures of patients in the different study groups.

7.3.2. Blood samples and ion concentrations

Whole blood samples were collected in Sarstedt Monovette tubes equipped with needles for trace metal analysis (Sarstedt, Montreal, QC) and kept at -80C until analysis. Co and Cr ions levels were measured as previously described by inductively coupled plasma mass spectrometry (ICP-MS, PerkinElmer SCIEX Elan 6100 DRC ICP-MS system; PerkinElmer Instruments, Norwalk, CT) at the Geochemical Laboratories of McGill University (22). The biological reference standard SeroNorm Trace Elements Whole Blood, Level 2 (Sero AS, Billingstad, Norway) was analyzed as a quality-control sample.

7.3.3. Plasma preparation

Whole blood of patients (1.5 ml) was also collected into Sarstedt Li-Heparin tubes and centrifuged at 500 x *g* for 10 min. Supernatant plasma was stored at -80ºC for later analysis. Plasma was chosen for this part of the study instead of whole blood because the assays for oxidative stress are not recommended for whole blood and can lead to erroneous data.

7.3.4. Oxidative stress markers

Total antioxidant status (TAS) was measured in plasma using the Oxford Biomedical total antioxidant power kit (Oxford, MI). This assay is based on the capacity to prevent the ABTS (2-2'-Azino-di-[3-ethylbenzthiazoline sulphonite]) oxidation by metmyoglobin and has an inter-assay coefficient of variation (CV) of 3%.

Lipid peroxidation was measured as the total peroxide concentration in plasma using the Biomedica OxyStat assay (Medicorp, Montreal, QC), which assesses the concentration of an orange complex formed by the oxidation of Fe^{2+} by peroxides contained in samples. The assay has a 5.1% CV inter-assay precision.

Plasma nitrotyrosine levels (nitrated proteins) were quantified using the BIOXYTECH® Nitrotyrosine-EIA assay (*Oxis*Research™, Portland, OR) that has an 11.2%CV inter-assay precision.

7.3.5.Antioxidant enzymes

The three types of superoxide dismutases (Cu/Zn-, Mn-, and Fe-SOD) present in plasma were assessed by a colorimetric assay (Superoxide Dismutase Assay kit, Cayman, Ann Arbor, MI). Cayman's superoxide dismutase assay kit utilizes a tetrazolium salt for detection of superoxide radicals generated by xanthine oxidase and hypoxanthine. One unit of SOD is defined as the amount of enzyme needed to exhibit 50% dismutation of the superoxide. It has a 3.2%CV inter-assay precision.

Catalase (CAT) activity was measured in plasma of patients using the Catalase Assay kit of Cayman, a colorimetric test based on the capacity of CAT to produce formaldehydes after hydrolysing H_2O_2. The inter-assay CV is 3.8%.

The Glutathione Peroxidase Assay kit of Cayman was used to determine the activity of all the glutathione peroxidases (GPX) present in patient plasma. This assay measures GPX activity indirectly by a coupled reaction with glutathione reductase and has a 5.7%CV inter-assay precision.

The presence of heme oxygenase-1 (HO-1) was assessed using the Human HO-1 ELISA kit from Assay Designs (Ann Arbor, MI) in which a mouse monoclonal antibody specific to human HO-1 is immobilized on wells and captured HO-1 present in samples. The sensitivity of the assay is 0.78 ng/mL.

7.3.6. Statistical analysis

TAS, peroxides, CAT, and GPX data were symmetrically distributed. Therefore, ANOVA followed by Scheffe's test was used to compare the different study groups. Metal ion, nitrotyrosine, SOD, and HO-1 data distributions were asymmetric and variability between groups was significant. The Kruskall-Wallis test that is a nonparametric equivalent of a one-way analysis of variance was used. It is calculated as a regular ANOVA, but uses the ranks of the data and is therefore resistant to outliers represented by the dots (•) in the box-plot visualization of results, in which the box by itself represent the middle 50% (25% to 75% percentiles) of the data. To facilitate calculations, all null values were defined as the half of lowest sensitivity range of the assay. A p value < 0.05 was considered as significant.

7.4. Results

Figure 7.1 shows the levels of Co and Cr ions in blood of patients with 28 mm-head MM prostheses. Results showed a significant increase of both Co (Fig. 7.1A) and Cr (Fig. 7.1B) in the blood of these patients within 6 month after their hip replacement surgery. There was no difference in the levels of both Co and Cr ions after the 1st year.

Figures 7.2 to 7.4 show the concentration of oxidative stress markers in plasma of patients with 28 mm-head MM prostheses. Results showed no differences between the various time groups for TAS (Fig. 7.2), peroxides (Fig. 7.3), and nitrotyrosines (Fig. 7.4), suggesting that the increased levels of Co and

Cr ions did not induce oxidative stress damage in plasma of these patients. Figures 7.5 to 7.8 shows the activity of antioxidant enzymes in patient plasma. Results showed that SOD significantly decreased by 65.8% in the plasma of patients up to 2 years after surgery (p=0.005) (Fig. 7.5).

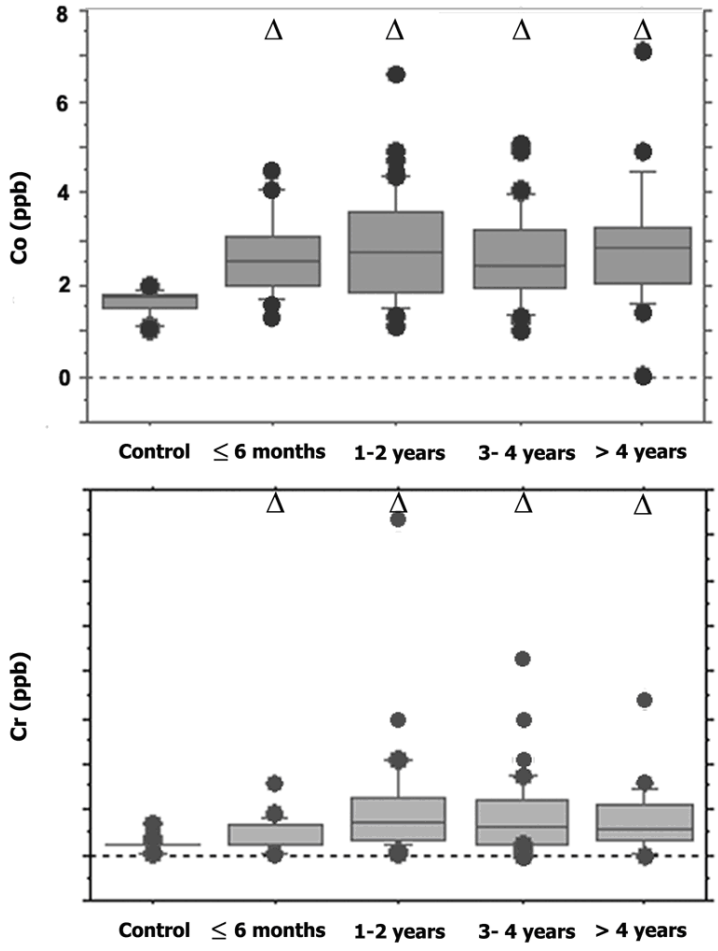

Figure 7.1: Co and Cr ion concentrations in the blood of patients with MM THAs. Co and Cr were measured in the blood of patients with 28 mm-head MM prosthesis up to 10 years post-operatively. Due to non-parametric distribution, results are presented as box plot in which outliers are represented by the dots (•)

and the box by itself represents the middle 50% (25% to 75% percentiles) of the data. Δ $p < 0.05$ versus control

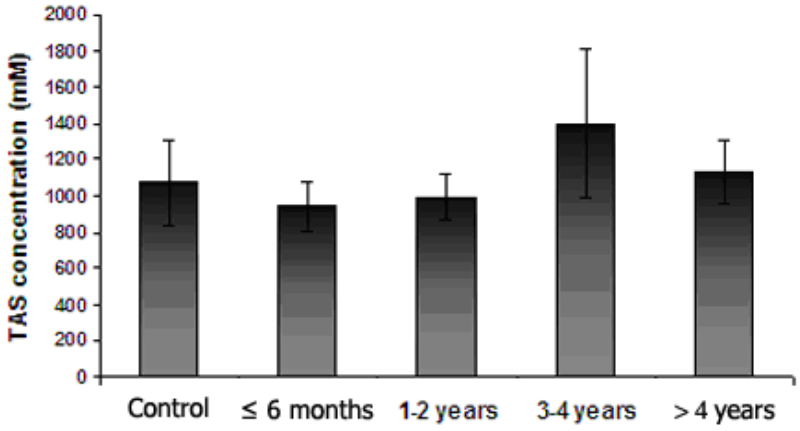

Figure 7.2: Total antioxidant status (TAS) in the plasma of patients with MM THAs. Total antioxidants were measured in the plasma of patients with 28 mm-head MM prosthesis up to 10 years post-operatively. Results are expressed as the mean ± standard deviation.

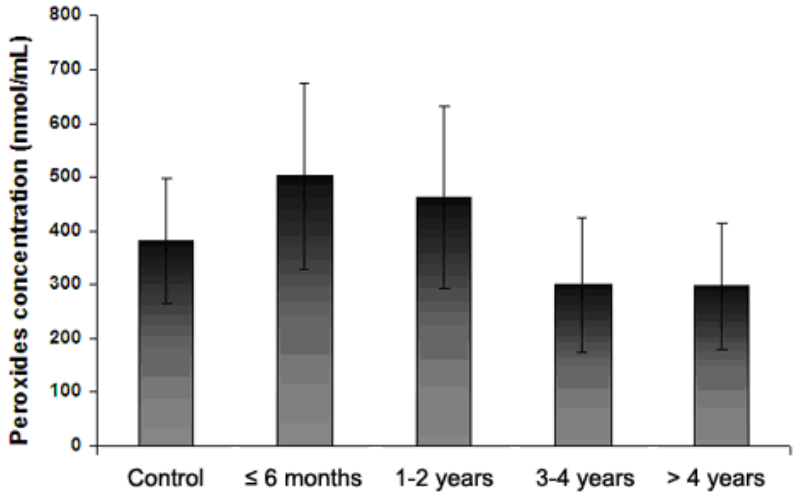

Figure 7.3: Peroxide concentrations in the plasma of patients with MM THAs. Lipid peroxides were measured in plasma of patients with 28 mm-head MM prosthesis up to 10 years post-operatively. Results are expressed as the mean ± standard deviation.

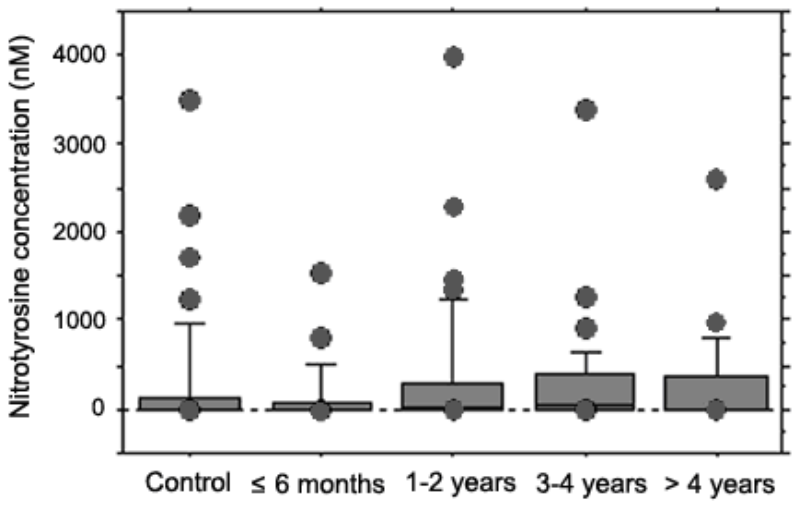

Figure 7.4: Nitrotyrosine concentrations in the plasma of patients with MM THAs. Nitrotyrosines were measured in plasma of patients with 28 mm-head MM

prosthesis up to 10 years post-operatively. Due to non-parametric distribution, results are presented as box plot in which outliers are represented by the dots (•) and the box by itself represents the middle 50% (25% to 75% percentiles) of the data.

This decrease was transient with a progressive return to control value after 3 years. The activity of SOD in the more than 4 year group was even higher than in the less than 6 month group (2.4 times; p= 0.04), the 1-2 year (7.8 times; p= 0.006), and the 3-4 year (1.3 times; p=0.02) groups (Fig. 7.5). These results suggest that Co and Cr ions may modify SOD activity in plasma of patients with 28 mm-head MM prostheses. Results also showed slow, not significant changes in CAT activity for all time intervals (Fig. 7.6). There were no statistical differences in the activity of GPX (Fig. 7.7) between the five groups.

Finally, the level of HO-1 decreased after implantation of the prostheses with statistical difference observed after 1 year (p= 0.03), at 3-4 years (p= 0.005), and after 4 years (p= 0.009) comparatively to the control group (Fig 7.8). In the more than 4 year group, the decrease reached 29.8% of the control group. The HO-1 level was also lower in the 1-2 year (p= 0.01) and the 3-4 year (p=0.006) groups compared to the less than 6 month group. These decreases in HO-1 levels suggest a role for Co and Cr ions in the modulation of circulating HO-1 in patients with 28 mm-head MM prostheses.

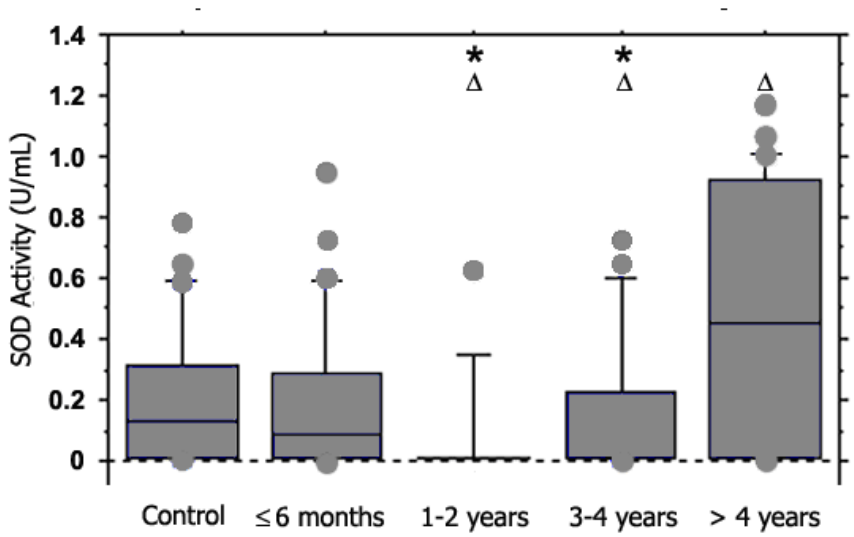

Figure 7.5: Superoxide dismutases (SODs) activity in the plasma of patients with MM THAs. SOD activity was measured in the plasma of patients with 28 mm-head MM prosthesis up to 10 years post-operatively. Due to non-parametric distribution, results are presented as box plot in which outliers are represented by the dots (•) and the box by itself represents the middle 50% (25% to 75% percentiles) of the data. Δ $p<0.05$ versus control; * $p< 0.05$ versus ≤ 6 months.

NB: The p value for the > 4 year group compared to ≤ 6 month group is 0.0486, which is at the limit of significance. The p value for the > 4 year group compared to control group is 0.038.

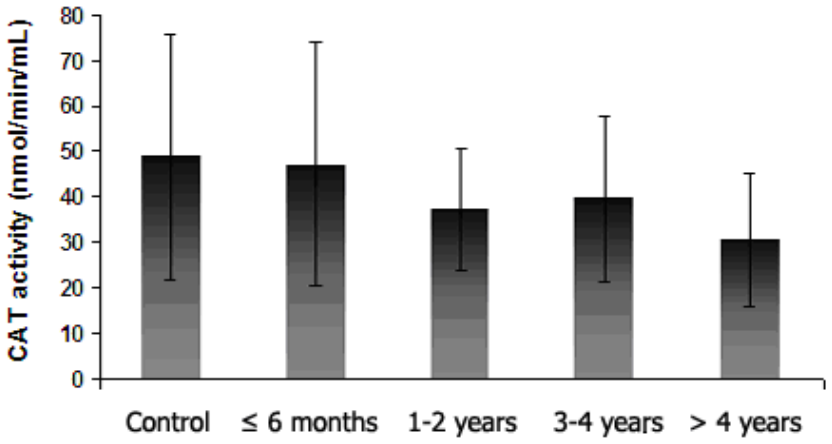

Figure 7.6: Catalase (CAT) activity in the plasma of patients with MM THAs. CAT activity was measured in the plasma of patients with 28 mm-head MM prosthesis up to 10 years post-operatively. Results are expressed as the mean ± standard deviation.

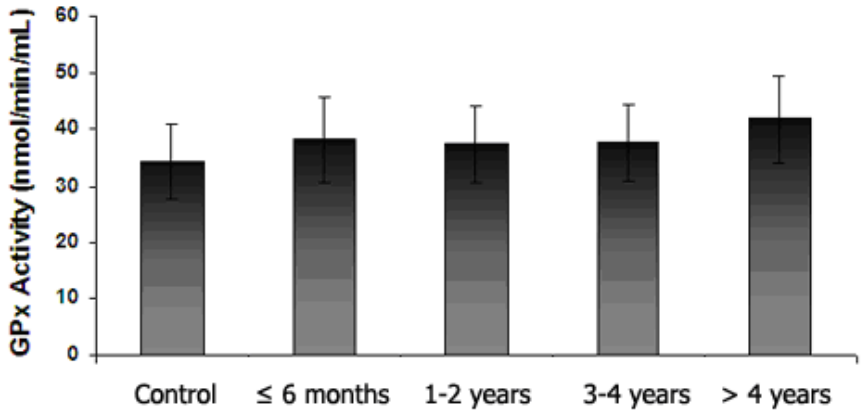

Figure 7.7: Glutathione peroxidase (GPX) activity in the plasma of patients with MM THAs. GPX activity was measured in the plasma of patients with 28 mm-

head MM prosthesis up to 10 years post-operatively. Results are expressed as the mean ± standard deviation.

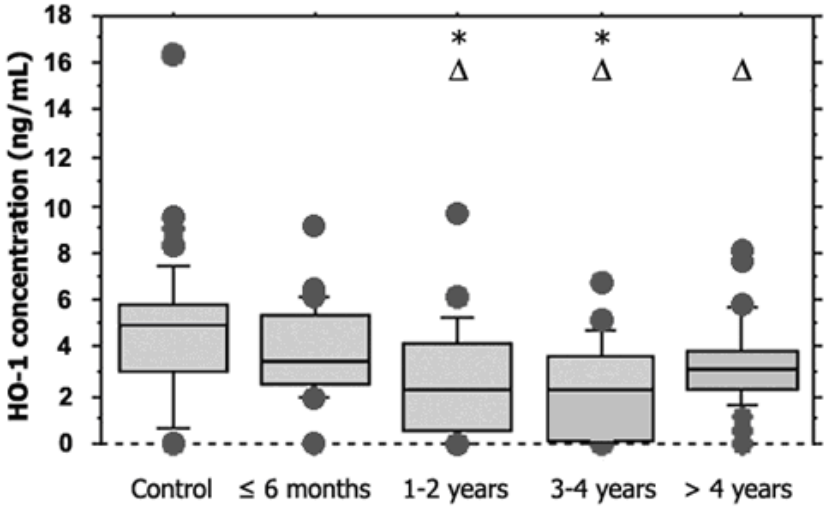

Figure 7.8: Heme oxygenase-1 (HO-1) concentrations in the plasma of patients with MM THAs. HO-1 was measured in the plasma of patients with 28 mm-head MM prosthesis up to 10 years post-operatively. Due to non-parametric distribution, results are presented as box plot in which outliers are represented by the dots (•) and the box by itself represents the middle 50% (25% to 75% percentiles) of the data. Δ $p < 0.05$ versus control; * $p < 0.05$ versus ≤ 6 months.

7.5. Discussion

The present study showed that levels of Co and Cr ions increased rapidly after surgery in blood of patients with 28 mm-head MM THA. The levels of both Co and Cr ions in our study were in the same range as those reported in previous

studies (23-30) using different prostheses, with mean (or median) Co ion levels varying from 0.7 to 2.2 ppb (12 to 38 nmol/L) and mean (or median) Cr ion levels varying from 1.3 to 2.8 ppb (24 to 53 nmol/L). However, due to differences in the choice of samples (erythrocyte vs. serum vs. whole blood) and in the methodology (digested samples vs. diluted samples; ICP-MS vs. graphite furnace), it is impossible to identify a prosthesis that releases the least amount of ions into patient circulation. Interestingly, the concentration of Cr and Co ions was much lower than those observed in periprosthetic fibrous tissue adjacent to the implants (31) but are comparable to those found in synovial fluid (32).

The rapid increase in blood ions found in the first year is also comparable to what was observed by other groups (28-30). This increase was followed by a plateau by 4 years. This suggests that, *in vivo*, the run-in phase of accelerated wear is indeed limited to the first 2 years postoperatively. A steady-state phase is reached from 6 months after surgery. In the present study, the number of patients per group and the fact that the study is not longitudinal (as the groups are formed of different patients) did not allow confirmation of this plateau. This suggests that after initial run-in-phase production, excretion of ions remains relatively constant to maintain constant level in patients. The similarity between previous longitudinal studies (28-30), and the present study supports the validity of our results even if their non-longitudinal aspect may represent a bias in the analysis of metal ions. Results from the present study have in counterpart the advantage of having been obtained with the same method of measurement (needles, tubes, solutions, standard, and technology (ICP-MS)) up to 10 years post-operatively.

Indeed, when we subdivided the more than 4 years group, there was no statistical differences in the levels of Co and Cr ions between the 5-6 years group (12 patients) and the ≥ 7 years group (7 patients) ($p > 0.8$) (results not shown). This remains to be confirmed with larger groups of patients. However, the role of renal excretion in the maintenance of metal ion levels has been shown by the dramatic increases in serum Co and Cr in patients with renal failure (29). Indeed, the observed constant levels of Co and Cr ions may also represent a change in the excretion of ions via the kidney that balances the generation of ions in patients with MM implants (3).

The single most significant obstacle preventing a broader application of MM hip arthroplasties and resurfacings continues to be the concerns regarding elevated metal ion levels in the blood, urine, and tissues of patients with these bearing surfaces, especially in young patients (2). An elevation of chromosomal aberrations was described in peripheral blood lymphocytes within 2 years postoperatively in patients with MM implants. However, as mentioned by the authors themselves, chromosomal aberrations are not necessarily associated with increased cancer incidence (33). Moreover, the same group also showed chromosome aberrations in patients with metal-polyethylene implants requiring revision (34). Visuri *et al*. initially reported a relative higher incidence of hematopoietic cancers in patients with MM prostheses (35). In the later study, however, the patient population was relatively small and no adjustments were made for co-morbidities that increase the patient risk of developing neoplasm (such as rheumatoid arthritis, Paget's disease, or bone infarcts) (35). More

recently, in a thorough evaluation of a larger cohort of patients, Visuri *et al.* were unable to demonstrate a relative increased risk of cancer in patients with MM prostheses (36). Finally, in a meta-analysis of 8 epidemiologic studies including over 130,000 patients with total hip and knee arthroplasties, no causal link could be established between MM hip bearings and cancer (37). Nevertheless, continued surveillance of patients with MM bearings is warranted to understand the clinical relevance of raised metal ions in these patients.

In an ongoing need to assess the potential consequences of elevated ion levels, we chose to evaluate oxidative stress markers in our patient population with MM THAs. Metal ions have the potential to induce the production of reactive oxygen species (ROS), making them prime suspects for disturbing the balance of oxidants/antioxidants in circulating cells (15,38,39). This oxidant/antioxidant unbalance has been identified in numerous degenerative processes including Alzheimer's disease, macular degeneration, rheumatoid arthritis, neoplasm, and aging (16). Three antioxidant groups of molecules constitute the antioxidant defense system of the organism: the primary system prevents the formation of ROS, the secondary system eliminates radicals to prevent chain reactions, and the tertiary system works to repair damaged molecules (39). TAS assesses these three antioxidant groups. In the present study, we showed that there were no changes in the levels of three oxidative stress markers (TAS, nitrotyrosine, and peroxides) and few changes in the activity of four antioxidant enzymes in patients with 28 mm-head MM prostheses compared to the control group, suggesting that the increased levels of metal ions in patients

with MM THA had no or little effect on oxidative stress in the blood of these patients. The results also stayed the same if we subdivided the more than 4 years group into a 5-6 years group and a more than 7 years group as observed for metal ions. Our results suggest that the increased levels of metal ions were not sufficient to disturb the overall defense antioxidant system (as measured by TAS) of patients with 28 mm-head MM prostheses. Furthermore, when looking at more specific markers of oxidative stress, namely lipid damage and nitrotyrosines, we were unable to show any macromolecule damage in our patient population. Further studies, with patients having prostheses with different designs, bigger head-size, as well as with hip resurfacing, are however necessary to conclusively determine the effects of elevated circulating ions on oxidative stress in the blood of patients with MM bearings.

Oxidative stress occurs when the balance of formation of oxidants exceeds the ability of antioxidant systems to remove ROS. In this regards, it was shown that Co and Cr could modify the expression of CAT and GPX in human MG-63 pre-osteoblasts (20) and that the lack of SOD in knockout mice have dramatic repercussions on phenotypes with perinatal or early postnatal mortality (40). Moreover, these enzymes are involved in many pathophysiological processes including neurodegeneration, cancer, and aging (18,41). Results of the present study show that the overall capacity of the antioxidant enzymes to remove ROS was not affected by metal ions in patients with 28 mm-head MM prostheses. We observed a transient decrease of SOD up to 2 years postoperatively group with a return to control values thereafter. The SOD activity we measured in the plasma

corresponded to SOD3 (extracellular SOD) that is present in low concentration compared to cellular SODs. Furthermore, SOD3 present in extracellular spaces of tissues accounts for 90-99% of the SOD3 present in the body. This low concentration of SOD3 circulating in plasma may make it more sensitive to minor changes of oxidative status (42). This may explain the variation of SOD activity observed in plasma of patients with 28 mm-head MM prostheses whereas the other antioxidant enzymes were not affected in the same conditions. Our results are in agreement with a previous study in COS7 cells where cobalt chloride led to a decrease in the resistance to oxidative damage by down-regulating the expression of SOD3 (43).

HO-1 is also known to be implicated in many human diseases such as Alzheimer and inflammatory diseases (21). Previous findings showed that Cr(VI) induced the expression of HO-1 in human dermal fibroblasts (44). This suggests that Cr ions were not implicated in the progressive decrease of HO-1 we observed in patients with MM THA up to 4 years post-operatively. However, HO-1 increased at longer term (> 4 years), suggesting that the effect might be reversible. A down-regulation of HO-1 was shown *in vivo* in patients with hepatitis C, while other antioxidant enzymes, such as CAT and SOD, were not affected (45). This suggests that parameters other than the presence of metal ions might be responsible for the decreased levels we observed in patients with MM prostheses.

7.6. Conclusion

This work is the first to determine the biological effects of metal ions released from MM hip implants with regards to mid-term systemic oxidative stress and showed that the increased levels of Co and Cr ions are not associated with significant oxidative stress damage.

7.7. References

1. Singh R, Dahotre NB. Corrosion degradation and prevention by surface modification of biometallic materials. J Mater Sci - Mater Med 2007, 18:725.
2. MacDonald SJ. Can a safe level for metal ions in patients with metal-on-metal total hip arthroplasties be determined? J Arthroplasty 2004; 8:71.
3. Cobb AG, Schmalzreid TP. The clinical significance of metal ion release from cobalt-chromium metal-on-metal hip joint arthroplasty. Proc Inst Mech Eng [H] 2006; 220:385.
4. Case CP, VG Langkamer, C James, et al. Wide spread dissemination of metal debris implants. J Bone Joint Surg [Br] 1994; 76-B:701.
5. Merritt K, SA Brown. Distribution of cobalt and chromium wear corrosion products and biological reactions. Clin Orthop Relat Res 1996; 329 (Suppl): S233.
6. Urban RM, JJ Jacobs, MJ Tomlinson, et al. Dissemination of wear particles to the liver, spleen, and abdominal lymph nodes of patients with hip or knee replacement. J Bone Joint Surg [Am] 2000; 82-A:457.

7. Rae T. A study on the effects of particulate metals of orthopaedic interest on murine macrophages in vitro. J Bone Joint Surg [Br] 1975; 57-B:444.

8. Haynes DR, Rogers D, Pearcy MJ, et al. The differences in toxicity and release of bone-resorbing mediators induced by titanium and cobalt-chromium-alloy wear particles. J Bone Joint Surg [Am] 1993; 75-A:825.

9. Hallab NJ, Merritt K, Jacobs JJ. Metal sensitivity in patients with orthopaedic implants. J Bone Joint Surg [Am] 2001; 83-A:428.

10. Gawkrodger DJ. Metal sensitivities and orthopaedic implants revisited: the potential for metal allergy with the new metal-on-metal joint prostheses. Br J Dermatol 2003; 148:1089.

11. Case CP. Chromosomal changes after surgery for joint replacement (Editorial). J Bone Joint Surg [Br] 2001; 83-B:1093.

12. Savarino L, Granchi D, Ciapetti, G, et al. Effects of metal ions on white blood cells of patients with failed total joint arthroplasties. J Biomed Mater Res 1999; 47:543.

13. Case CP, Langkamer VG, Lock RJ, et al. Changes in the proportions of peripheral blood lymphocytes in patients with worn implants. J Bone Joint Sur [Br] 2000; 82-B:748.

14. Granchi D, Savarino L, Ciapetti G, et al. Immunological changes in patients with primary osteoarthritis of the hip after total joint replacement. J Bone Joint Surg [Br] 2003; 85-B:758.

15. Stohs SJ, Bagchi D. Oxidative mechanisms in the toxicity of metal ions. Free Radic Biol Med 1995; 18:321.

16. Spector A. Oxidative stress and disease. J Ocul Pharmacol Ther 2000; 16:193.

17. Argüelles S, García S, Maldonado M, et al. Do the serum oxidative stress biomarkers provide a reasonable index of the general oxidative stress status? Biochim Biophys Acta 2004; 1674:251.

18. Matés JM, Pérez-Gómez, Núnez de Castro T. Antioxidant enzymes and human diseases. Clin Biochem 1999; 32:595.

19. Foresti R, Motterlini R. The heme oxygenase pathway and its interaction with nitric oxide in the control of cellular homeostasis. Free Radic Res 1999; 31:459.

20. Fleury C, Petit A, Mwale F, et al. Effect of cobalt and chromium ions on human MG-63 osteoblasts in vitro: morphology, cytotoxicity, and oxidative stress. Biomaterials 2006; 27:3351.

21. Applegate LA, Luscher P, Tyrrell RM. Induction of heme oxygenase: a general response to oxidant stress in cultured mammalian cells. Cancer Res 1991; 51:974.

22. Antoniou J, Zukor DJ, Mwale F, et al. Metal ion levels in the blood of patients after hip resurfacing: a comparison between twenty-eight and thirty-six-millimeter-head metal-on-metal prostheses. J Bone Joint Surg [Am] 2008; 90-A (Suppl) 3:142.

23. MacDonald SJ, McCalden RW, Chess DG, Bourne RB, Rorabeck CH, Cleland D, Leung F. Metal-on-metal versus polyethylene in hip arthroplasty: a randomized clinical trial. Clin Orthop Relat Res 2003; 406:282.

24. Clarke MT, Lee PTH, Arora A, et al. Levels of metal ions after small- and large-diameter metal-on-metal hip arthroplasty. J Bone Joint Surg [Br] 2003; 85-B:913.

25. Savarino L, Granchi D, Ciapetti G. et al. Ion release in patients with metal-on-metal bearings in total joint replacement: a comparison with metal-on-polyethylene bearings. J Biomed Mater Res – Applied Biomater 2002; 63:467.

26. Damie F, Favard L. [Metal serum levels in 48 patients bearing a chromium-cobalt total hip arthroplasty with a metal-on-polyethylene combination] [French]. Rev Chir Orthop Rep App Moteur 2004; 90:241.

27. Daniels J, Ziaee H, Salama A, et al. The effect of the diameter of metal-on-metal bearings on systemic exposure to cobalt and chromium. J Bone Joint Surg [Br] 2006; 88-B:443.

28. Savarino L, Granchi D, Ciapetti G, et al. Ion release in stable hip arthroplasties using metal-on-metal articulating surfaces: a comparison between short- and medium-term results. J Biomed Mater Res Part A 2003; 66-A:450.

29. Brodner W, Bitzan P, Meisinger V, et al. Serum cobalt levels after metal-on-metal total hip arthroplasty. J Bone Joint Surg [Am] 2003; 85-A:2168.

30. Lhotka C, Szekeres T, Steffan I, et al. Four-year study of cobalt and chromium blood levels in patients managed with two different metal-on-metal total hip replacements. J Orthop Res 2003; 21:189.

31. Dorr LD, Bloebaum R, Emmanual J, et al. Histologic, biochemical, and ion analysis of tissue and fluids retrieved during total hip arthroplasty. Clin Orthop Relat Res 1990; 261:82.

32. Brien WW, Salvati EA, Betts F, et al. Metal levels in cemented total hip arthroplasty. Clin Orthop Relat Res 1992; 276:66.

33 Bhamra MS , Case CP. Biological effects of metal-on-metal hip replacements. Proc Inst Mech Eng [H] 2004; 220:379.

34 Doherty AT, Howell RT, Ellis LA, et al. Increased chromosome translocations and aneuploidy in peripheral blood lymphocytes of patients having revision arthroplasty of the hip. J Bone Surg Br 2001; 83(7):1075.

35 Visuri T, Pukkala E, Paavolainen P, et al. Cancer risk after metal on metal and polyethylene on metal total hip arthroplasty. Clin Orthop Relat Res 1996; 329:S280.

36 Visuri T, Pukkala E, Pulkkinen P, et al. Cancer incidence and causes of death among total hip replacement patients: a review based on Nordic cohorts with a special emphasis on metal-on-metal bearings. Proc Inst Mech Eng [H] 2006; 220:399.

37 Tharani R, Dorey FJ, Schmalzried TP. The risk of cancer following a total hip or knee arthroplasty. J Bone Joint Surg Am 2001; 83(5):774.

38. Stohs SJ, Bagchi D, Hassoun E, et al. Oxidative mechanisms in the toxicity of chromium and cadmium ions. J Environ Pathol Toxicol Oncol 2001; 20:77.

39. Chaudière J, Ferrari-Iliou R. Intracellular antioxidants : from chemical to biochemical mechanisms. Food Chem Toxicol 199; 37:949.

40. Sentman ML, Granström M, Jakobson H, et al. Phenotypes of mice lacking extracellular superoxide dismutase and copper- and zinc-containing superoxide dismutase. J Biol Chem 2006;281:6904.

41. Matés JM, Sánchez-Jiménez F. Antioxidant enzymes and their implications in pathophysiologic processes. Frontiers Biosci 1999; 4:339.

42. Rodriguez C, Mayo JC, Sainz RM, et al. Regulation of antioxidant enzymes: a significant role for melatonin. J Pineal Res 2004; 36:1.

43. Kamiya T, Hara H, Yamada H, et al. Cobalt chloride decreases EC-SOD expression through intracellular ROS generation and p38-MAPK pathways in COS7 cells. Free Radic Res 2008; 42:949.

44. Joseph P, He Q, Umbright C. Heme-oxygenase 1 gene expression is a marker for hexavalent chromium-induced stress and toxicity in human dermal fibroblasts. Toxicol Sci 2008; 103:325.

45. Abdalla M.Y, Britigan B.E, Wen F, et al. Down-regulation of heme oxygenase–1 by hepatitis C virus infection in vivo and by the in vitro expression of hepatitis C core protein. J Infect Dis 2004; 190:1109.

CHAPTER 8

GENERAL DISCUSSION

Even though no epidemiologic studies could relate the presence of Co and Cr ions to an increased risk of cancer, the presence of these ions in the blood of patients with metal-on-metal prosthesis remains the main concern associated with CoCrMo bearing. The objectives of this thesis have been established to bring some insights into the fate of metal ions and the role they play in affecting the general health of patients with metal-metal hip prostheses. To fulfill the objectives of this thesis, the experimental approach was designed around two main pillars:

1) the biological aspects of the thesis aimed at establishing the effects of Cr(III), Co(II) and Cr(VI) ions *in vitro* on human macrophages-like cells and *in vivo* in blood of patients with MM hip prosthesis, and

2) the chemical aspects aimed at explaining the difference in toxicities of these ions by analyzing their fate in simulated-physiological fluids.

8.1. Achievements of the Thesis Objectives

In the following sections, the different segments of our work will be outlined in demonstrating the fulfillment of the objectives of this thesis.

8.1.1 Effect of Cr and Co ions on the expression of antioxidant enzymes in human macrophages in vitro

We demonstrated the toxicity of Cr and Co ions *in vitro* in both macrophages (1) and osteoblasts (2). The effect of four different concentrations of Cr(VI), Cr(III), and Co(II) on the expression (protein and mRNA) of Mn-SOD, Cu/Zn-SOD, CAT, GPx, and HO-1 was investigated after 24h, 48h and 72h of incubation. We demonstrated that Cr(VI) induced protein and gene expression of all studied antioxidant enzymes. Co(II) induced the expression of both protein (translation) and mRNA (transcription) of HO-1 only, whereas Cr(III) had no effect on these enzymes. Our results confirmed the higher toxicity of Co(II) and Cr(VI) compared to Cr(III) and suggest that ions released from MM prostheses may affect the antioxidant potential of patients with these hip implants.

8.1.2. Formation of Cr(III) complexes in simulated biological fluids

Our electron microscopy results showed that Cr(III) can form precipitable complexes of about 60-100 nm in RPMI 1640 and DMEM high glucose. While Co(II) and Cr(VI) did not form noticeable complexes, the presence of inorganic and organic compounds in the complexes of Cr(III) complexes formed in both media was confirmed by TEM and EDXA. XPS analyses, FT-IR investigations along with elemental analysis revealed a difference in the nature of compelled amino acids between two media. All analyses together indicated that Cr(III) complexes are composed of an organic phase (amino acids) tangled with an inorganic phase made of Cr(III), Ca(II) and Na(I). This work provided us with

important information on the fate of Cr in a simulated biological environment and the difference in toxicity of various metal ions.

8.1.3. Interaction of bovine and human serum proteins with Cr(III) complexes

We showed the predominant role of organic compounds, particularly proteins, in the formation of Cr(III) complexes by comparing the interaction of Cr(III) complexes with both bovine and human serum proteins. We demonstrated that Cr(III) could interact only with albumin in the presence of FBS in both RPMI 1640 and DMEM high glucose media. Seven other human proteins, namely transferrin, immunoglobulins, apolipoprotein B, complement C3, ceruloplasmin, alpha-2-macroglobulin, and plasminogen were also involved in the complex formation in both media when they are supplemented with HS. As a result of these interactions, the internalization of Cr(III) complexes were increased by macrophages. This result highlighted the role of human proteins as opsonins to make Cr(III) complexes easily recognizable by macrophages.

8.1.4. Clinical relevance of increased levels of Co and Cr ions in patients with MM hip implants

We first showed a rapid increase of Co and Cr ions in the blood of 4 groups of patients bearing a primary MM hip over 1 to 4 years. However, the presence of Co and Cr ions did not induce significant modifications in the levels of oxidative stress markers, namely peroxides and nitrotyrosines. We also

revealed no modification in the activity of the antioxidant enzymes CAT and GPx, but a slight decrease of SOD activity and HO-1 after 1-2 years post-operatively was observed. Although the long term biological effects of Co and Cr ions released from MM hip implants remain unanswered, we concluded that the levels of Co and Cr in our groups of patients were not sufficient to induce significant oxidative stress.

8.2. A Model Integrating the Different Results

Results of this global approach suggest that Cr(III) ions are less toxic than Co(II) and Cr(VI) in terms of oxidative stress, probably due to the formation of Cr(III) complexes constituted by an organic phase (amino acids, phosphates) tangled with an inorganic phase (chromium, calcium, chloride, and sodium) (Fig. 8.1), whereas neither Co(II) nor Cr(VI) could form any complexes in the same experimental conditions.

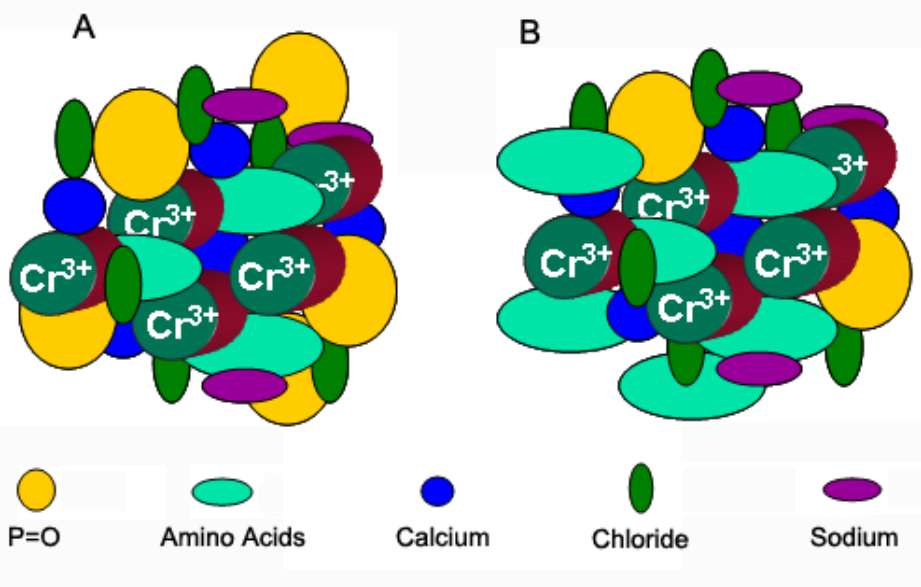

Figure 8.1: A proposed model for the nanoscale Cr(III) complexes formed in RPMI 1640 (A) and DMEM high glucose (B) media. The main difference between the complex A and the complex B is the ratio between amino acids and phosphates. Complexes A contain more P=O and less amino acids than complexes B.

These Cr(III) complexes have the capacity to bind to proteins, especially opsonins (immunoglobulins and complement C3), making them easily identifiable by macrophages, which most likely internalize them in a phagocytosis-like pathway (Fig 8.2). Cr(VI) and Co(II) are believed to enter into the cells via anionic channels.

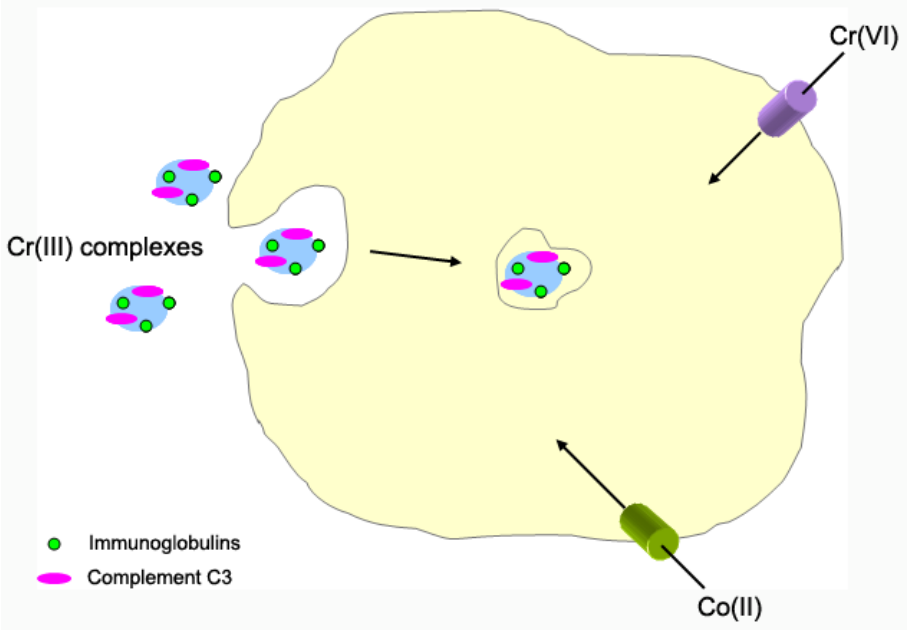

Figure 8.2: **Internalization of Cr(III), Co(II), and Cr(VI) by cell.**

We can suggest that once Cr(III) complexes are internalized, the endocytotic vesicles become endosomes or fuse with a pre-existing endosomes (pre-endosomes), a digestive vesicle with a very low pH. However, our data presented in Chapter 5 demonstrated that this acidic condition was not sufficient to alter Cr(III) complexes. It is likely that they are then held in the macrophage or finally released by an exocytosis process (Fig. 8.3). *In vivo*, it is also probable that macrophages die after internalization of the Cr(III) complexes and release them. The complexes may then be internalized for a second time by other cells within the tissues and this may explain, to some extend, the low clearance of Cr ions compared to those of Co.

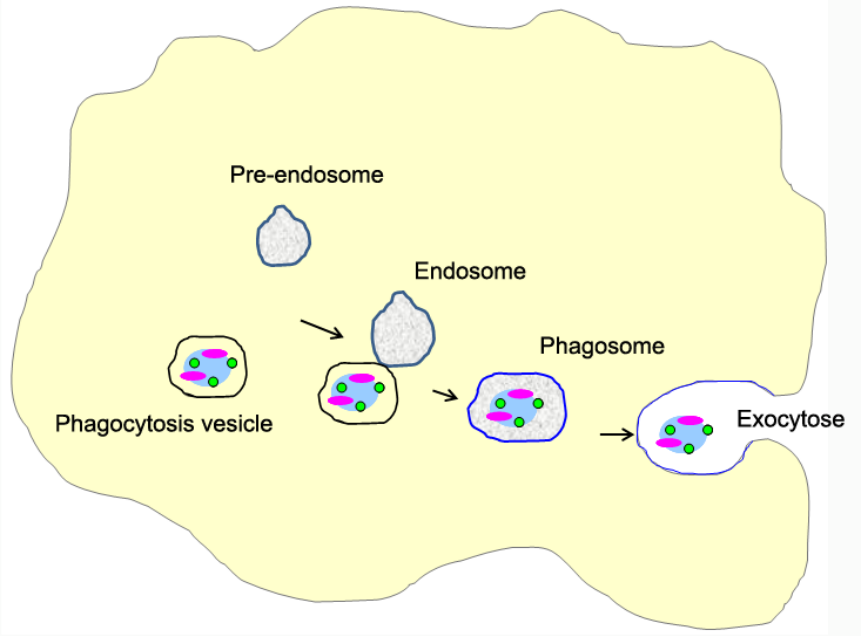

Figure 8.3: Fusion of pre-endosome and phagocytosis vesicle to form an endosome containing Cr(III) complexes.

As previously mentioned, Co(II) can penetrate into cells via ion channels. In U937 macrophages-like cells, this led to the induction of both protein and mRNA expression of HO-1, indicating that this enzyme constitute the primary defense against this ion. The activation of HO-1 by Co(II) is possibly mediated by the metal-responsive metal transcription factor-1 already described in BHK cells (3) (Fig. 8.4). In contrast, Cr(VI) induced the protein expression of all studied antioxidant enzymes, suggesting that ROS induction is more important in the presence of Cr(VI) than in the presence of Co(II) (Fig. 8.4). However, Cr(VI) did not induce the expression of their mRNA. This means that the response to Cr(VI) is at the level of translation of the protein but not at the transcription of the gene.

The absence of Cr(III) effect may be explained by the protective role of the phagocytosis phenomenon, which embeds the ions in endosome-like structures. Although our results indicated the deleterious effects of Co(II) and Cr(VI) ions on lipids or proteins, the fact that oxidative stress could not be detected in patients with MM hip prostheses may be due to insufficient levels of ions in the circulation. However, the combination of both *in vitro* and *in vivo* results suggests that at low ion concentrations, the antioxidant systems are efficient enough to prevent the oxidative stress. We cannot, however extrapolate with regards to the effects of long term exposure at the latencies involved.

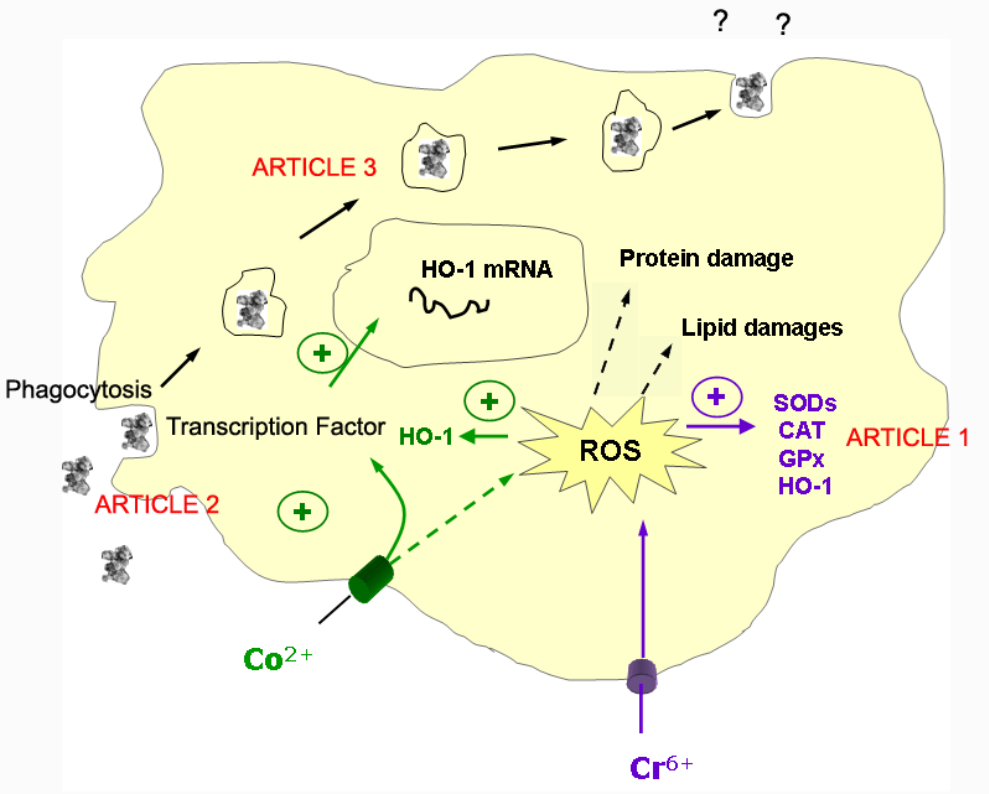

Figure 8.4: Effects of Cr(III), Co(II), and Cr(VI) in cells: A model.

8.3. Future Work

8.3.1. *In vitro*

8.3.1.1. Determination of tridimensional structure of Cr(III) complexes

One of the challenges of the future study would be to determine the tridimensional structure of the complexes and validate the proposed model. Despite the use of advanced analytical techniques and efforts, we could not solubilise and crystallize the Cr(III) complexes. The complexes were analyzed by solid-phase Nuclear Magnetic Resonance (NMR) and by X-ray. Inorganic and organic database of NMR and X-Ray indicated that no such material had been studied before, and as far, it is still classified as "unknown".

8.3.1.2. Cytotoxicity of Cr(III) complexes

The work of the present thesis combined with previous studies on the toxicity of Cr and Co in macrophages (1) and osteoblasts (2) strongly suggest that the lower toxicity of Cr(III), compared to Cr(VI) and Co(II) may be due to the formation of organic-inorganic complexes in cell culture media and in body fluid. Since Cr(III) complexes formed in RPMI 1640 and DMEM high glucose are visually and chemically different, the potential difference of toxicity of these complexes should be meticulously investigated in different cell types (i.e. macrophages, monocytes, osteoblasts) to better understand the implication of their formation in toxicity and clearance. Preliminary results in U937 macrophage-like

cells showed that Cr(III) complexes formed in DMEM seem to be more toxic (induction of cell death) than Cr (III) complexes formed in RPMI. Moreover, the disparity in their interactions with human and bovine serum proteins is another avenue of investigation full of promising results.

8.3.1.3. Long term fate of Cr(III) complexes

The present thesis described the internalization of Cr(III) complexes after a short incubation period with U937 cells and showed that the composition of the complexes may affect this internalization. However, the long term fate of these complexes in macrophages is still unknown. Can prolonged presence in endosomes, in an acidic environment coupled with strong enzymatic conditions, disrupt the complexes? Can the structure be reformed thereafter? To answer these questions, we used immunogold labeling of albumin to visualize the complexes containing albumin. However, the Cr(III) complexes appeared too dark and it was impossible to visualize the gold particles by TEM (results not shown). The alternative is the use of radio-labeled Cr(III) ($^{51}CrCl_3$) and follow the structures inside the cells by electron microscopy autoradiography.

8.3.1.4. Fate of Co(II) and Cr(VI) ions in cells

Since no complex could be visualized by TEM, the question remains unanswered on the fate of Co(II) and Cr(VI). We do not know if these ions are distributed in the cytoplasm or if they have tendency to accumulate into specific organelles. In a future study, a Luminol probe could be used to visualize Co ions

by fluorescence microscopy while Nano-Secondary Ion Mass Spectroscopy (NanoSIMS) could be used to visualize both Co(II) and Cr(VI) ions.

8.3.1.5. Internalization of the Cr(III) complexes

Phagocytosis is a very complex process which requires extensive studies to better understand it in various contexts. In this thesis, we narrowly covered the internalization of the Cr(III) complexes. The use of a clathrin-dependant endocytosis inhibitor such as chlorpromazine, the use of a caveolin-dependent endocytosis inhibitor such as genistein, and the use of a stimulator of pinocytosis such as phorbol myristate can be considered as a follow-up of our investigation on the internalization process of Cr (III) complexes (4). It is also possible to use radio-labeled Cr (^{51}Cr) and isolate organelles by ultracentrifugation. Early endosomes can then be detected by Western blot using anti-rab5-GDP and the late endosomes using anti-lamp1. Radioactivity can then be counted in the different maturation steps of endosomes.

8.3.2. *In vivo*

8.3.2.1. Effect of ions on blood cells

One of the concerns about MM prosthesis is the potential carcinogenic effect of Co and Cr ions. In this regard, an increase in chromosomal aberrations was observed in the bone marrow adjacent to metal-on-polyethylene THA, in the blood of patients undergoing revision arthroplasty of metal-on-polyethylene THA,

and in the blood of patients with MM THA (5). However, the relationship between these aberrations and the levels of ions is not known. This relationship could be analyzed by relating the Co and Cr ion levels in patients with metal-on polyethylene and MM THA to the levels of chromosomal aberrations (genomic instability, asymmetrical chromosomes, chromosome translocation, and aneuploidy) in circulating lymphocytes and monocytes. This study should be longitudinal and a long follow-up of the patients would be necessary.

8.3.2.2. Effects of ions on young patients

There is an urgent need to better understand the clinical relevance of raised serum Co and Cr levels in young patients with MM total hip replacements due to prolonged period of metal ion circulation. Several of these patients are still at the age of mothering or fathering a child. Certain metals (e.g., cadmium and lead) are toxic to embryonic and fetal tissues and can induce teratogenicity (6). However, the passage of metals through the placenta varies significantly (7) and the passage of Co and Cr is not well understood (8,9). The comparison of the concentrations of Co and Cr ions in the umbilical cord and in the blood of patients with MM THA and without THA could be realized to better understand the potential effect of these ions on the newborn. To date, two studies with a limited number of patients showed that Co and Cr seems to cross the placenta but the placenta exerts a modulatory effect on the rate of transfer (8,9).

In young men, it is well known that exposure to heavy metals (lead, copper, mercury, nickel, cadmium) may lead to significant alterations in human sperm

morphology and motility (11). Lastly, to better understand the implication, if any, of elevated ion levels on men with a MM THR and of the age of fathering a child, a prospective study should be designed to correlate the levels of Co and Cr ions in blood and seminal plasma of these patients to their semen parameters.

8.4. References.

1- Catelas I, Catelas I, Petit A, Zukor DJ, Antoniou J, Huk OL. TNF-alpha secretion and macrophage mortality induced by cobalt and chromium ions in vitro-qualitative analysis of apoptosis. Biomaterials 2003;24:383-91.

2- Fleury C, Petit A, Mwale F, Antoniou J, Zukor DJ, Tabrizian M, Huk OL. Effect of cobalt and chromium ions on human MG-63 osteoblasts in vitro: morphology, cytotoxicity, and oxidative stress. Biomaterials 2006;27:3351-60.

3- Palmiter RD. Regulation of metallothionein genes by heavy metals appears to be mediated by a zinc-sensitive inhibitor that interacts with a constitutively active transcription factor, MTF-1. Proc Natl Acad Sci (USA) 1994;91:1219-23.

4- Douglas KL, Piccirillo CA, Tabrizian M. Cell line-dependent internalization pathways and intracellular trafficking determine transfection efficiency of nanoparticle vectors. Eur J Pharm Biopharm 2008;68:676–87.

5- Bhamra MS, Case CP. Biological effects of metal-on-metal hip replacements. Proc IMechE – J Eng Med. 220: 379-384, 2006.

6- Domingo JL. Metal-induced developmental toxicity in mammals: A review. J Toxicol Environ Health. 42: 123-141, 1994.

7- Osman K, Åkesson A, Berglund M, Bremme K, Schütz A, Ask K, Vahter M. Toxic and essential elements in placentas of Swedish women. Clin Biochem. 33: 131-138, 2000.

8- Brodner W, Grohs JG, Bancher-Todesca D, Dorotka R, Meisinger V, Gottsauner-Wolf F, Kotz R. Does the placenta inhibit the passage of chromium and cobalt after metal-on-metal total hip arthroplasty? J Arthroplasty. 19 (suppl 3): 102-106, 2004.

9- Ziaee H, Daniel J, Datta AK, Blunt S, McMinn DJW. Transplacental transfer of cobalt and chromium in patients with metal-on-metal hip arthroplasty: A controlled study. J Bone Joint Surg [Br]. 89-B: 301-305, 2007.

10- Kozac K, Amneus M W, Pusey SM, Su F, Luong M N, Luong S A, Reddy S T, Farias-Esner R. Identification of biomarkers for ovarian cancer using strong anion-exchange ProteinChips: Potential use in diagnosis and prognosis. Proc Natl Acad Sci (USA) 2003; 21:12343-8.

11- Gerhard I, Monga B, Waldbrenner A, Runnebaum B. Heavy metals and fertility. J Toxicol Environ Health Part A. 54: 593-611, 1998.

CHAPTER 9

General Conclusion

Biological studies established the effects of Cr(III), Co(II) and Cr(VI) ions *in vitro* on human macrophages-like cells and *in vivo* in blood of patients with MM hip prosthesis. The physicochemical characterization demonstrated that the difference of toxicities and clearance mechanism of Cr (III) and other studied ions could originate from the formation of nanoscale complexes composed of organic and inorganic phases in the case of Cr (III). Despite higher level of metal ions in the blood of patients bearing MM implants comparing to control, the clinical studies indicated their insufficient levels to induce significant oxidative stress. Further clinical assessments are required to establish the relevance of our finding in a clinical set-up.